Structural fire and post-fire resistance of self-drilling screw connections for cold-formed steel structures

（冷間成形鋼構造のドリリングスクリューねじ接合部の構造耐火と火災後構造性能）


LIU Ying

（劉　　穎）


Doctor of Engineering

Graduate School of Environmental Studies, Nagoya University

（名古屋大学大学院環境学研究科 博士（工学））


2024

# Contents

# Chapter 1 Introduction

## 1.1 Research background

In recent years, there has been significant economic development, leading to the promotion of green, lightweight, prefabricated buildings. Cold-formed steel (CFS) is commonly used to represent light steel structures. CFS is commonly used in mid-to-low-rise residential buildings, industrial buildings, public buildings, and commercial buildings. CFS is typically formed through the cold rolling, molding, or bending of steel sheets, strips, or plates, with a material thickness ranging from 0.4mm to 6.4mm. CFS possesses the following characteristics: ① CFS allows for the production of various cross-sectional shapes through cold forming, enabling the selection of the most economical and practical cross-section based on specific requirements. ② The components of CFS are easy to produce and manufacture, with a lightweight, low transportation cost, short installation time, and low labor demand, which is conducive to the development of construction industrialization. ③Although wide and thin plates that make up the cross-section are susceptible to local buckling, they possess high post-buckling strength and do not immediately lose their load-bearing capacity. Therefore, these structures are widely used in Europe, North America, Japan, Australia, and other countries and regions. The structural regulations and technical standards followed in these countries have been proposed by EN 1993-1-3 [1.1], AISI S100-12 [1.2], Architectural Institute of Japan (AIJ) [1.3], and AS100-1998 [1.4], respectively.

The connection methods for cold-formed steel components include screw connection, welding, bolt connection, and rivet connection [1.5]. These different methods of connection can have a direct impact on the structural performance and can result in significant differences in construction cycles. It is important to note that there are significant differences in the calculation formula for the load-bearing capacity design of different connection methods, as specified by various countries. Regarding bolted connections, the thin thickness of cold-formed thin-walled steel plates results in a smaller pressure-bearing area, which leads to poor force transmission performance. Whereas, welded and riveted joints have certain disadvantages, including low deformation capacity, low construction efficiency and high cost [1.6]. Self-drilling screws are commonly used to connect cold-formed thin-walled steel members (thickness ≤ 6 mm) due to their economic benefits, ease of construction, high connection stiffness, and high shear strength [1.7], as shown in Fig1.1[1.8].

Due to the reduction of land resources in various countries and regions worldwide, some have started researching and constructing high-rise cold-formed steel structure residential buildings. In the past decade, the number of mid-rise buildings made of cold-formed steel structures has gradually increased worldwide, as shown in Fig 1.2 [1.9]. The construction technology of high-rise cold-formed steel structure buildings is also gradually maturing. Due to frequent natural disasters, such as earthquakes and typhoons, many low-rise, multi-story cold-formed steel buildings have recently been built in Japan. Additionally, with the large population

base and scarce land resources in China, as well as the critical stage of prefabricated housing industrialization and the rapid development of new rural construction and rural revitalization, China is advocating the development of green and energy-saving buildings to accelerate the achievement of "dual carbon" targets. As a result, there is significant potential for the construction of cold-formed steel (CFS) structures in China.



Fig 1.1 screw connections of Cold-formed steel structure [1.8]



Fig1.2 Mid-Rise Construction with Cold-formed steel structure [1.9]

The density of urban buildings is increasing with the development of the economy, leading to a higher probability of building fires. The damage caused by such fires in buildings is also becoming more and more significant. During the 911 attacks in 2001, two high-rise buildings in New York, USA, collapsed due to a plane impact. Investigations revealed that the primary cause of the collapse was the intense fire ignited by aviation fuel leaking after the plane struck the buildings [1.10]. Recently, the use of cold-formed thin-walled steel structures in high-rise buildings has increased owing to their sustainability and resilience. Accordingly, research into the fire safety of building structures has attracted more attention. Ensuring fire resistance and safety of these structures is critical. The connection is recognized as one of the weakest parts of the structure, and its load-bearing performance during fire directly determines the fire safety of the whole structure. In addition to focusing on the fire resistance performance of cold-formed steel structures, the reuse of steel members after fire incidents is also an important research topic in civil engineering for a sustainable society; the research on which, however, is still in the early stages and there is currently no assessment method for post-fire cold-formed steel structures. In Japan, the reuse of steel structures after a fire is determined by empirical judgment due to a lack of scientific data, as stated in the Recommendations for the Diagnosis and Repair Methods of Fire-damaged Buildings [1.11]. Although there are current design rules for screw connections have been specified by EN 1993-1-3 (EC3) [1.1], AISI S100-12 (AISI) [1.2], Architectural Institute of Japan (AIJ) [1.3], and AS100-1998 [1.4], the evaluation methods for the strength of screw connections at elevated temperatures and after heating and cooling processes are still completely unknown.

As a consequence, it is challenging to ascertain whether steel structures, including cold-formed steel structures, can be effectively reused. Especially, in Japan, not only the basic structural capacity (useable, strength, and beauty) but also the seismic-resistance capacity needs to be considered when a steel structure is reused after fire. The fire heating may alter the residual mechanical properties; therefore, having a comprehensive understanding of their post-fire mechanical properties is necessary to assess the reusability and repair of structures after fire exposure.

## 1.2 Studies and Previous researches
### 1.2.1 Shear/tensile tests of self-drilling screws at elevated temperatures

In order to gain insight into the fire resistance of cold-formed steel structure, it is essential to examine the fire resistance of the screws at first, which are the widely used to connect the components of cold-formed steel structure. However, in the fire resistance of steel structures, most past studies on the connections are related to bolted connections rather than screwed connections. For instance, for the high-strength bolted connection at elevated temperatures, Hirashima et al. [1.12] examined the load-bearing capacities of double-shear strength of friction-type high-strength bolted connections using JIS SS400 steel plate with JIS F10 T high-strength bolts. The shear

strength of Grade 8.8 high strength bolts at elevated temperatures was examined by Kirby [1.13], and the bolted connection using Grade 8.8 bolts under natural fire was examined by Hanus and Franssen et al. [1.14]. The shear strengths of two types of high-strength bolts (ASTM A325 and ASTM A490) under double-shear loading tests at elevated temperatures were examined by Seif et al. [1.15]. Pang et al. [1.16] conducted tensile tests on three types of high-strength bolts with steel grades of 8.8, 10.9 and 12.9, at elevated temperatures and reported their mechanical properties. Furthermore, other past studies [1.17-20] have reported the load-bearing capacities of bolted connections at elevated temperatures. However, for the fire resistance performance of the self-drilling screw, past research was very limited. In 1996, RL. Daudet et al. [1.21] presented the results of 264 shear tests on self-drilling screws at ambient temperature. The tests conducted include single screws in single shear, two screws in single shear, and single screws in double shear, which provided a large database for the study of screw connections. Since the failure modes of screw connections differ from those of bolt connections—for example, sheet bearing and screw tilting occur in screw connections but not in bolt connections—the existing evaluation methods for bolt connections cannot be directly applied to screw connections. Therefore, it is crucial to study screw connections at elevated temperatures to develop accurate and reliable evaluation methods. However, basic information on the both tensile and shear strength for the drilling screw and the relationships at elevated temperatures have not been clarified, because the tensile test for the drilling screw has not been conducted.

**1.2.2 Shear loading tests for self-drilling screw connections at elevated temperatures**

Previous research on screw connections has predominantly concentrated on their structural properties at ambient temperature. For the structural performance of the screw connections at ambient temperature, the design methodologies were reported by Pekoz in 1990 [1.22]. Regarding the past research using the Japan Industrial Standard (JIS) steel grade sheets and self-drilling screws, the shear loading tests of single and double-overlapped screwed connections were conducted to clarify the connection strength and failure modes at ambient temperature [1.23-25]. Furthermore, Oki Koji and Sakamoto [1.26] examined the collapse modes and deformation capacity of the single overlapped screwed connections combining several steel sheet thicknesses (1.6, 2.3, 3.2 and 4.5 mm) of JIS SCG340 and 400 grades using the drilling screws (the nominal diameter: 6 mm). They reported that several failure modes such as the pull-out and bearing failure for the screw connections occurred. Regarding the past studies on the screwed connections except for the Japanese steel grades, for example, Rogers and Hancock [1.27] reported the test results of single overlapped screwed connections under shear force using G550 and 300 sheet steels (thickness: 0.42–1.00 mm). LaBoube and Sokol [1.28] focused on fastener patterns, screw spacing, stripped screws and the number of screws, respectively, and examined the influence that those caused to the structural performance of the screwed connection. The verification method on the load-bearing capacity corresponding to each failure mode of the screwed connection at the

ambient temperature was proposed by Yu and LaBoube [1.29]. Furthermore, Roy et al. [1.30] reported the test results on the single-overlapped self-drilling screwed connections of G550 sheet steels and discussed the failure modes (bearing, tilting, pullout, shear and those combined failures), and proposed the detailed finite element modeling to be able to analyze the elastoplastic behaviors of the connections corresponding to the failure modes. Jing et al. [1.31] conducted shake table tests for the Cold-Formed Steel (CFS) modular buildings constructed by using self-tapping screws, which had a novel slide device, and reported that the numerical results well agreed with the test results. In 2020, Huynh and Pham et al. [1.32] conducted experimental research on the shear test of cold-formed high-strength steel screw connections. Different screw types and plate thickness combinations were used to investigate the compression and failure behavior of screwed connections. These experimental results, knowledge and novel systems on the connections of the cold-formed steel structures have been accumulated and contributed to the improvement of the structural performance under the ambient temperature environment.

Due to the research on fire safety in building structures, more attention has been paid. Some researchers have investigated the screwed connections at elevated temperatures, and the mechanical performance indicators for the screwed connections under high-temperature conditions were proposed recently. Chen et al. [1.33] conducted single-shear experiments on cold-formed steel-to-steel screwed connections with one screw at ambient and elevated temperatures including a total of 189 steady-state tests and 36 transient-state tests. It was considered that the failure mode of the screwed connection at elevated temperatures is established to be quite similar to that of the same screwed connection under the steady-state condition of below 100 °C. This indicates that the failure modes of threaded connections remain relatively consistent as temperature increases under steady-state conditions. Moreover, the shear strengths of screws at elevated temperatures were not examined in the research. Instead, it was assumed that the deterioration of the cold-formed steel material properties could be considered a reduction in the shear strength of the screw connection at elevated temperatures. Roy et al. [1.34] investigated the effect of screw patterns, number of screws, and screw spacing on the connection strength. Then, the experimental test and finite element analysis results were compared in terms of connection strength and failure modes, including bearing, tilting, pullout, and shear failures. Lu et al. [1.35] developed a 3D finite element (FE) model for a single-lap shear screwed connection using ABAQUS software. This model was used to predict the ultimate resistance of connections at both ambient and elevated temperatures after the validation by tests, and design equations were proposed to predict the connection resistance based on the analyses results. Yan and Young [1.36-37] investigated the structural behavior of single-shear screwed connections fabricated using thin sheet steels by varying the size of screws, sheet thickness, and arrangement of the screws using steady and transient state test methods at elevated temperatures. Additionally, the single-shear screwed-connection strengths were also compared with the nominal values determined using the cold-formed steel construction requirements from North America, Australia/New Zealand, and

Europe. The results demonstrated that the connection strengths predicted by the European code, derived from the reduction factors of cold-formed steel material properties, are typically more conservative at all temperature levels than those predicted by North American and Australian/New Zealand specifications. Vy et al. [1.38] investigated the shear behavior and load-bearing capacity of the screwed connections as used in built-up back-to-back CFS members at both ambient and elevated temperatures. They also proposed design equations to predict the tilting and bearing capacity of these screwed connections at elevated temperatures. However, a significant amount of fundamental data regarding the performance and transition of failure modes in screwed connections is still required, as research in this area is still in its early stages.

### 1.2.3 Shear tests of self-drilling screws after fire

The reuse of steel members after fire incidents is also an important research topic in civil engineering for a sustainable society [1.39]. The fire heating may alter the residual mechanical properties; therefore, having a comprehensive understanding of their post-fire mechanical properties is necessary to assess the reusability and repair of structures after fire exposure. A review of previous studies on post-fire mechanical characteristics provides a credible basis for evaluating the behavior of steel structures after exposure to fire [1.40-41]. Recently, some researchers investigated the post-fire behavior of steel bolts. Kodur et al. [1.42] and Ketabdari et al. [1.43] studied the residual mechanical properties of high-strength steel bolts and proposed predictive equations to evaluate residual mechanical properties after a fire. According to these studies, when heated >400 °C, the residual strength of bolts decreases rapidly. However, the post-fire behaviors of the screws of the cold-formed steel structure have not been investigated.

### 1.2.4 Shear loading tests for self-drilling screw connections after fire

Recent research on post-fire connections of cold-formed steel structures is bolted connections rather than screwed connections. Cai and Young [1.44] conducted tests on cold-formed single and double shear bolted connections of stainless steel under post-fire conditions. They indicated that the failure modes of the cold-formed stainless-steel bolted connection specimens under post-fire conditions were similar to those without post-fire conditions. Sulayman et al. [1.45] performed post-fire tensile tests on bolted connections; they demonstrated that the yield stress and elastic modulus of heated coupons were mainly affected by the heating temperature and time, with an insignificant effect of cooling. In Japan, KODAMA T et al. [1.46] and Seokhyeon et al. [1.47] have conducted shear tests for JIS 4.8/8.8/12.9 bolts and super high strength bolts F14T under post-fire conditions. However, the postfire behaviors of the screws of the cold-formed steel structure have not been investigated. However, the post-fire behaviors of screwed connections of the cold-formed steel structure have not been investigated. To estimate the members for safe repair, demolition, and reuse after a fire, the residual load-bearing capability of the screwed connections must be assessed. Therefore, an experimental investigation of the post-fire structural behavior of

the cold-formed steel screwed connections was required.

## 1.3 Research Purpose and Organization of the Thesis

The main objective of this study is to examine the fire resistance and post-fire performance of self-drilling screwed connections in cold-formed steel structures. While Chen et al. [1.33] and Yan and Young et al. [1.36-37] conducted single-shear experiments on screwed connections at elevated temperatures, their research did not explore the shear and tensile strengths of screws under these conditions. Additionally, their studies did not address the transitions in failure modes with changing temperatures. Consequently, there is still a lack of fundamental data and methods for evaluating the fire resistance of self-drilling screwed connections under fire conditions. Moreover, past research has not adequately addressed the post-fire strength of screwed connections, making it essential to clarify the post-fire performance of self-drilling screwed connections. Ultimately, this study aims to advance fire resistance design guidelines and post-fire repair diagnostic methods, thereby enhancing the safety and sustainability of cold-formed thin-walled steel structures.

This thesis is organized into seven Chapters. Fig1.3 shows the organization of the thesis.
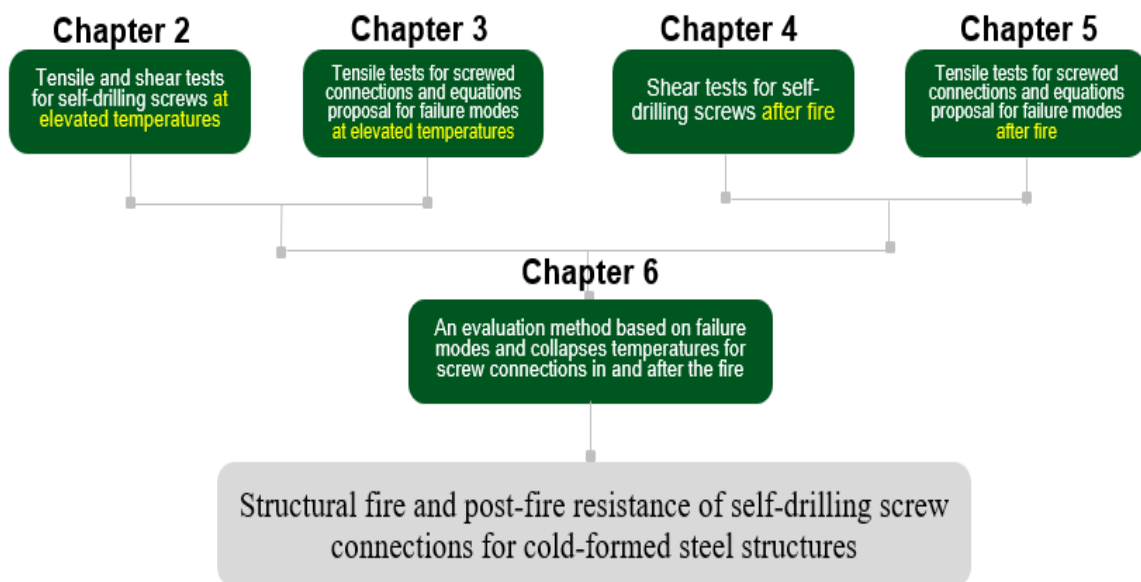


Fig1.3 The organization of the thesis

A brief description of the content of each Chapter is listed as follows:

In Chapter 1, research background and previous studies for screwed-connections were presented.

In Chapter 2, tensile and shear tests were conducted on three types of self-drilling screws at elevated temperatures under steady-state conditions, which were manufactured from high-strength steel, martensitic high-strength stainless steel and austenitic stainless-steel bar. The test clarified the shear strength and tensile strength at elevated temperatures, as well as the deformation behavior under these conditions, and the relationship between shear strength and tensile strength of self-drilling screws at elevated temperatures was elucidated. Furthermore, the high-strength

(HS) screws possessed similar reduction factors to the high-strength (AIJ F10T) bolts for the shear strength.

In Chapter 3, tensile tests for single overlapped screwed connections at elevated temperatures were conducted. This chapter examined the transition of the failure modes between the ambient and elevated temperatures by tensile loading for two screwed-connection specimens and eight screwed-connection specimens, which are made of two thin steel sheets with a thickness of 1.6 mm and a width of 120 mm, connected by 2 and 8 self-drilling screws respectively. Moreover, sheet bearing failure mode and screw shear failure mode were observed after tensile tests at elevated temperatures. Equations for the screw connection strength corresponding to each failure mode at elevated temperatures was proposed, referring to the design codes EN 1993-1-3 [1.1] and AISI S100 [1.2] at ambient temperatures.

In Chapter 4, three types of self-drilling screws, manufactured using high-strength steel, martensitic high-strength stainless steel, and austenitic stainless-steel bars, were used in the tests, which was the same batch as used in Chapter 2. Shear loading tests were conducted on the self-drilling screws after the heating and cooling procedures. It was clarified that the reduction factor of HS screws decreased significantly when <500℃, compared with JIS Grade 4.8/8.8/12.8, super high-strength F14T, and high-strength F10T bolts. The post-fire shear strengths of HS and super high-strength F14T bolts reduced by more than 40% when the heated temperature reached 800 ℃. The post-fire shear strengths and load-bearing capacities of the self-drilling screw were examined. Furthermore, the post-fire shear strengths were compared with the shear strengths at elevated temperatures. The reduction of post-fire shear strength was clarified, which provided the fundamental data necessary for the study of screwed-connections at post-fire conditions, as detailed in Chapter 5.

In Chapter 5, the post-fire shear strengths and load-bearing capacities of screwed connections have been examined by using two screwed-connection specimens, four screwed-connection specimens and eight screwed-connection specimens. Tensile loading tests were conducted on single overlapped screwed connections after the heating and cooling procedures to examine the transition of the failure modes between the ambient and exposed temperatures. Evaluation equations were proposed for each failure mode, which could predict the post-fire strength of screwed-connections.

Chapter 6 presents an evaluation method based on failure modes and failure temperatures for screw connections in/after fire. This evaluation method involves varying parameters, including different sheet thicknesses of screwed-connections and loads which are based on designing by Guide for Designing Cold-formed Steel Structures 2nd Edition [1.48]. Subsequently, the theoretical evaluation formulas proposed in Chapters 3 and 5 for elevated temperatures and post-fire conditions, are employed to calculate and investigate the failure modes and failure temperatures. This ensures the structural integrity and safety of cold-formed steel structures at elevated temperatures and provides essential data for post-fire repair and reuse efforts, as well as

investigating the residual strength after fire.

In Chapter 7, the research is summarized. Conclusions from the study are stated and directions for further research are suggested.

**References**

[1.1] EN 1993-1-3 (2006). Eurocode 3 – Design of Steel Structures – Part 1-3: General Rules Supplementary Rules for Cold-Formed Members and Sheeting.

[1.2] American Iron and Steel Institute. North American Specification for the Design of CFS Structural Members, AISI S100-12[S]. Washington, DC, USA, 2012.

[1.3] Architectural Institute of Japan (AIJ) (2012). AIJ Recommendation for Design of Connections in Steel Structures, Maruzen Publishing Co., Tokyo (in Japanese).

[1.4] Australian Standard. Steel Structures. AS100-1998[S]. Australia, 1998.

[1.5] Yu W, Roger A. Cold-Formed Steel Design: 4th (fourth) edition. Wiley, John & Sons, Incorporated, 2010, 263

[1.6] Lee, Y.H., Tan, C.S., Mohammad, S., Md Tahir, M., Shek, P.N., 2014. Review on Cold-Formed Steel Connections. The Scientific World Journal 2014, 1–11.

[1.7] Serrette R, Nolan D. Pullout strength of steel pins in cold-formed steel framing. Journal of Structural Engineering, 2015, 141(5): 04014144

[1.8] Vincent E. Sagan, P.E.(2014). "STRUCTURE magazine | Cold-Formed Steel Design: Where Do I Find Help?". *https://www.structuremag.org/?p=2628.* (viewed 22 Jul 2024)

[1.9] Ardy Sherafati, PhD, PE, SE(2021). "Mid-Rise Construction with Cold Formed Steel - Artin Engineering&Design". *Mid-Rise Construction with Cold Formed Steel - Artin Engineering & Design (artined.com).* (viewed 22 Jul 2024)

[1.10] Salvatore Ancona.(2023). "The World Trade Center Construction and Collapse, Part 4". Fire Engineering. *https://www.fireengineering.com.* (viewed 22 Jul 2024)

[1.11] Architectural Institute of Japan (AIJ), Recommendation for diagnosis and repair Methods of fire-damaged Buildings, 2015 (in Japanese)

[1.12] Hirashima, T., Orimo, T., Kikuta, S., Takahashi, K., Hori, A., Nakagome, A., Mtsudo, M., Yoshida, M., Yamanouchi, H., Nakamura, K., Uesugi, H. and Saitou, H. (2001), "Experiments about shear strength of friction type high tension bolted joints at elevated temperature", Journal of Structural Engineering, Architectural Institute of Japan (AIJ) (in Japanese), Vol. 47B, pp. 311-316.

[1.13] Kirby, B.R. (1995), "The behaviour of high-strength grade 8.8 bolts in fire", Journal of Constructional Steel Research, Vol. 33, pp. 3-38.

[1.14] Hanus, F., Zilli, G. and Franssen, J.M. (2011), "Behaviour of Grade 8.8 bolts under natural fire conditions—tests and model", Journal of Constructional Steel Research, Vol. 67, pp. 1292-1298.

[1.15] Seif, M.S., Weigand, J.M., Peixoto, R. and Vieira, L. (2017), "Behaviour of high-strength bolts at elevated temperatures under double-shear loading", Proceedings of Eurosteel, Vol. 1 Nos 2-3, pp. 2648-2657.

[1.16] Pang, X.-P., Hu, Y., Tang, S.-L., Xiang, Z., Wu, G., Xu, T. and Wang, X.-Q. (2019), "Physical properties of high-strength bolt material at elevated temperatures", Results in

Physics, Vol. 13, 102156.

[1.17] Zhang, J.-F., Zhao, J.-J., Tian, G.-F., Zhang, P., Deng, E.-F., He, J.-M., Yu, H.-X. and Fan, Y.-F. (2020), "Tensile behavior of the connection between nut-free high-strength bolt and endplate", Journal of Constructional Steel Research, Vol. 174, 106301.

[1.18] Akagwu, P., Ali, F. and Nadjai, A. (2020), "Behaviour of bolted steel splice connections under fire", Journal of Constructional Steel Research, Vol. 170, 106103.

[1.19] Cai, Y. and Young, B. (2015), "High temperature tests of cold-formed stainless steel double shear bolted connections", Journal of Constructional Steel Research, Vol. 104, pp. 49-63.

[1.20] Yang, K.C., Hsu, R.J. and Chen, Y.J. (2011), "Shear strength of high-strength bolts at elevated temperature", Construction and Building Materials, Vol. 25, pp. 3656-3660. Yang, K.C., [1.20] Hsu, R.J. and Hsu, C.F. (2013), "Strength criteria for bolted connections at elevated temperature", Journal of Constructional Steel Research, Vol. 88, pp. 43-52.

[1.21] Daudet, Randy L. and LaBoube, Roger A., "Shear Behavior of Self Drilling Screws Used in Low Ductility Steel" (1996). *CCFSS Proceedings of International Specialty Conference on Cold-Formed Steel Structures (1971 - 2018)*. 3.

[1.22] Pekoz, T. (1990), "Design of cold-formed steel screw connections", Proceedings of the 10th International Specialty Conference on Cold-Formed Steel Structures University of Missouri Rolla, pp. 575-587.

[1.23] Sasaki, T. et al. (1996), "Experimental study on screw connections between thin steel plates", Summaries of Technical Papers of Annual Meeting, Architectural Institute of Japan (AIJ), pp. 511-512, (in Japanese).

[1.24] Yamamoto, T., Sakamoto, Y. and Ninomiya, J. (1997), "Structural properties, durability and thermal insulation of steel-framed houses (Part 7. Shear loading test for self-drilling tapping screw connections (2) analysis of experiment)", Summaries of Technical Papers of Annual Meeting, Architectural Institute of Japan, pp. 857-858, (in Japanese).

[1.25] Sakamoto, Y., Miyamoto, T. and Ninomiya, J. (1997), "Study on structural properties, durability and thermal insulation of steel-framed houses (Part 6. Shear loading test for self-drilling tapping screw connections (1) outline of experiment)", Summaries of Technical Papers of Annual Meeting, Architectural Institute of Japan (AIJ), pp. 855-856, (in Japanese).

[1.26] Oki Koji, K. and Sakamoto, Y. (2000), "Shear loading test for self-drilling tapping screw connections (2) (steel and steel connections)", Summaries of Technical Papers of Annual Meeting, Architectural Institute of Japan (AIJ), pp. 857-858, (in Japanese).

[1.27] Rogers, C.A. and Hancock, G.J. (1999), "Screwed connection tests of thin G550 and G300 sheet steels", Journal of Structural Engineering, ASCE, Vol. 125 No. 2, pp. 128-136.

[1.28] LaBoube, R.A. and Sokol, M.A. (2002), "Behavior of screw connections in residential construction", Journal of Structural Engineering, ASCE, Vol. 128 No. 1, pp. 115-118.

[1.29] Yu, W.W. and LaBoube, R.A. (2010), Cold-Formed Steel Design, 4th ed., Journal of

Structural Engineering, John Wiley & Sons, Hoboken, New Jersey.

[1.30] Roy, K., Lau, H.H., Ting, T.C.H., Masood, R., Kumar, A. and Lim, J.B.P. (2019a), "Experiments and finite element modelling of screw pattern of self-drilling screw connections for high strength cold-formed steel", Thin-Walled Structures, Vol. 145, 106393.

[1.31] Jing, J., Clifton, G.C., Roy, K. and Lim, J.B.P. (2020), "Three-storey modular steel building with a novel slider device: shake table tests on a scaled down model and numerical investigation", ThinWalled Structures, Vol. 155, 106932.

[1.32] Huynh M T, Pham C H, Hancock G J. Design of screwed connections in cold formed steels in shear. Thin-Walled Structures, 2020, 154(5): 106817

[1.33] Chen W, Ye J, Zhao M. Steady- and transient-state response of cold-formed steelto-steel screwed connections at elevated temperatures. Journal of Constructional Steel Research 2018, 144: 13–20

[1.34] Roy, K., Lau, H.H., Huon Ting, T.C., Masood, R., Kumar, A., Lim, J.B.P., 2019. Experiments and finite element modelling of screw pattern of self-drilling screw connections for high strength cold-formed steel. Thin-Walled Structures 145, 106393.

[1.35] Lu W, Pentti M, Outinen J, et al. Design of screwed steel sheeting connection at ambient and elevated temperatures. Thin-Walled Structures, 2011, 49(12): 15261533

[1.36] Yan, S., Young, B., 2012. Screwed connections of thin sheet steels at elevated temperatures – Part I: Steady state tests. Engineering Structures 35, 234–243.

[1.37] Yan, S., Young, B., 2012. Screwed connections of thin sheet steels at elevated temperatures – Part II: Transient state tests. Engineering Structures 35, 228–233.

[1.38] Vy, S.T., Mahendran, M., 2022. Screwed connections in built-up cold-formed steel members at ambient and elevated temperatures. Journal of Constructional Steel Research 192, 107218. https://doi.org/10.1016/j.jcsr.2022.107218

[1.39] Rehman, M.; Sakalle, R. Finite elemental analysis of industrial structure using cold formed steel. *AIP Conf. Proc.* **2019**, *2158*, 020014.

[1.40] Ye, K., Ozaki, F., 2021. Post-fire mechanical properties and buckling strength of cold-formed steel hollow section columns. Journal of Constructional Steel Research 184, 106806.

[1.41] Yamaguchi, T., Ozaki, F., 2023. Tensile strengths of super high-strength steel strand wire ropes and wire rope open swaged socket connections at fire and post fire. JSFE.

[1.42] Kodur, V., Yahyai, M., Rezaeian, A., Eslami, M., Poormohamadi, A., 2017. Residual mechanical properties of high strength steel bolts subjected to heating-cooling cycle. Journal of Constructional Steel Research 131, 122–131.

[1.43] Ketabdari, H., Saedi Daryan, A., Hassani, N., 2019. Predicting post-fire mechanical properties of grade 8.8 and 10.9 steel bolts. Journal of Constructional Steel Research 162, 105735. https://doi.org/10.1016/j.jcsr.2019.105735

[1.44] Cai, Y., Young, B., 2019. Structural behaviour of cold-formed stainless steel bolted connections at post-fire condition. Journal of Constructional Steel Research 152, 312–321. https://doi.org/10.1016/j.jcsr.2018.03.024

[1.45] Sulayman, Q., Mahmood, M., 2022. Post-fire block shear strength of thin-walled carbon steel bolted connections. Journal of Constructional Steel Research 198, 107528. https://doi.org/10.1016/j.jcsr.2022.107528

[1.46] KODAMA T., Ozaki, F., 2023. "Shear strength of a bolt at elevated temperature and after heating and cooling processes", Summaries of technical papers of annual meeting, Architectural Institute of Japan. No.3084, pp. 177-178. (in Japanese)

[1.47] Seokhyeon HAN, Fuminobu OZAKI, Kenji TADA, Junichi SUZUKI, 2022. "Damage evaluation for super high-strength bolted(F14T) connections after heating and cooling processes". Summaries of technical papers of annual meeting, Architectural Institute of Japan. No.3018, pp.35-36. (in Japanese)

[1.48] Guide for Designing Cold-formed Steel Structures 2nd Edition, Gihodo Shuppan Co.,Ltd., 2014 (in Japanese)

# Chapter 2 Tensile and shear tests of self-drilling screws at elevated temperatures

## 2.1 Introduction

In Chapter 2, tensile and shear tests were conducted on three types of self-drilling screws at elevated temperatures under steady-state conditions, which were manufactured from high-strength steel, martensitic high-strength stainless steel and austenitic stainless-steel bar. The test clarified the shear strength and tensile strength at elevated temperatures, as well as the deformation behavior under these conditions, and the relationship between shear strength and tensile strength of self-drilling screws at elevated temperatures was elucidated. Furthermore, the high-strength (HS) screws possessed similar reduction factors to the high-strength (AIJ F10T) bolts for the shear strength.

## 2.2 Tensile test of self-drilling screws at elevated temperatures

### 2.2.1 Overview of tensile test for self-drilling screws at elevated temperatures

In total, three types of self-drilling screws were used as test specimens (Fig 2.1), namely, high-strength steel screw manufactured from carbon steel wire for cold heading and cold forging JIS SWCH A18 (hereinafter referred to as HS), which have been heat treated, martensitic stainless-steel screw manufactured from the original stainless-steel bar JIS SUS410 (hereinafter referred to as MSUS) and austenitic stainless steel screw manufactured from the original stainless-steel bar JIS-SUS304J3 (hereinafter referred to as ASUS). These three types of screws are commonly used in various components of cold-formed structures. HS screws are typically employed for connecting structural elements of cold-formed steel, while MSUS screws are primarily used in stainless steel components of cold-formed structures. On the other hand, ASUS screws are used for non-structural components with corrosion resistance and waterproof properties, such as a window sash frame, the installation of interior and exterior decorative materials or aluminum sheets in metal roofing systems, where water and corrosion resistance are important [2.1, 2.2]. Therefore, it is crucial to clarify the fire resistance of the screws. The inspection certificates of the original bars for the three kinds of screw specimens show in Appendix A. The chemical components of the original steel bars are listed in Table 2.1 by OZAKI et al. [2.3]. The amounts of nickel and chromium alloys included in the ASUS and MSUS screws were higher than those in the HS screw to improve rust prevention. However, it is known that these alloys contribute to improving the tensile strength at elevated temperatures, in comparison with general mild steels or high-strength carbon steels by Fushimi et al. [2.4]. The nominal diameter and length under the head position of the screw were 5 and 70 mm, respectively, for the three types of screws. The length of the screw specimen (70 mm) was larger than that of the general screw to meet the specifications of experimental jigs for tensile tests and shear tests shown in Fig 2.2 and Fig 2.7.

HS     ASUS     MSUS

Fig 2.1 Test specimens

Table 2.1 Chemical compositions of screws [2.3]

| Chemical(mass%) Metal | C | Si | Mn | P | S | Al | Cu | Ni | Cr |
|---|---|---|---|---|---|---|---|---|---|
| SWCH18 A(HS) | 0.19 | 0.03 | 0.8 | 0.01 | 0.007 | 0.03 | 0.02 | 0.03 | 0.03 |
| SUS304J3(ASUS) | 0.025 | 0.25 | 1.6 | 0.034 | 0.001 | | 2.55 | 9.05 | 18.28 |
| SUS410(MSUS) | 0.1 | 0.4 | 0.37 | 0.023 | 0.001 | | | 0.23 | 12.03 |

To obtain the basic experimental results on the tensile strength of the screw, tensile tests were conducted at elevated temperatures under steady-state conditions. Table 2.1 shows lists of the screw specimens (HS, MSUS and ASUS) using tensile and shear testes, respectively. To apply tensile force to the screw, the testing jigs, as shown in Fig 2.2, were used. A total of two columnar steel jigs (Fig 2.2(a)) were used to clamp the screw in the testing jig. The screw was installed into a groove in the columnar jig and sandwiched by two columnar jigs, which were set into a hole in a steel plate jig, as shown in Fig 2.2(b). The hole diameter in the plate was smaller than the columnar diameter; therefore, the columnar jigs were tightly attached to the hole in the lower steel plate jig (Fig 2.2(e)) when applying a tensile force to the upper and lower steel plate jigs, and finally, the tensile force acted on the screw. The screw specimen in the testing jigs was set in the middle of a cylindrical electric furnace (height: 500 mm, inside diameter: 250 mm) and heated up to the target test temperatures, which were given by the ambient temperature (20$^\circ$C), 400, 600, 700 and 800$^\circ$C. A dummy screw specimen with a thermocouple for the measurement of the screw temperature, which had the same shape and size as the screw specimen, was set in the testing jigs near the screw specimen (Fig 2.2(f)). It was assumed that the temperature of the screw specimen was given by the temperature measured from the dummy screw specimen. After the specimen temperature reached approximately the above target temperatures (see Fig 2.3), the specimen was maintained under the target test temperature for approximately 30 min to achieve a uniform temperature; subsequently, the tensile force P was applied. The number of screw specimens subjected to the tensile test at each temperature was one, whereas the same tests were conducted three times for the ASUS specimens at 400$^\circ$C, because of the verification of the dispersion tendency of the test results at elevated temperatures. The relative deformation between the upper and lower steel plate jigs in the furnace was measured. The measurement steel-bar jigs were attached to the steel plate jigs and both the upper and lower parts of the steel bar jigs were taken from the furnace, and displacement meters were set to the steel bar jigs outside the furnace (Fig 2.2(g)).

Table 2.2 Details of screw specimens

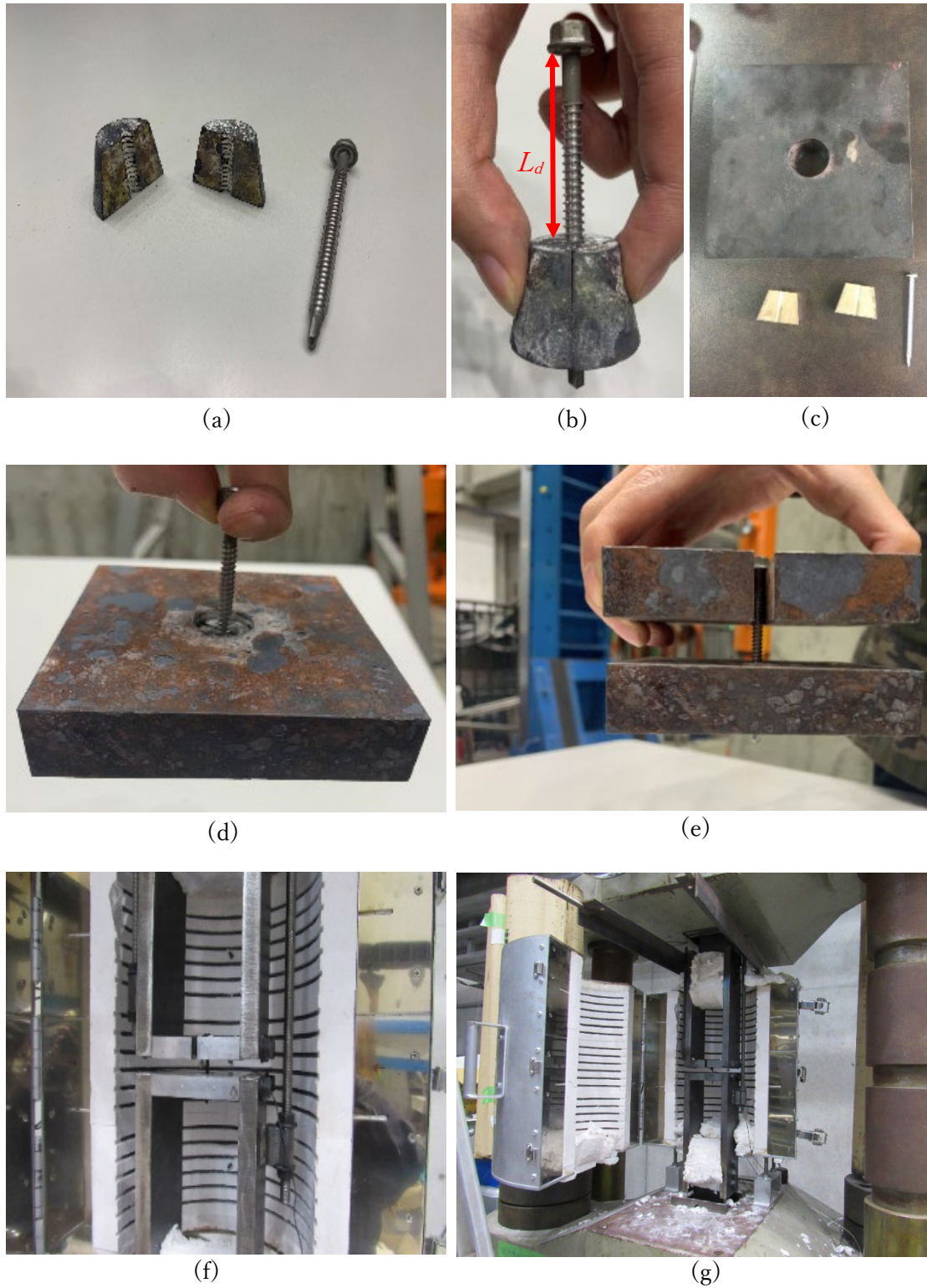| specimens | Screw nominal diameter | Length screw position | under head | Number of screws Tensile test | Shear test |
|---|---|---|---|---|---|
| HS | 5.0mm | 70mm | | 1 | 2 |
| MSUS | 5.0mm | 70mm | | 1 | 2 |
| ASUS | 5.0mm | 70mm | | 1 | 2 |

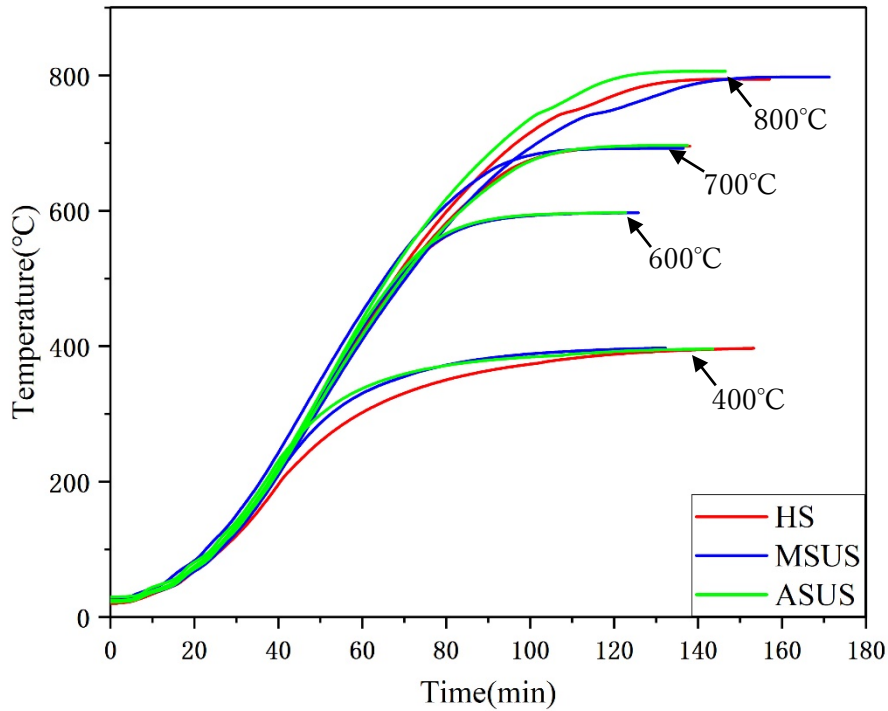Fig 2.2 Testing jigs and test systems

Fig 2.3 Relationships between time and specimen temperature for tensile testes

### 2.2.2 Experimental results of tensile strength for self-drilling screws at elevated temperatures

Fig 2.4 shows the photographs of the screw specimens after the tensile test at elevated temperatures. Many screw specimens were fractured at those thread parts, except for the ASUS specimen at 800℃ (screw head fracture) and 400℃ (shaft part fractures near the head). It was considered that the latter failure modes (shaft part fractures near the head) occurred by shape imperfection or stress concentration owing to the screw head. Fig 2.5 shows the experimental results for the screw specimens. The horizontal axis shows the non-dimensional deformation, which was denoted by a quotient dividing the relative displacement, $\Delta L$, measured from the displacement meters by the deformed region length, $L_d$ =39.5 mm, of the screw set in the testing jig. The deformed region length, $L_d$, was assumed to be the axial distance of the screw clamped between the upper and lower steel plate jigs. The vertical axis of Fig 2.5 is the tensile stress calculated by dividing the tensile force, $P$, by the nominal cross-sectional area, $A_s$= 19.6 mm$^2$, of the screw. The vertical axis of Fig 2.5 indicates the nominal stress $\sigma$, which was evaluated by $\sigma$ = $P/A_s$.

As shown in Fig 2.5, the maximum tensile force decreased with increasing test temperature. For the ASUS specimens, the tensile strength at the ambient temperature was the lowest; however, the tensile strength at 800℃ reached approximately 100 N/mm$^2$ and was the highest among the three types of screw specimens. The ASUS test results were conducted three times at 400℃ and exhibited almost the same behavior (Fig 2.5(c)); therefore, it was considered that the variation in

18

tensile strength at each temperature was small. For the MSUS specimens, the tensile strengths at both 400℃ and ambient temperatures were almost the same. Conversely, the tensile strength above 400℃ decreased sharply. The HS and MSUS specimens possessed a large tensile strength at ambient temperature; however, the tensile strength at 800℃ was less than 1/10 of that at ambient temperatures.

Fig 2.6(a) shows the reduction factors on the tensile strength for three kinds of specimens. Each value of the reduction factor as shown in Fig 2.6(a) was given by dividing the tensile strength at the ambient temperature from that at the elevated temperature. The reduction factors of both the HS and MSUS specimens sharply decreased above 400℃, as mentioned above. The reduction factor of the ASUS specimen above 400℃ was the largest because of included a high amount of nickel and chromium alloys (Table 1). Fig 2.6(b) shows the comparison results of the reduction factors of the HS specimens with the past test results on the tensile strength of high-strength steel bolts, which were JIS F10T ones (the specified design tensile strength at the ambient temperature is given by 1,000 MPa) [2.5] and 12.9, 10.9 and 8.8 ones tested by Pang et al. [2.6]. JIS F10 T high-strength bolts are widely used for the connection of steel structures in Japan. As illustrated in Fig 2.6(b), the tensile strength of HS screws at 400 degrees is 20% lower than that of F10T. The observed reduction in tensile strength is thought to be associated with the processing of the HS screw. As detailed in Appendix A, the tensile strength of the carbon steel wire is 439 N/mm², whereas the tensile strength of the HS screw tested in this experiment is 746 N/mm². As a consequence of the heat treatment and processing, the tensile strength of the HS screw is enhanced at ambient temperature(20℃), while its tensile strength is significantly reduced at 400℃. Fig2.6(c) shows the reduction factors of ASUS specimens have a similar tendency with past research for SUS630 by Sakumoto et al. [2.7] at elevated temperatures.

20℃        400℃        600℃

700℃        800℃

(a) HS



20℃        400℃        600℃

700℃        800℃

(b) MSUS

Fig 2.4 Photographs of ASUS after tensile test

|  |  |  |
|:---:|:---:|:---:|
| 20°C | 400°C | 600°C |
| 700°C | 800°C | Three specimens at 400°C |
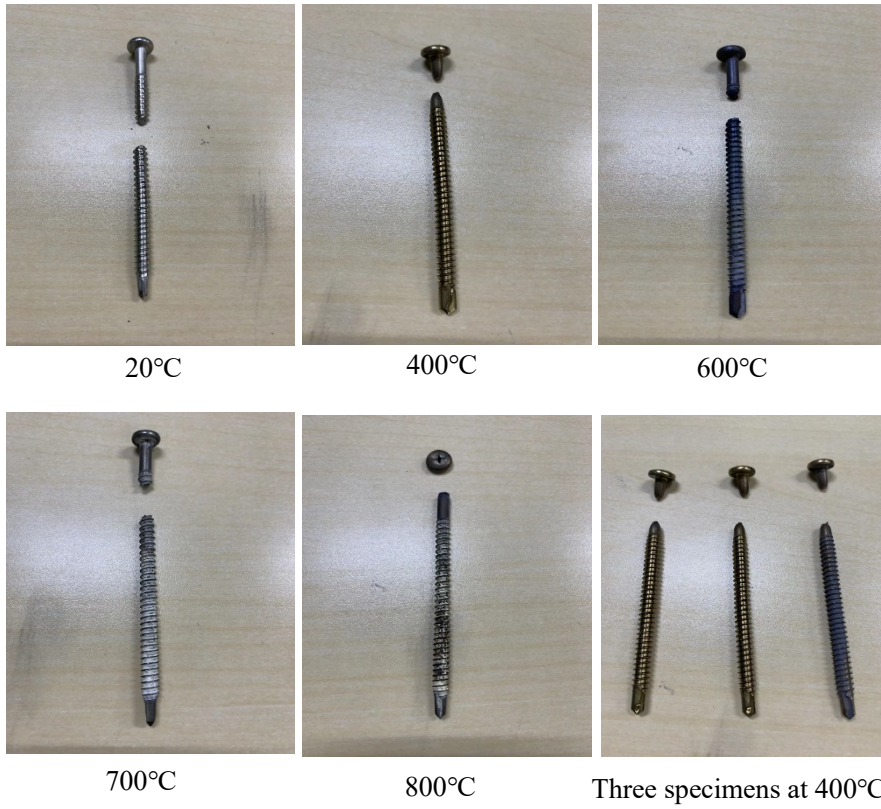
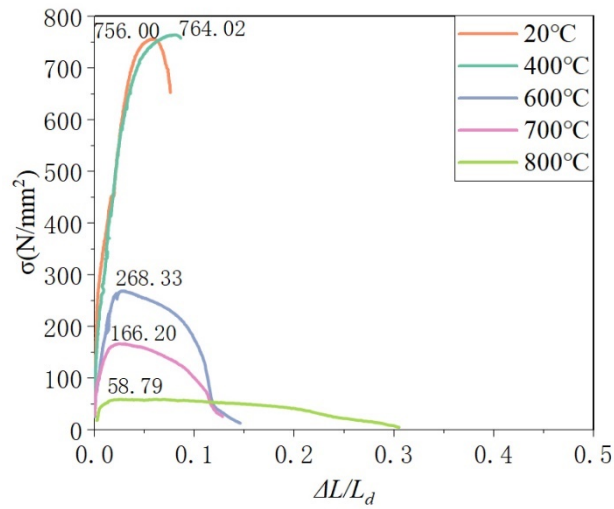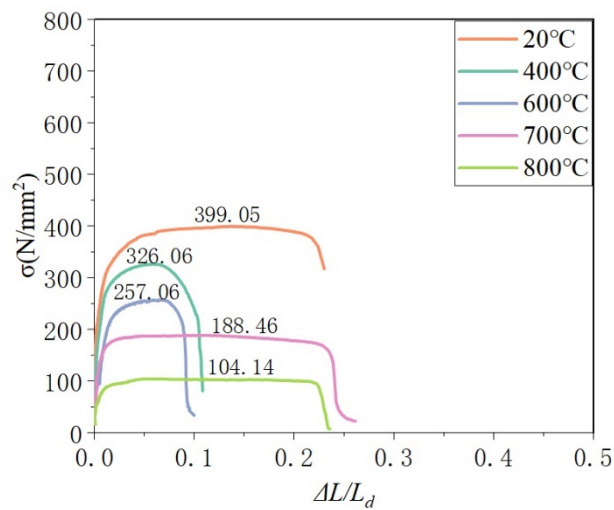(c) ASUS

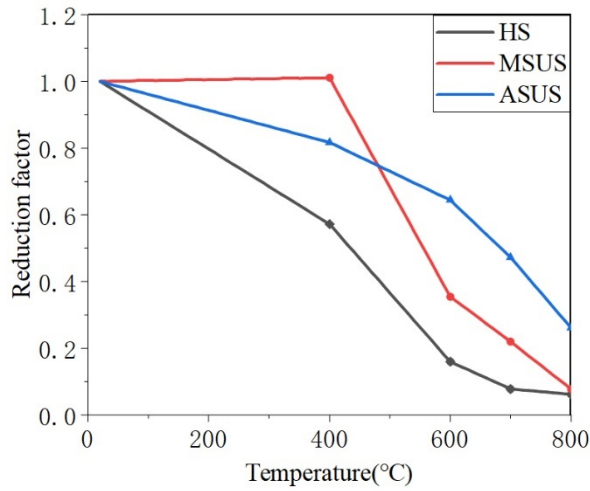Fig 2.4 Photographs of ASUS after tensile test (Connected)
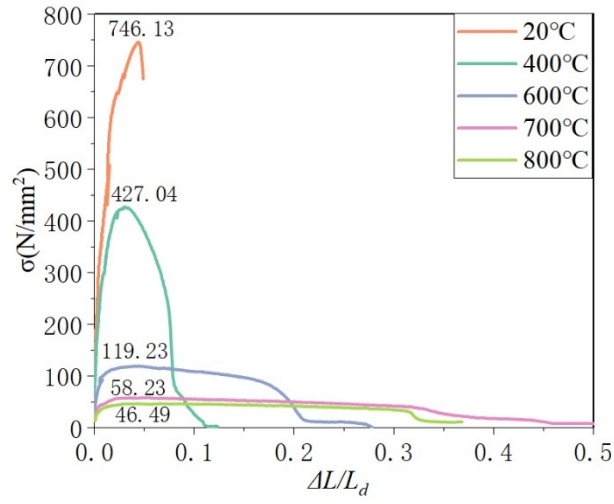
(a) HS



(b) MSUS


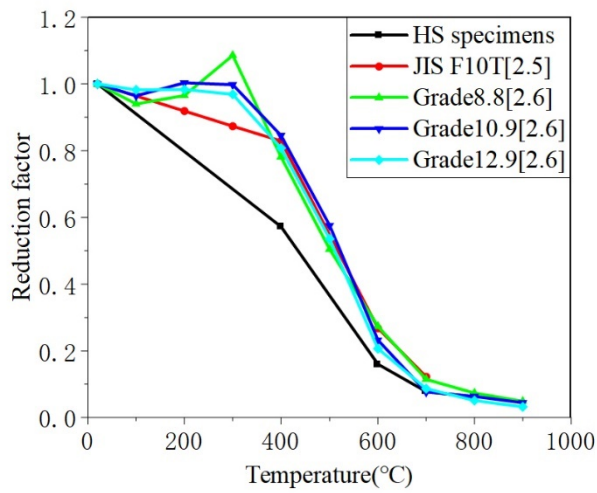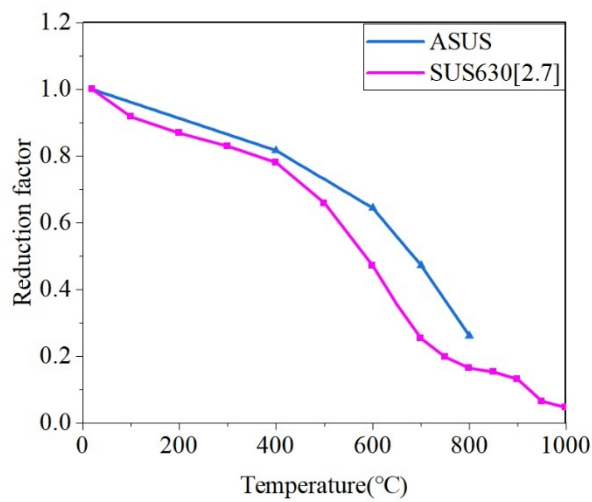
(c) ASUS

Fig 2.5 Experimental results of screw tensile tests

(a)Reduction factors of HS, MSUS and ASUS specimens



(b) Comparison results between the HS specimens and the past research



(c) Comparison results between the ASUS specimens and the past research

Fig 2.6 Reduction factors of tensile tests

## 2.3 Shear test of self-drilling screws at elevated temperatures
### 2.3.1 Overview of shear test for self-drilling screws at elevated temperatures

To examine the shear strength of the screw, double-shear testing jigs consisting of three steel plates were used (Fig 2.7(a)). The testing jigs possessed sufficient stiffness and strength compared to the screw. The two screws that were the same as the tensile test specimen were inserted into the upper holes (hole diameter: 6 mm) in the testing jig because the single shear test using the screw was unstable such that the testing jigs were easily rotated. However, the tests using the single-overlapped screwed connection are described later in this paper. To apply the shear force to the screw specimens, the three steel plates in the testing jig were tightly connected using four bolts at the lower part (Fig 2.7(a) and (d)), and the shear force, $P$, as shown in Fig 2.7(b), was applied to the top of the testing jig. The testing jig with two screw specimens was set in an electric furnace (Fig 2.7(a)) and heated to test temperatures from 400 to 800℃. The thermocouple was attached to the center hole in the testing jig (Fig 2.7(a)), and it was confirmed that the measured temperature reached the target temperature. After reaching the target temperature, the specimen was maintained for approximately 30 min at this temperature, after which the shear force, $P$, was applied. The deformation of the testing jig was measured using displacement meters set at both the upper and lower positions on the outside of the furnace (Fig 2.7(b) and (c)).
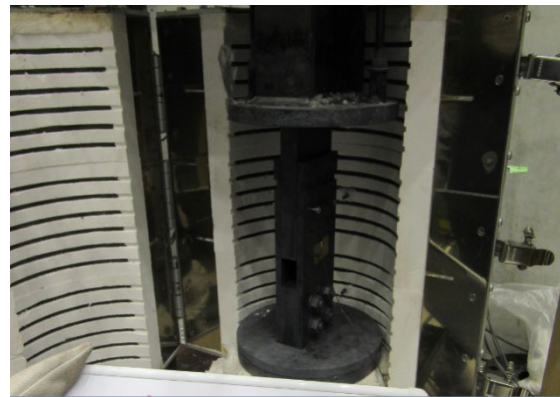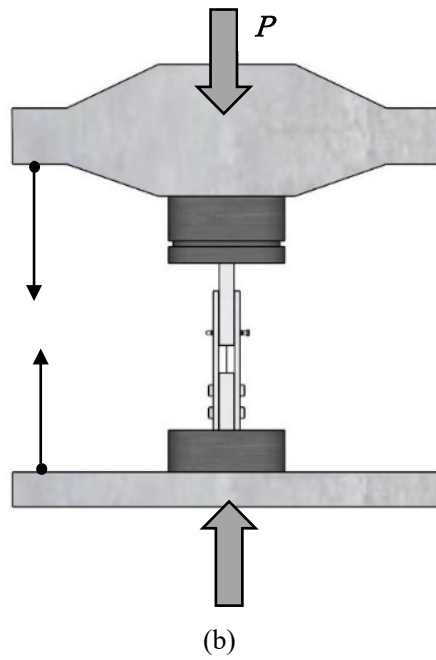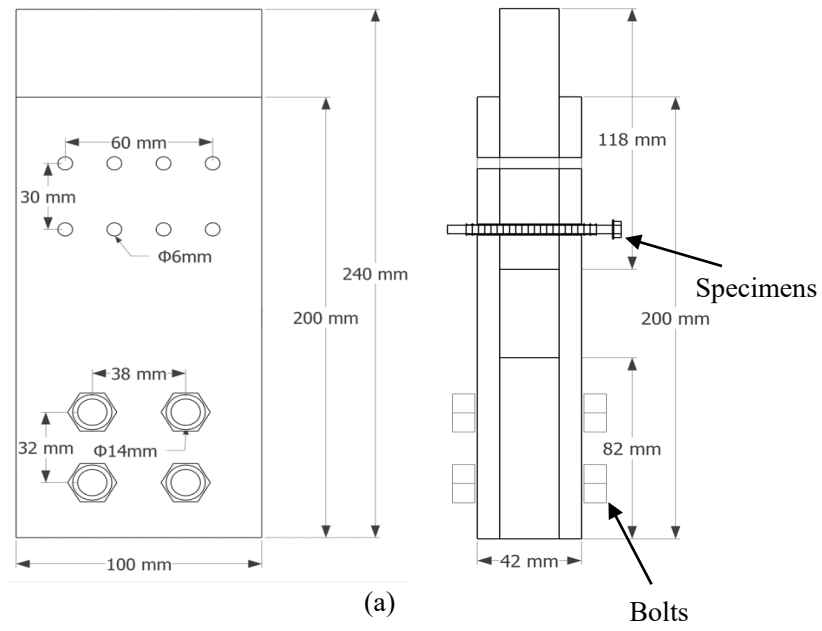
(a)

(b)

(c) Outside

(d) Inside

Fig 2.7 Testing jig for shear tests and test systems

**2.3.2 Experimental results of shear strength for self-drilling screws at elevated temperatures**

Fig 2.8 shows the relationship between the heating time and specimen temperature. In the case of the ASUS test at 400°C, the temperature slowly increased because the heat insulation treatments for the openings in the furnace were insufficient. However, it was considered that the long heating time under low temperatures below 400°C and the unloading condition at the heating time did not significantly affect the mechanical properties of the screw specimens. Fig 2.9 shows the shear test results for the HS, MSUS and ASUS specimens. The horizontal axis indicates the relative deformation, δ, measured by the displacement meters divided by the nominal screw diameter d = 5 mm. The vertical axis of Fig 2.9 indicates the nominal shear stress $\tau$, which was calculated by

$$\tau = P/(m \cdot n \cdot As) \tag{2.1}$$

where $m$ and $n$ are the numbers of the shear planes and screws ($m$ = 2 and $n$ = 2), respectively. Table 2.3 shows the test results of shear strength $\tau_s$ and the design shear strength (=$0.6\sigma_t$, see section 2.4) evaluated from the tensile strength $\sigma_t$ obtained from the tensile tests. As shown in Fig 2.9, the shear strength decreased with increasing temperature, and the screw specimens at elevated temperatures possessed a large deformation capacity in comparison with the ambient temperature. A stiffness-change point was observed in the test result curve from the start of loading to the shear strength. During the loading process up to this point, the test results included the bending deformation of the screw itself that occurred in the hole of the testing jig. The stiffness increased after exceeding that point because the shear deformation became dominant as the bent screw touched the side wall of the hole and was approximately under the sheared condition. Fig 2.10(a) – (c) shows photographs of the screw specimens after the shear tests. All the specimens were fractured in the shear failure mode at the double shear plane positions. It was understood that bending deformation remained in the screw specimen, as mentioned above.

Fig 2.11 shows the reduction factors for the shear strength obtained from the test results. The past test results on the shear strengths of the high-strength bolts by AIJ [2.5] and Yang et al. [2.8] and high-strength stainless steel bolts by AIJ [2.5] are shown in Fig 2.11, respectively. As shown in Fig 2.11, the HS screws possessed similar reduction factors to the past high-strength bolts for the shear strength. The ASUS screws possess 20% higher reduction factors above 600°C than the MSUS screws and high-strength stainless steel bolts (Fig 2.11(b)).

Table 2.3 Shear test results of screws

| Temperature(°C) | HS specimens | | MSUS specimens | | ASUS specimens | |
|---|---|---|---|---|---|---|
| | $\tau_s$ (N/mm$^2$) | $0.6\sigma_t$ (N/mm$^2$) | $\tau_s$ (N/mm$^2$) | $0.6\sigma_t$ (N/mm$^2$) | $\tau_s$ (N/mm$^2$) | $0.6\sigma_t$ (N/mm$^2$) |
| 20 | 397.2 | 447.7 | 439.0 | 453.6 | 343.9 | 239.5 |
| 400 | 280.5 | 256.2 | 425.8 | 458.4 | 235.0 | 195.7 |
| 600 | 97.3 | 71.5 | 164.7 | 161.0 | 144.5 | 154.3 |
| 700 | 48.4 | 34.9 | 88.8 | 99.7 | 130.2 | 113.1 |
| 800 | 40.8 | 27.9 | 38.0 | 35.3 | 81.7 | 62.5 |
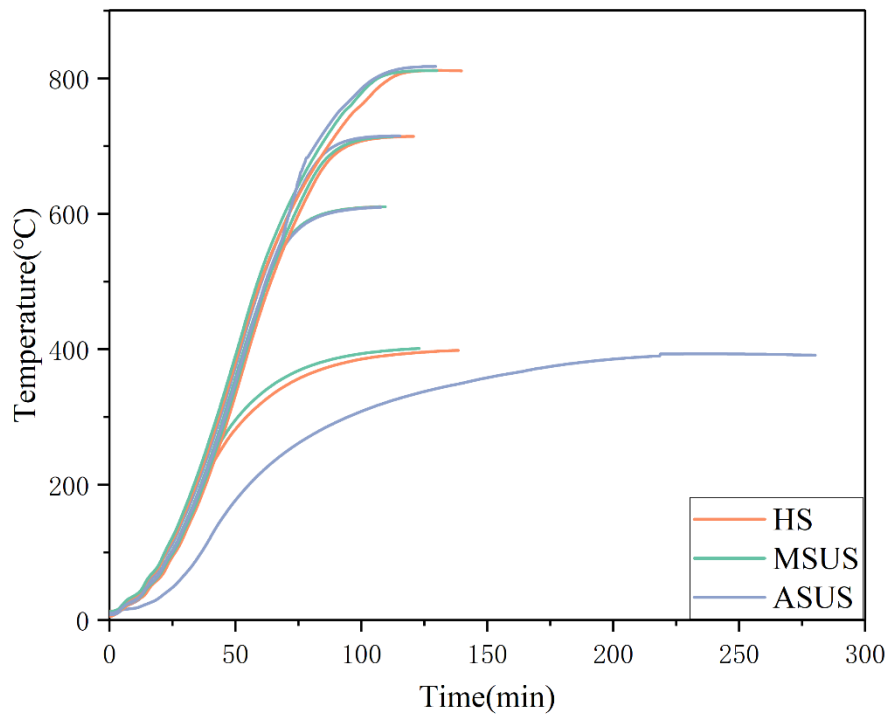


Fig 2.8 Relationships between time and specimen temperature for shear testes
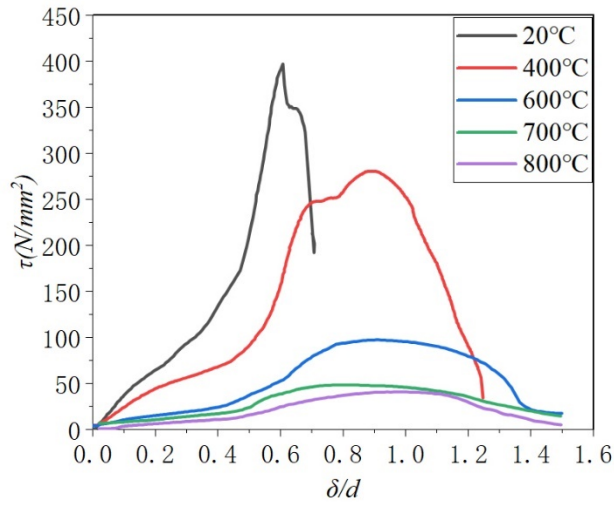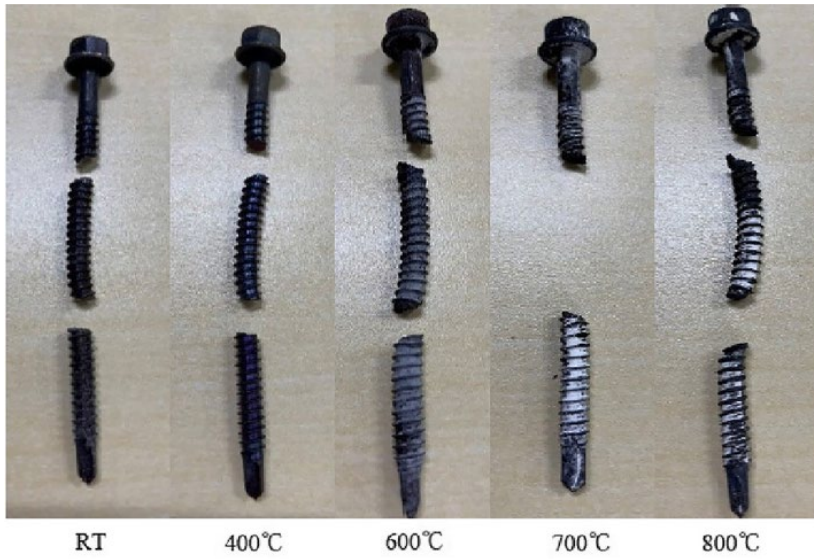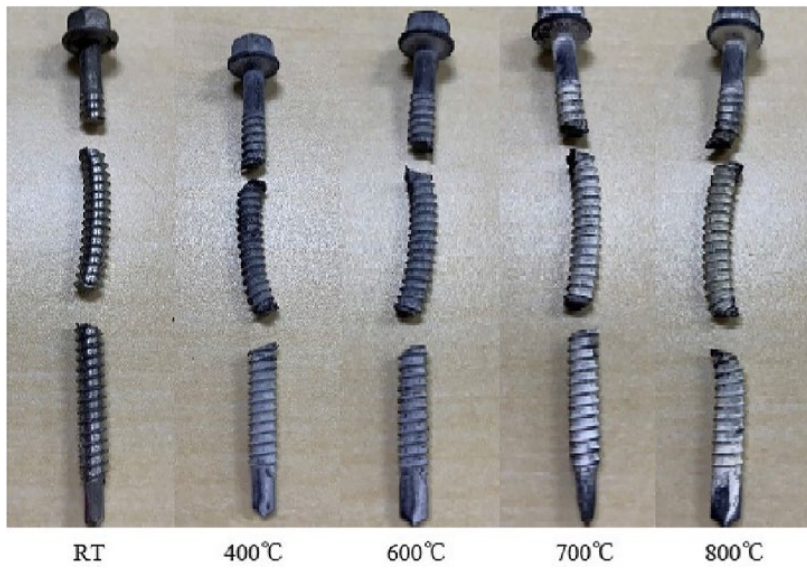
(a) HS
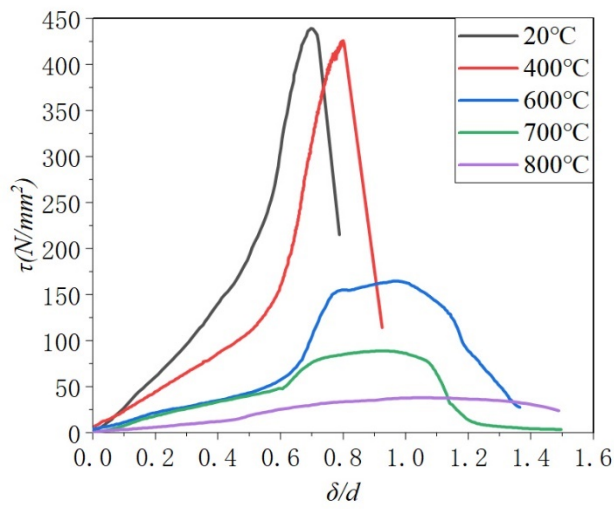


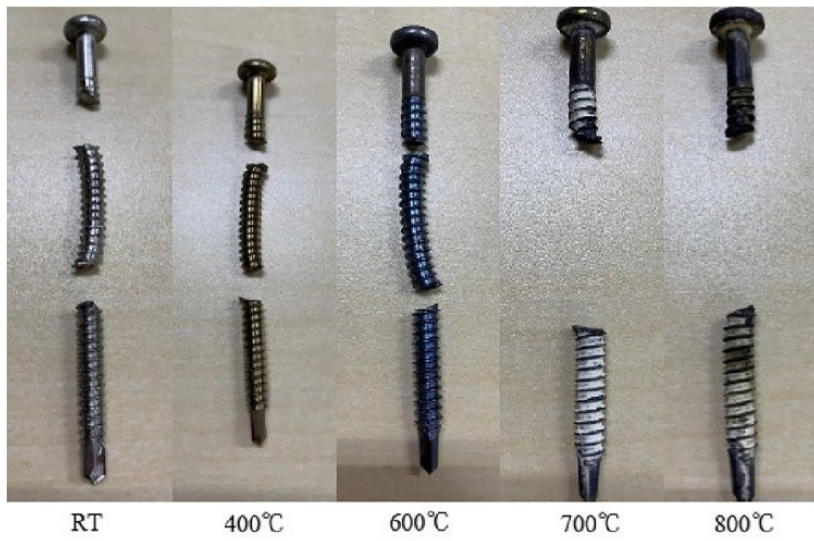(b) MSUS
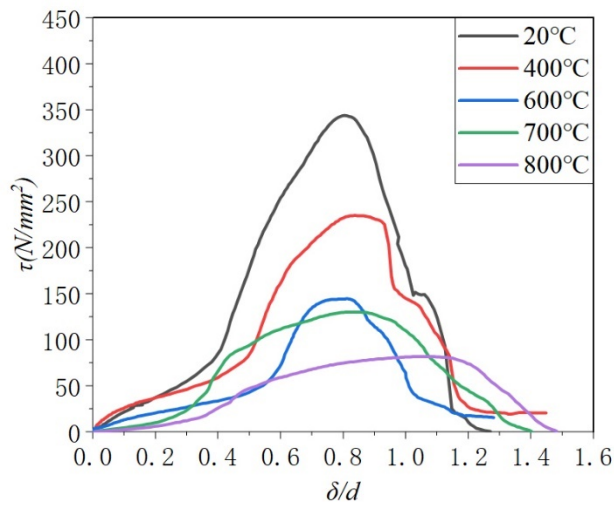


(c) ASUS

Fig 2.9 Experimental results of screw shear tests
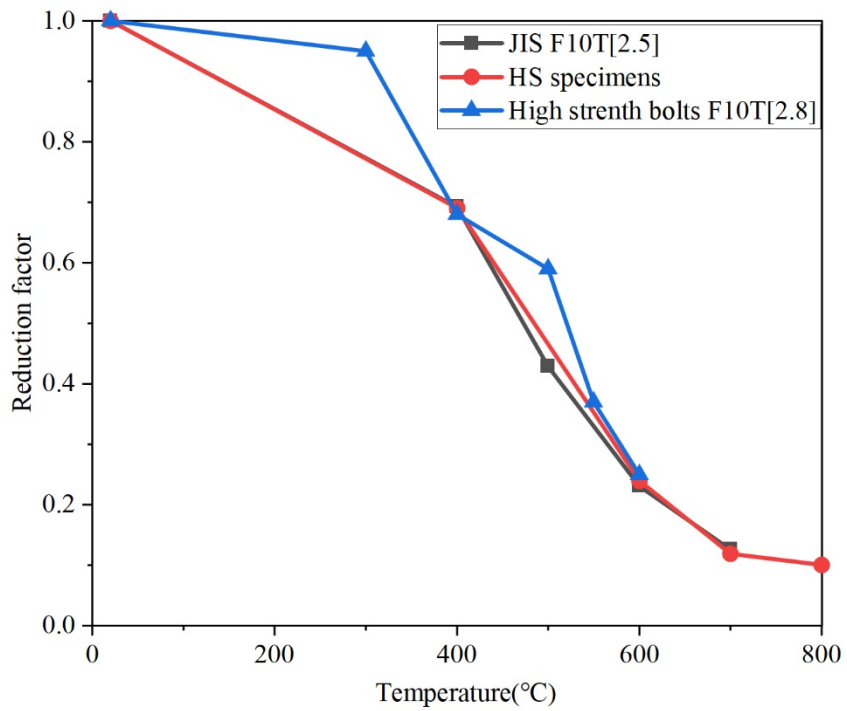
(a) HS specimens
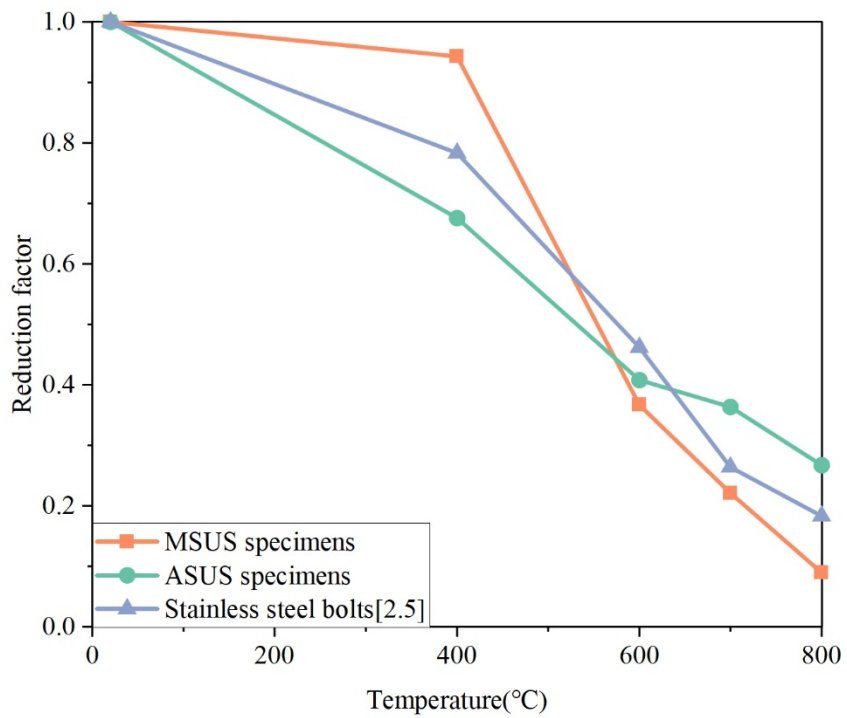


(b) MSUS specimens



(c) ASUS specimens

Fig 2.10 Photographs for test specimens after shear tests

(a) HS specimens



(b) MSUS and ASUS specimens

Fig 2.11 Comparison results between screw specimens and the past researches for shear strength

## 2.4 Comparison of tensile and shear test results for the screw specimen at elevated temperatures

Both the tensile and shear tests for the same steel rot screw specimens were conducted in this study, allowing for a discussion of the relationship between the tensile and shear strength relationships for the drilling screw at elevated temperatures. Fig 2.12 shows the tensile reduction factor, $\kappa_t$, and the shear reduction factor, $\kappa_s$, for the three types of specimens. As shown in Fig 2.12(b), the MSUS specimens possessed the same reduction factors for the tensile and shear strengths at elevated temperatures. For the HS specimen (Fig 2.12(a)), the reduction factor on the shear strength, $\kappa_s$, was higher than that on the tensile strength, $\kappa_t$, whereas the ASUS specimens had the opposite results (Fig 2.12(c)). Fig 2.13 shows the strength ratio, $k$, of the shear strength, $\tau_s$, to the tensile strength, $\sigma_t$, at the same temperature, which is denoted by Eq. (2.2):

$$k = \tau_s / \sigma_t \qquad\qquad (2.2)$$

At the ambient temperature, the strength ratio, $k$, of the HS screw was 0.58, which was similar to the value evaluated from the high-strength bolt $\tau_s = 0.6\sigma_t$ at the ambient temperature (AIJ) [2.6]. The variation tendency of $k$ at elevated temperatures is related to the relative relationship between $\kappa_t$ and $\kappa_s$, as shown in Fig 2.12. That is, the MSUS screws possessed almost the same reduction factors, $\kappa_t$ and $\kappa_s$ (Fig 2.12(b)), resulting in constant values of k ≒ 0.6 at elevated temperatures (Fig 2.13). The HS screws possessed a larger shear reduction factor, $\kappa_s$, than the tensile reduction factor, $\kappa_t$ (Fig 2.12(a)), resulting in an increase in k at elevated temperatures. In contrast, the values of $k$ for the ASUS screws decreased from the ambient temperature to 600°C, because the gaps between $\kappa_t$ and $\kappa_s$ gradually increased (Fig 2.12(c)). Furthermore, the latter gaps decreased above 600°C, resulting in an increase in $k$. Regarding the test results at ambient temperature, the value of $k$ for the ASUS screw was larger than that of the HS and MSUS screws (Fig 2.13). This is because the ASUS screw in the tensile test possessed a larger deformation capacity ($\Delta L/L_d = 0.2$), as shown in Fig 2.5(c). In this case, the effect of the tensile stress on the stress component on the shear plane of the screw under the shear test increased with the increasing deformation capacity of the screw. That is, the tensile stress gradually became dominant instead of the shear stress by delaying the shear fracture with increasing deformation capacity, and the shear force, $P$, at the shear test increased by adding the above tensile stress. For this reason, it was considered that the strength ratio, of the ASUS screw at ambient temperature became larger than that of the HS and MSUS screws. However, as shown in the tensile test results on the HS screw (Fig 2.5(a)), the deformation capacity increased at elevated temperatures, resulting in a large value of the strength ratio, $k$. Furthermore, the deformation capacities of the ASUS screws in the tensile test gradually decreased from the ambient temperature to 600°C and increased when the temperature increased to over 600°C(Fig 2.5(c)), resulting in a corresponding behaviour of the strength ratio, $k$ (Fig 2.13).
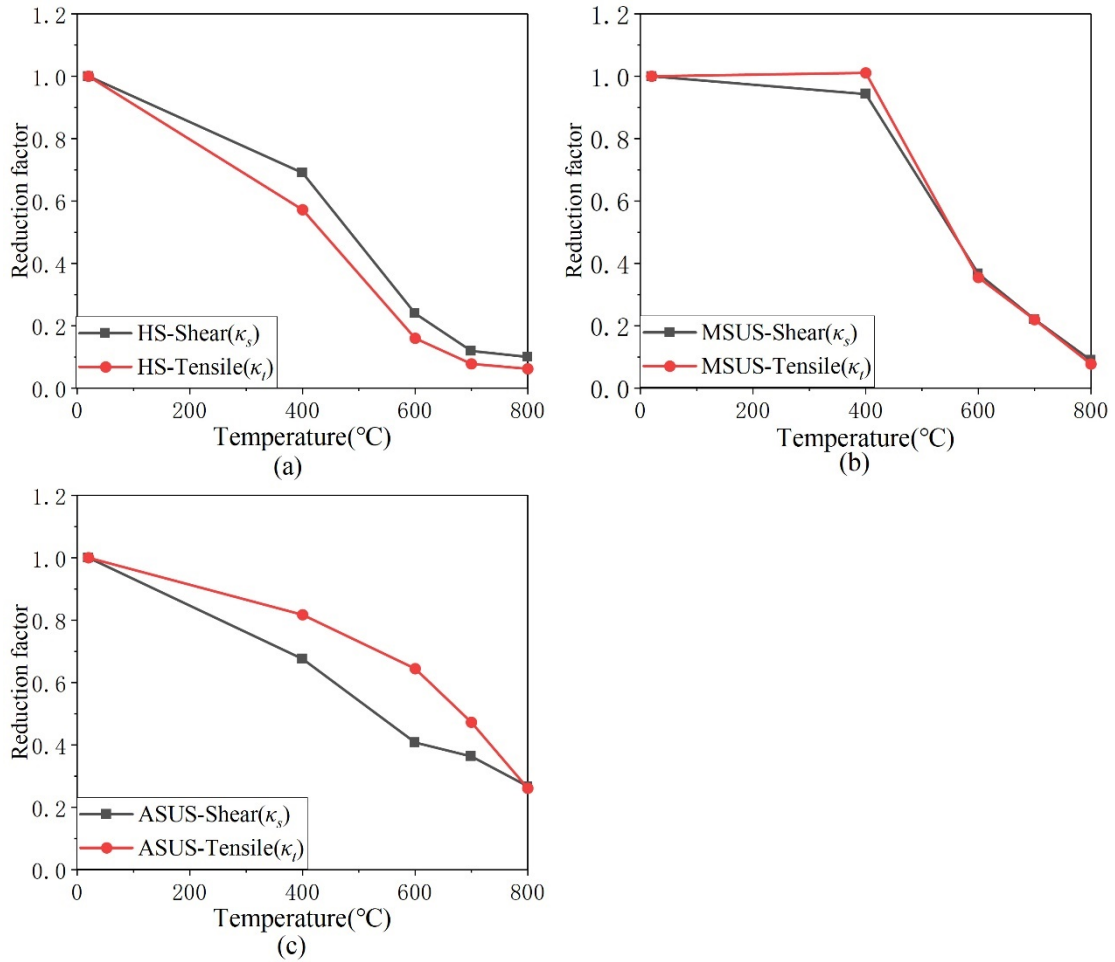
Fig 2.12 Reduction factors of screw specimens at elevated temperatures
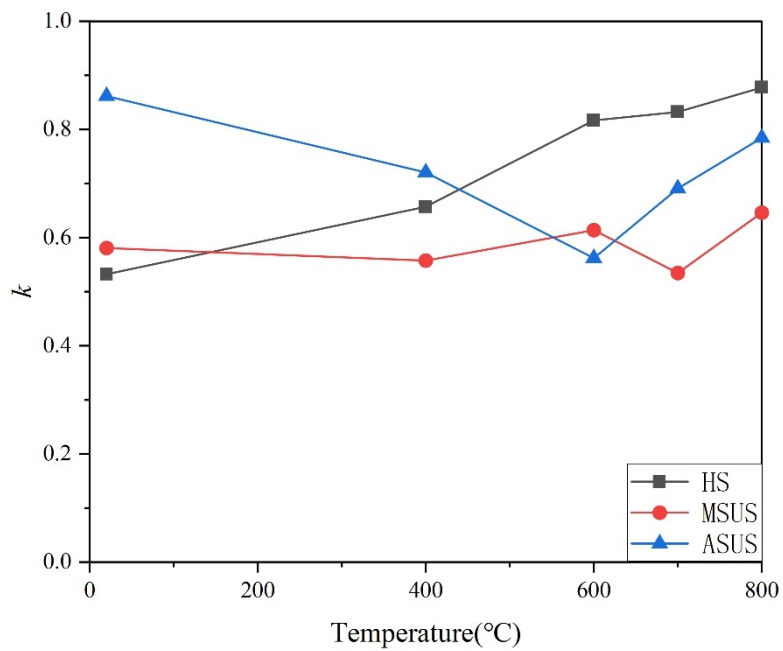


Fig 2.13 Strength ratios $k$ of shear to tensile strength

## 2.5 Conclusions

Tensile and shear tests were conducted on three types of self-drilling screws (nominal diameter: 5 mm, steel grade: HS, MSUS and ASUS) at elevated temperatures. The summary is as follows:

(1) To obtain basic information on the tensile strength of the self-drilling screw, tensile tests were conducted at elevated temperatures. The HS screw possessed a higher tensile strength at the ambient temperature, with a larger reduction factor at the elevated temperature than the high-strength bolts (JIS F10 T and Grade 8.8–12.9) reported in previous studies. The MSUS screw manufactured from high-strength stainless steel, which mostly has the same tensile strength at the ambient temperature as the HS screw, possessed a higher tensile strength than the HS screw up to 700℃, whereas both screws possessed a similar tensile strength at 800℃. The ASUS screw possessed the lowest tensile strength at ambient temperatures; however, the highest tensile strength was above 700℃ because of the nickel and chromium alloys in the austenitic stainless steel, which increase the strength at elevated temperatures.

(2) Shear tests of the self-drilling screw at elevated temperatures were conducted. The HS screws exhibited a reduction factor on the shear strength at elevated temperatures above 600℃ similar to those of the high-strength bolts (JIS F10 T) reported in previous studies. The MSUS screws possessed higher shear strength at elevated temperatures than the HS screws. The ASUS screws possessed the highest shear strength at elevated temperatures above 700℃, although they had the lowest shear strength at ambient temperature. Furthermore, according to the test results of both the tensile and shear tests using the above three types of drilling screws, the strength ratio of the shear to tensile strength at each elevated temperature was clarified.

**References:**

[2.1] KUROSAWA Miku, KISHIKI Shoichi, 2022. "Ultimate Strength of Screw Joint for Exterior Wall of Metal Panel", Summaries of technical papers of annual meeting, Architectural Institute of Japan, No.22442, pp. 883-884. (in Japanese).

[2.2] Jun Zhao, Zhuang Wang, Feng Qian, Yang Peng, Jun Dong, 2022. Finite element analysis of the shear capacity of stainless-steel screw connections, Structures, Vol.41, ISSN 2352-0124, pp.957-968.

[2.3] Fuminobu OZAKI, Ying LIU, Ye, Kai, Tensile and shear strength for a self-drilling screw and transition of failure modes and shear-strengths for self-drilling screwed connections at elevated-temperatures, Journal of Structural Fire Engineering, Vol. 13 No. 3, pp. 321-346. https://doi.org/10.1108/JSFE-10-2021-0063

[2.4] Fushimi, M., Keira, K. and Chikaraishi, H. (1995), "Development of fire-resistant steel frame building structures", Nippon Steel Technical Report, No. 66, pp. 29-36.

[2.5] Architectural Institute of Japan (AIJ) (2017), AIJ Guide Book for Fire-Resistive Performance of Structural Materials, Maruzen Publishing Co., Tokyo (in Japanese).

[2.6] Pang, X.-P., Hu, Y., Tang, S.-L., Xiang, Z., Wu, G., Xu, T. and Wang, X.-Q. (2019), "Physical properties of high-strength bolt material at elevated temperatures", Results in Physics, Vol. 13, 102156.

[2.7] Yoshifumi Sakumoto, Fukujiro Furumura, Takeo Ave. Mechanical Properties of High-Strength Stainless Bolts at High Temperatures. Journal of Structural Engineering, Architectural Institute of Japan, Vol.39B, pp405-413, 1993.03.

[2.8] Yang, K.C., Hsu, R.J. and Chen, Y.J. (2011), "Shear strength of high-strength bolts at elevated temperature", Construction and Building Materials, Vol. 25, pp. 3656-3660.

[2.9] Architectural Institute of Japan (AIJ) (2012), AIJ Recommendation for Design of Connections in Steel Structures, Maruzen Publishing Co., Tokyo (in Japanese).

# Chapter 3 Tensile tests for screwed connections at elevated temperatures

## 3.1 Introduction

In Chapter 3, tensile tests for single overlapped screwed connections at elevated temperatures were conducted. This chapter examined the transition of the failure modes between the ambient and elevated temperatures by tensile loading for two screwed-connection specimens and eight screwed-connection specimens, which are made of two thin steel sheets with a thickness of 1.6 mm and a width of 120 mm, connected by 2 and 8 self-drilling screws respectively. Moreover, sheet bearing failure mode and screw shear failure mode were observed after tensile tests at elevated temperatures. Equations for the screw connection strength corresponding to each failure mode at elevated temperatures was proposed, referring to the design codes EN 1993-1-3(EC3) [3.1] and AISI S100 [3.2] at ambient temperatures.

## 3.2 Current design rules of screwed connections for cold-formed steel structures

The current design rules of cold-formed steel screwed connections in the North American Specification [3.2] and EC3 [3.1] are categorized by different types of failure modes.

### 3.2.1 The design rules in the North American Specification (AISI)

In 1993, the AISI design guidelines for screw connections were created [3.3]. Pekoz [3.4] provides an overview of the background data regarding the AISI design criteria. The AISI stipulates that the distance between the centers of screws shall not be less than $3d$ ($p_1, p_2 \geqslant 3$d) and the distance from the center of a screw to the edge of any part shall not be less than 1.5$d$ ($e_1, e_2 \geqslant 1.5d$), as shown in the Fig 3.1. AISI presents several types of screw connection failure modes in shear:

(a) Sheet longitudinal shear failure (Type 1)

Sheet longitudinal shear failure, also known as connection shear limited by end distance, occurs when the parallel length extended from the screw hole along the direction of the applied load to the end of the plate is insufficient, as shown in Fig 3.2(a). The nominal sheet longitudinal shear strength per screw, $P_{ns}$, specified in the AISI S100 [3.2] is given as follows,

$$P_{ns} = F_u te \tag{3.1}$$

where $e$ is the distance measured in the line of the applied force from the center of the screw hole to the nearest end of the connected part, and t is the thickness of the part in which the end distance is measured.

(b) Sheet bearing failure (Type 2)

Sheet bearing failure with screw tilting is defined in the AISI S100 as the failure of connection shear limited by tilting and bearing, as shown in Fig 3.2(b).

The nominal shear strength per screw in the case of $t_2/t_1 \leqslant 1.0$ shall be taken as the

smallest value obtained from the following design equations:

$$P_{ns} = 4.2(t_2^3 d)^{1/2} F_{u2} \tag{3.2}$$

$$P_{ns} = 2.7t_1 d F_{u1} \tag{3.3}$$

$$P_{ns} = 2.7t_2 d F_{u2} \tag{3.4}$$

where $t_1$ is the thickness of member in contact with screw head; $t_2$ is the thickness of member not in contact with screw head; $F_{u1}$ is the tensile strength of member in contact with screw head; $F_{u2}$ is the tensile strength of member not in contact with screw head; and 2.7 is the bearing factor.

The nominal shear strength per screw for the case of $t_2/t_1 \geqslant 2.5$ can be found using the smaller value of the following formulae,

$$P_{ns} = 2.7t_1 d F_{u1} \tag{3.5}$$

$$P_{ns} = 2.7t_2 d F_{u2} \tag{3.6}$$

For the case of $1.0 < t_2/t_1 < 2.5$, $P_{ns}$ shall be calculated by linear interpolation between the aforementioned two situations.

(c) Sheet net-section failure (Type 3)

The nominal tensile strength of the net section for a single screw or a single row of screws perpendicular to the force is provided as follows, as shown in Fig 3.2(c),

$$F_t = (2.5d/s)A_n F_u \leq A_n F_u \tag{3.7}$$

The nominal tensile strength of the net section for several screws in the line parallel to the force is provided as follows:

$$F_t = A_n F_u \tag{3.8}$$

where $d$ is the nominal screw diameter; $s$ is the sheet width divided by number of screw holes in cross section being analyzed; $A_n$ is the net area of connected part; and $F_u$ is the tensile strength of connected part being analyzed.

(d) Screw shear failure (Type 4)

The screw shear failure is due to the deficiency of the strength or quality of the screws, as shown in Fig 3.2(d). The nominal shear strength ($P_{ss}$) of screw can be determined either by the manufacturer report or by testing as specified in the AISI S100.

### 3.2.2 The design rules in the Eurocode 3 (EC3)

(a) Sheet longitudinal shear failure (Type 1)

The limited end distances in EC3 are identical to AISI. However, the nominal sheet longitudinal shear strength did not be given in EC3.

(b) Sheet bearing failure (Type 2)

In EC3, the nominal shear strength per screw for tilting and bearing failure of thin sheet steel screwed connections is given as follows,

$$P_{ns} = \alpha d t F_u \tag{3.9}$$

in which, if $t_2/t_1 = 1.0$, $\alpha = 3.2\sqrt{t/d} \leq 2.1$; if $t_2/t_1 \geq 2.5$ and $t_1 < 1.0mm$, $\alpha = 3.2\sqrt{t/d} \leq 2.1$;

if $t_2/t_1 \geq 2.5$ and $t_1 \geq 1.0mm$, $\alpha = 2.1$; otherwise, if $1.0 < t_2/t_1 < 2.5$, then obtain $\alpha$ by linear interpolation.

(c) Sheet net-section failure (Type 3)

The nominal tensile strength of the net section of screwed connections of thin sheet steels is directly calculated by the EC3 using Eq. (3).

$$F_t = A_n F_u \qquad (3.10)$$

(d) Screw shear failure (Type 4)

The nominal shear strength of screw in the EC3 requires by testing, and should be at least 20% higher than $P_{ns}$ and the nominal tensile strength ($F_t$) of the net section of the screwed connection.
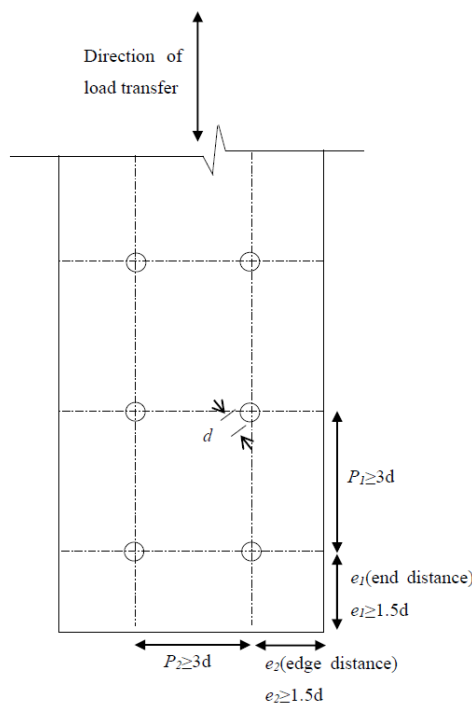


Fig 3.1 Details of end distance $e_1$, edge distance $e_2$, and spacings for connection specimen from EN 1993-1-3 (2006)
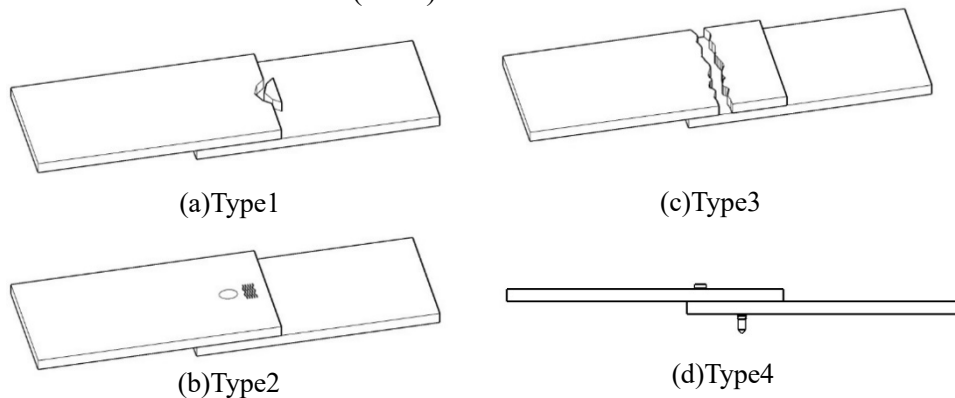


(a)Type1

(c)Type3

(b)Type2

(d)Type4

Fig 3.2 Failure modes of screwed connections

## 3.3 Tensile tests of screwed connections at elevated temperatures

### 3.3.1 Test specimens

Tensile tests using single overlapped screwed connection specimens were conducted to examine the load-bearing capacity of screwed connections at elevated temperatures. In particular, these tests focused on the shear failure mode of screws arranged in the screwed connection and the transition phenomenon of the failure modes between the ambient and elevated temperatures for the screwed connection at the same specification. Screws with the same chemical components as the HS specimens were used for the connection tests (Fig 3.3). The single overlapped connection specimen consisted of two steel sheets (both having a thickness 1.6 mm and steel grade JIS SS400) and HS screws (nominal diameter: 5 mm; length under the head position of the screw: 13 mm). Fig 3.4 shows the details of the screwed connection specimen, in which the edge and end distance were designed to adhere to the EC3/AISI S100 requirements [3.1-3.2]. In total, two types of specimens were used in this study. The number of HS screws in the connection was different between these specimens, which were two and eight, respectively (Fig 3.4(b)). The two screwed connection specimens were used to examine the shear strength of the screws in the steel sheet connections and were designed such that the steel sheet possessed sufficient strength in comparison with the shear strength of two screws at both ambient and elevated temperatures. A total of eight screwed specimens with a higher shear strength of screws were used to examine the possibility of a change in failure modes (screw shear failure or steel sheet failure) between the ambient and elevated temperatures. Table 3.1 shows the lists of the screwed connection specimens. For the screwed connection specimens, the end distance, $e_1$, from the center of the screw hole to the end line of the steel sheet was 20 mm (two screwed-connection) and 13mm (eight screwed-connection), which was more than 1.5 times the nominal screw diameter (d=5 mm) and designed to adhere to the EN 1993-1-3/AISI S100 requirements [3.1-3.2] for end distance ($e_1 \geq 1.5$d), to prevent steel sheet failure ahead of the screw failure. According to EN 1993-1-3/AISI S100 requirements [3.1-3.2], the end distance ($e_1$) (Fig 3.1) refers to the edge that is oriented in the same direction as the axial force. According to the specifications, the distance between the centers of screws must be less than 3d, and the distance from the center of a screw to the edge of the steel sheet must be at least 1.5d ($p_1, p_2 \geq 3$d, $e_2 \geq 1.5$d), as shown in Fig 3.1.

Fig 3.3 HS specimens

Table 3.1 Details of screwed connection specimens

|  | Screw type | Steel sheet | Connection |
|---|---|---|---|
| Screwed connection | HS specimen Diameter: 5 mm | JIS SS400 Thickness:1.6 mm Number of sheets: 2 | Single one lapped connection Pitch length between screws: 40 and 20 mm Edge distance: $e_1$=20 and $e_1$=13 mm |
|  | Length under screw head position: 13 mm Number of screws: $n$=2 and $n$=8 |  |  |
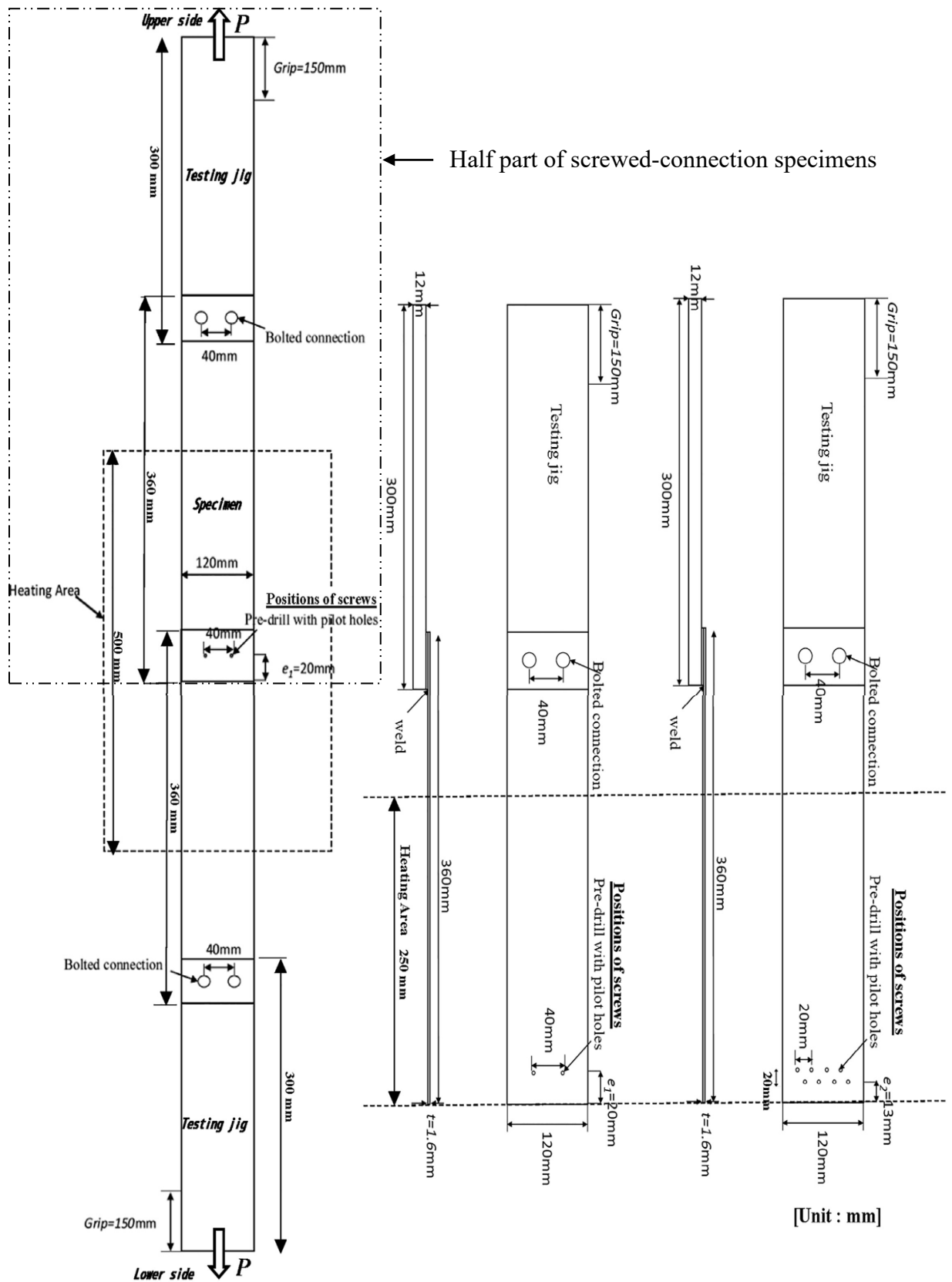
(a) Overview of two screwed-connection  (b) Half part of screwed-connection specimens

Fig 3.4 Details of screwed-connection specimens

### 3.3.2 Test details

To apply the shear force to the screwed connection specimen in the electric furnace, steel plate jigs were used (Fig 3.5(a)). Both the steel plate jigs and screwed connection specimens were connected by bolts, and shear force, $P$, for the screwed connection was applied at both the top and bottom of the steel plate jigs. To prevent bearing failure of the steel sheet around the bolted holes at the part connected with the steel plate jig, cover steel sheets (thickness: 1.6 mm) were welded at the end of the connection part. Pilot holes of 1 mm in the screwed connection part were made to shoot the screws at the correct positions. The steel plate jigs and screwed connection specimens were set to the loading test machine (Fig 3.5(a)). The test temperatures of the screwed connection specimen were obtained at the ambient temperature and temperatures of 400, 600, 700 and 800℃. A thermocouple was attached to the steel sheet close to the screws. To measure the displacement in the axial direction of the specimen, the steel displacement jigs were attached to both the upper and lower steel plate jigs, and the displacement meters were set at the end of the steel bars outside the furnace. After the specimen temperature reached the target test temperature, the specimen was held for approximately 30 min in an electric furnace, and the tensile force, $P$, was applied to the screwed connection.
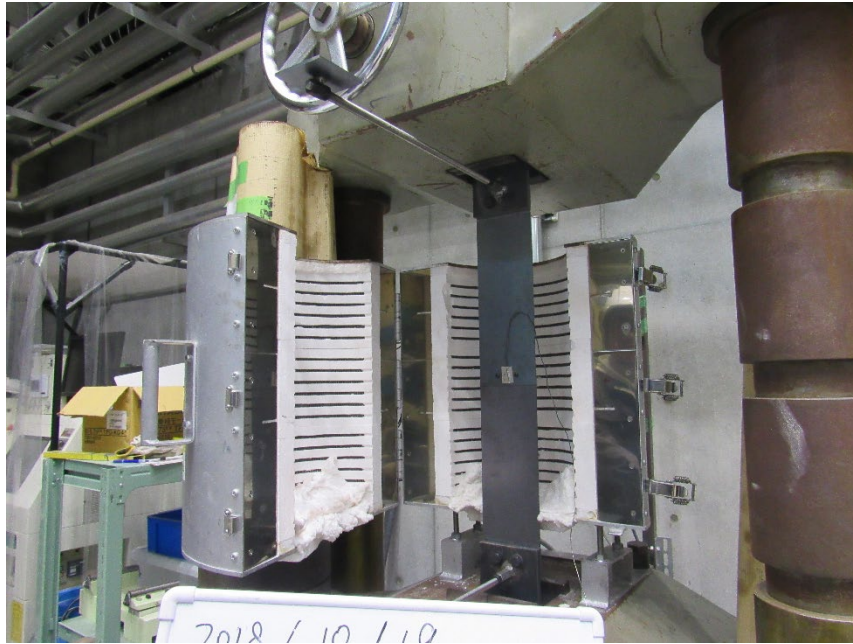
(a) Test jig in the furnace
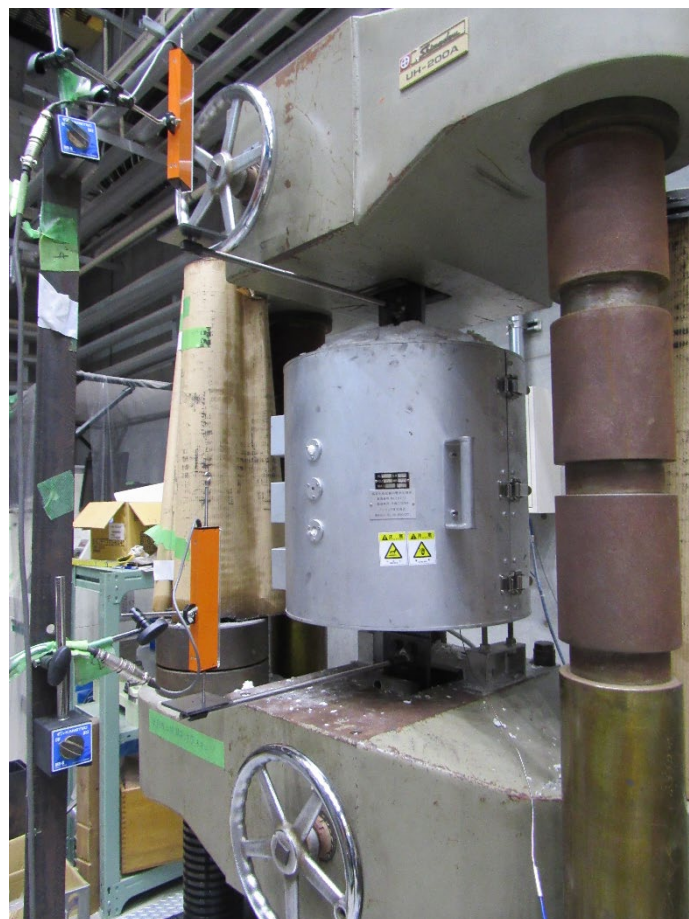

(b) Test jig outside the furnace
Fig 3.5 Photographs for setting up the test jigs

## 3.4 Experimental results of screwed connections at elevated temperatures

### 3.4.1 Two-screwed connections

Fig 3.6 shows the relationship between the heating time and specimen temperature. Fig 3.7 shows the relationship between the deformation and tensile forces for the two screwed-connection specimens. Table 3.2 shows the test results on the maximum load obtained from the shear tests of screwed connections. In Table 3.2, the maximum load calculated from the shear strength of screws in the connection (Type 4) was shown, respectively. Fig 3.8 shows photographs of the specimens after the tests. Screw shear failure was observed in both the ambient and elevated temperature tests (Fig 3.8). Other failures (sheet longitudinal shear failure and sheet-bearing failure) around the holes of the steel sheets were not observed. As shown in Fig 3.7, the strength of the connection decreased with increasing temperature; in particular, for the specimen above 600℃, the shear force after the tensile strength gradually decreased because of the large deformation capacity of the screw (Fig 2.5(a)). Furthermore, the experimental results of the two-screw connection specimens at elevated temperatures, which exhibited screw shear failure modes, were compared to the shear test results for HS screws presented in Chapter 2, as shown in Fig 3.9. The comparison revealed a close consistency between the two sets of results, indicating that the screw length did not have a significant impact on the outcomes of the experiments.
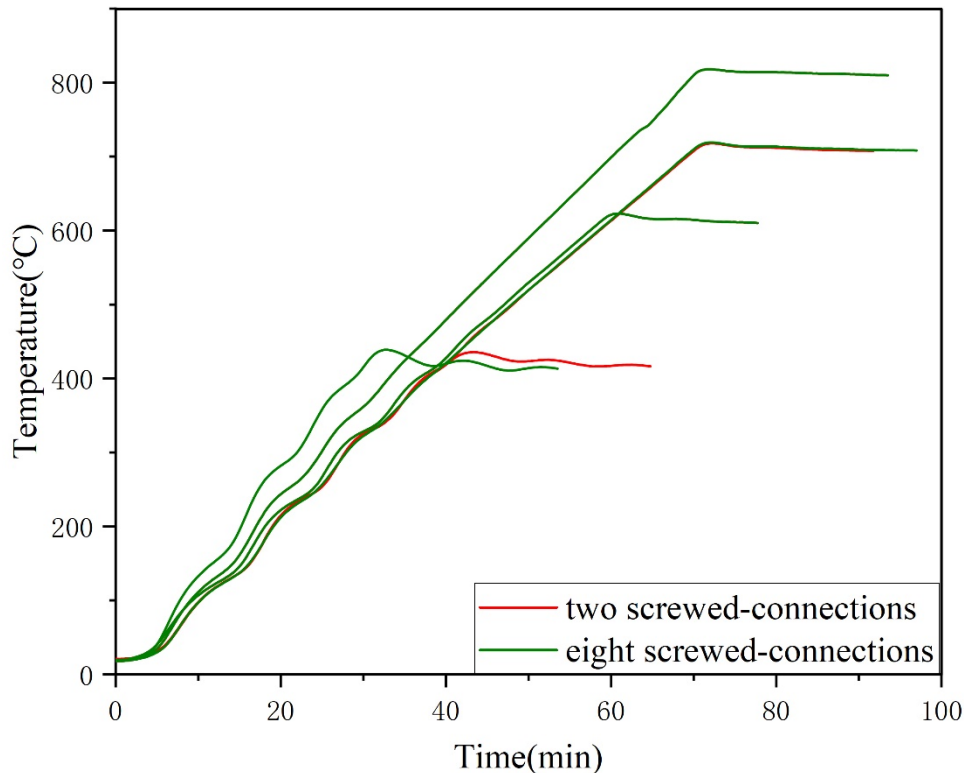


Fig 3.6 Relationship between time and temperature at screwed connection tests
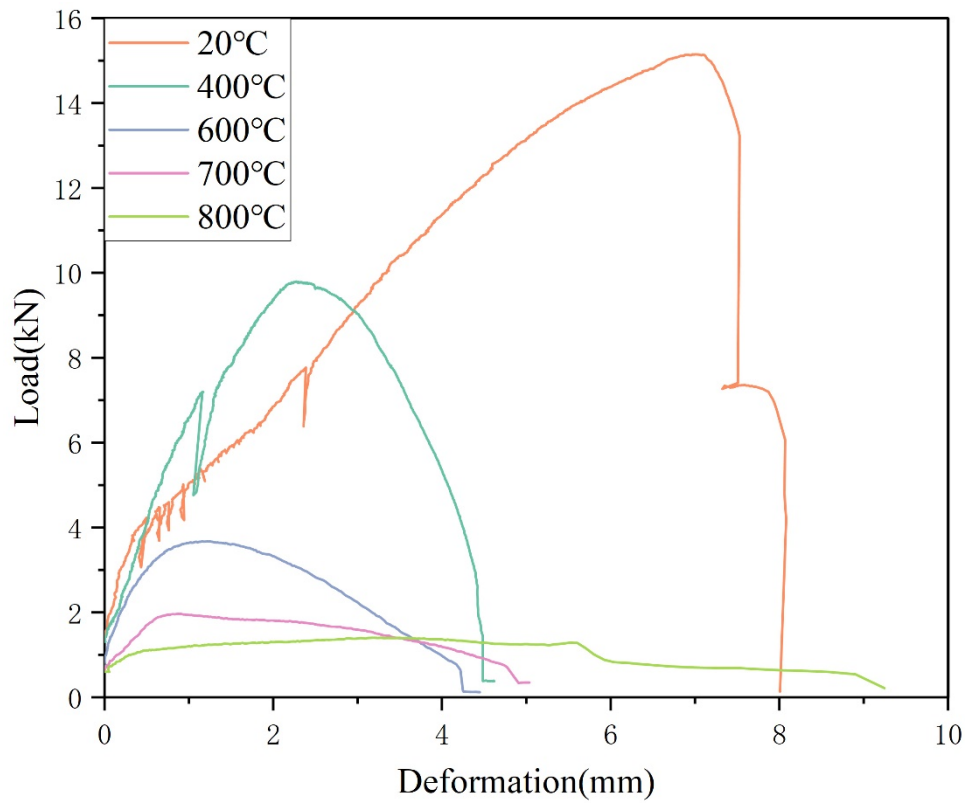
Fig 3.7 Relationships between load and deformation for two-screwed connections



RT
screw shear failure (Type4)



400°C
screw shear failure (Type4)



600°C
screw shear failure (Type4)



700°C
screw shear failure (Type4)



800°C
screw shear failure (Type4)
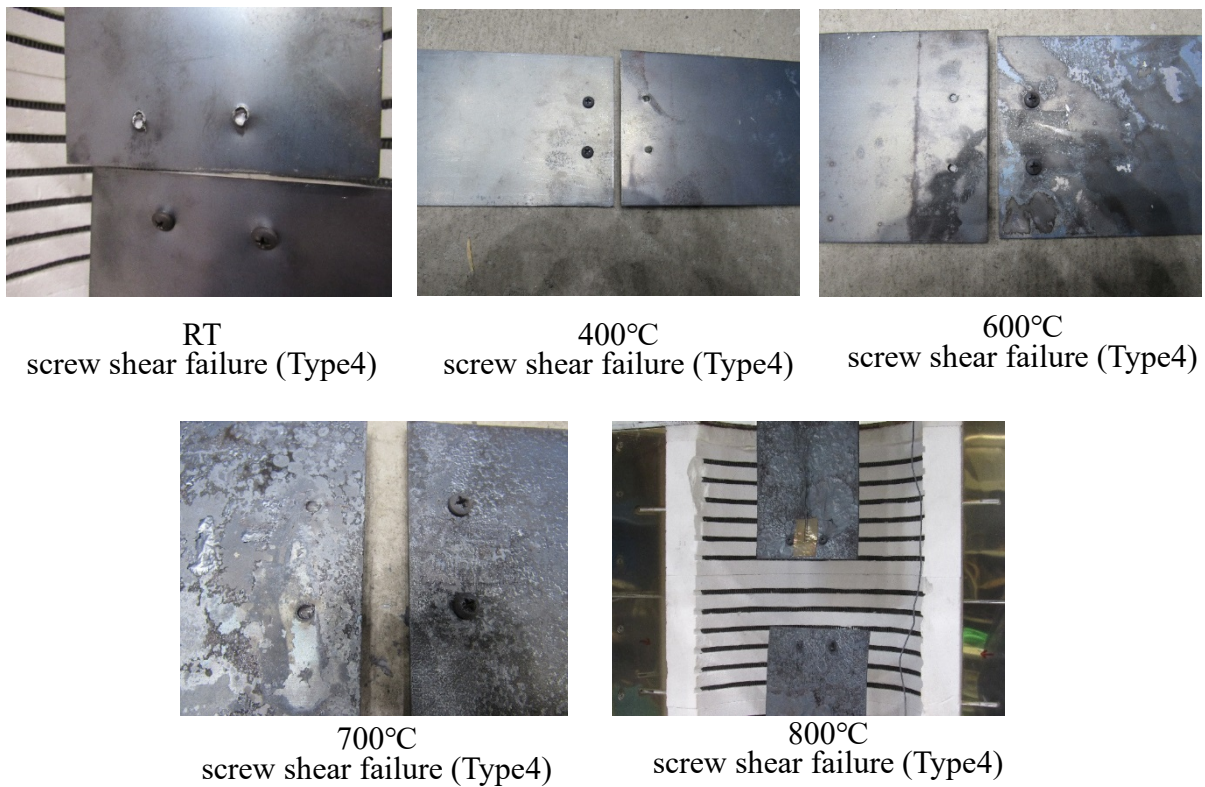
Fig 3.8 Two-screwed connection specimens after tests
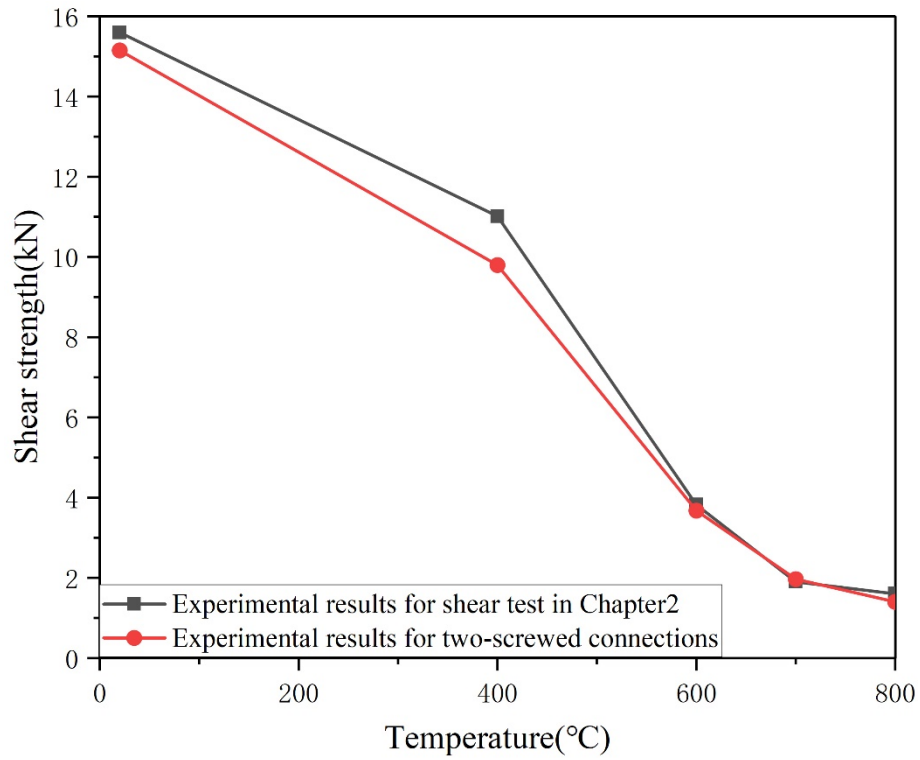
Fig 3.9 Comparison results between the shear tests of HS screws and the two-screwed connection specimens at elevated temperatures

**3.4.2 Eight-screwed connections**

Fig 3.10 shows the relationship between the deformation and shear forces for the eight screwed specimens. Fig 3.11 shows photographs of the specimens after the tests. Regarding the eight screwed connection specimens, remarkable results on the failure modes were observed: in the cases of both the ambient temperature (20℃) and 800℃ experiments, the sheet failure mode was observed, which was the bearing failure around the screw holes, and the screws were not fractured. For the 400℃ experiment, damage due to bearing failure around the holes of the sheet was also observed; however, the specimens collapsed because of screw shear failure. In the 600 and 700℃ experiments, the shear failure modes of the screws were observed. From the above test results, the failure modes of the eight screw connections changed depending on the test temperatures. As shown in Fig 3.10, both the ambient and 800℃ specimens possessed a larger deformation capacity than the 400–700℃ specimens, because the former specimens included plastic deformations accompanying bearing failure around the screw holes.
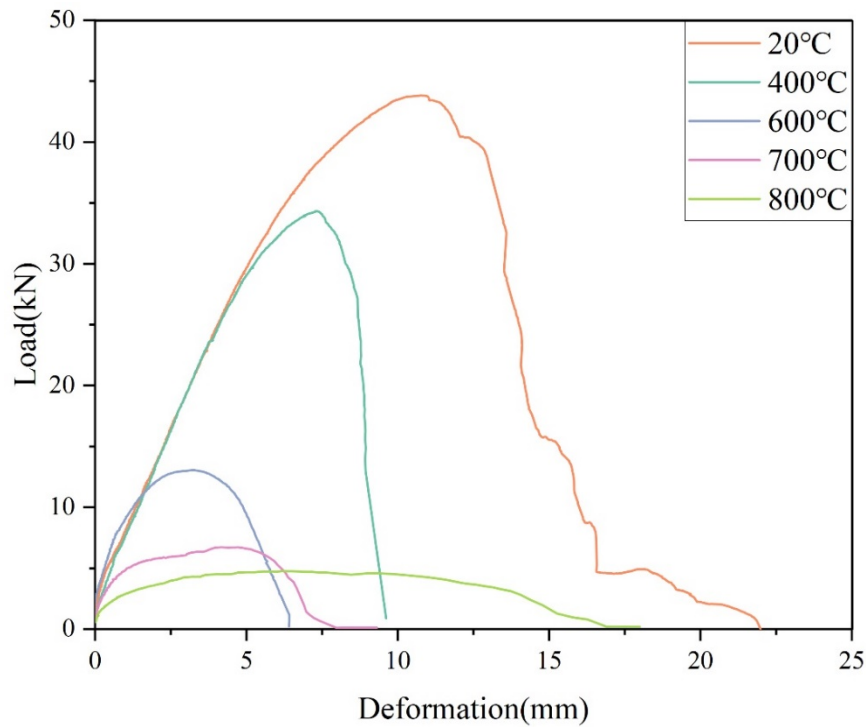


Fig 3.10 Relationships between load and deformation for eight-screwed connections

RT
Sheet bearing failure (Type2)
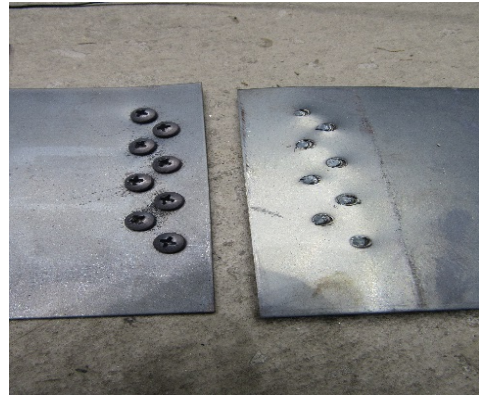
400°C
Screw shear failure (Type4)

600°C
Screw shear failure (Type4)
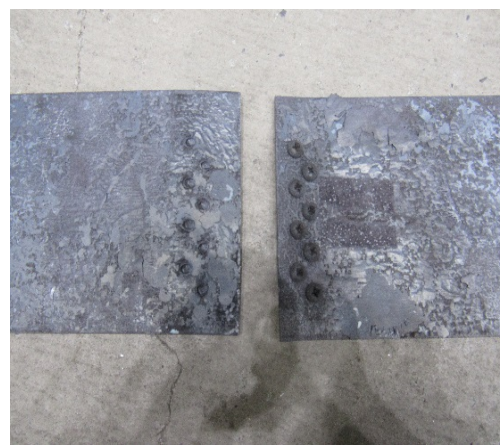
700°C
Screw shear failure (Type4)

800°C
Sheet bearing failure (Type2)

Fig 3.11 Eight-screwed connection specimens after tests

Table 3.2 Shear test results of screwed connections

| Temperature °C | Two-screwed connection | | | Eight-screwed connection | | |
|---|---|---|---|---|---|---|
| | Maximum load values kN | Collapse mode | Shear strength based on Eq. (3.14) kN | Maximum load values kN | Collapse mode | Shear strength based on Eq. (3.14) kN |
| 20 | 15.1 | Type 4 | 15.6 | 43.8 | Type 2 | 62.5 |
| 400 | 9.8 | Type 4 | 10.8 | 34.3 | Type 4 | 43.2 |
| 600 | 3.7 | Type 4 | 3.7 | 13 | Type 4 | 15 |
| 700 | 2 | Type 4 | 1.9 | 6.2 | Type 4 | 7.5 |
| 800 | 1.4 | Type 4 | 1.6 | 4.8 | Type 2 | 6.3 |

## 3.5 Discussion on failure modes for screwed connection at elevated temperatures

### 3.5.1 Coupon test of steel sheets at elevated temperatures.

Coupon tests of steel sheets at elevated temperatures have already been conducted by Sato and Ozaki [3.5], who used the same steel sheet sets as the screwed connections used in this study. The tests were conducted at ambient temperature and temperatures of 400, 600, 700 and 800°C, based on the JIS 0567 standard coupon test methods for metallic materials at high temperatures (JIS, 1998). The strain rate for the coupon test was 0.003 [1/min.], which was a constant value during the loading test. The reduction factor, $\kappa_u (T)$, on the tensile strength at the elevated temperature, $T$, is shown in Fig 3.12, which was divided by the tensile strength of 418 N/mm² at each temperature. Table 3.3 shows the mechanical properties obtained from the coupon tests by Sato and Ozaki [3.5]. The reduction factor, $\kappa_u (T)$, on the tensile strength was used to evaluate the shear strength of the screw connection.

Table 3.3 Coupon test results of steel sheets by Sato and Ozaki [3.5]

| Temperature °C | Effective strength (Stress at strain 1.0%) N/mm² | Tensile strength N/mm² |
|---|---|---|
| 20 | 318 | 418 |
| 400 | 280 | 377 |
| 600 | 110 | 111 |
| 700 | 55 | 64 |
| 800 | 24 | 25 |

## 3.6 Proposal equations for screwed connections at elevated temperatures

To discuss the change in the failure modes for the screwed connection at elevated temperatures, the tensile strength of the screwed connection corresponding to each failure mode at the elevated temperature was proposed based on the current design codes at the ambient temperature. The design rules of the cold-formed steel screwed connections at ambient temperature were proposed by EN 1993-1-3[3.1] and AISI S100 [3.2]. In this study, four failure modes proposed by AISI S100 (2016) and EN 1993-1-3 (2006), which were the sheet longitudinal shear failure (Type 1), sheet bearing failure (Type 2), sheet net-section failure (Type 3) and screw shear failure mode (Type 4) under shear loading were studied, as shown in Fig 3.2. Table 3.4 shows the shear strength of the screwed connections obtained from the experiment and calculated from EC3 and AISI at ambient temperature. It can be seen that the shear strength for an eight-screwed connection at ambient temperature is closer to the experimental result than that calculated from AISI, in which the failure mode was sheet bearing failure (Type2).

Table 3.4 Comparison of experimental results for screwed connections with those of EC3 and AISI at ambient temperature

| Strength for Two-screwed connection | | | Strength for Eight-screwed connection | | |
|---|---|---|---|---|---|
| Type4 | | | Type2 | | |
| Test | EC3 | AISI | Test | EC3 | AISI |
| 15.15kN | / | / | 43.23kN | 48.43kN | 63.56kN |
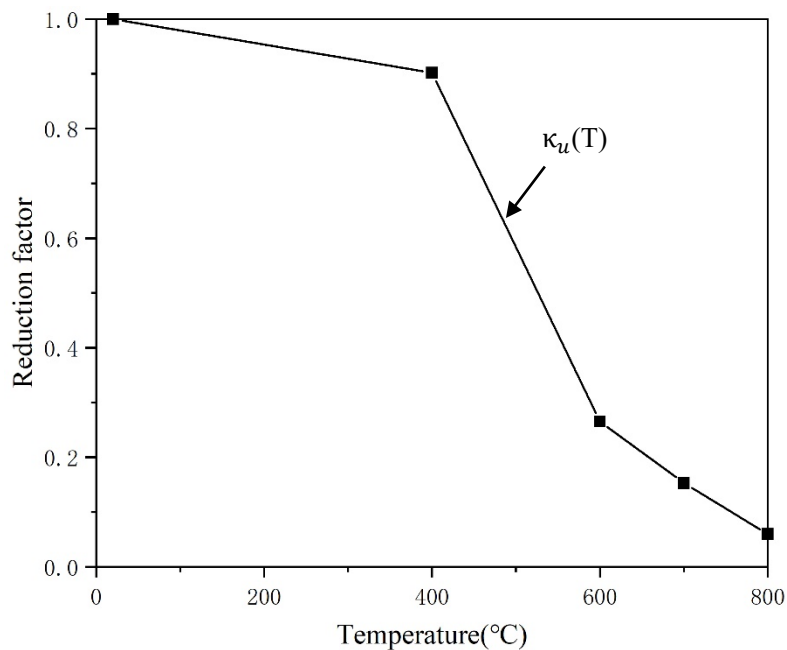


Fig 3.12 Reduction factor on tensile test for coupon test

The shear strength equations proposed for the ambient temperature environment were extended to the high-temperature region using the reduction factors of both the screw and sheet. The four types of failure modes above are shown in Fig 3.2. For these failure modes, the sheet longitudinal shear failure mode at ambient temperature (Type 1, Fig 3.2(a)) was proposed by AISI S100, which the failure mode is not specified in EC3, and the other failure modes at ambient temperatures (Types 2–4, Fig 3.2(b–d)) were proposed by EC3.

(1) Sheet longitudinal shear failure at the elevated temperatures (Type 1, Fig 3.2(a))

Regarding this failure, the sheet fractures because of the small edge distance in the screwed connection. However, the screwed connection specimens used in the tests were designed to possess a large edge distance. The shear strength at the sheet longitudinal shear failure $P_u$ can be estimated by

$$P_u = nF_u te\kappa_u(T) \tag{3.11}$$

where $F_u$ is the tensile strength of the steel sheets at the ambient temperature, $e$ is the edge distance (in this study, two-screwed specimen: 20 mm, eight-screwed specimen: 13 mm) in the connection, $t$ is the sheet thickness (in this study, $t$ =1.6 mm); and $\kappa_u(T)$ is the reduction factor of the tensile strength of the sheet at temperature $T$, as shown in Fig 3.12.

(2) Sheet bearing failure at the elevated temperatures (Type 2, Fig 3.2(b))

Regarding this failure, the sheet fractures because of the large hole diameter made in the thin sheet. This failure mode easily occurs for the screwed connection with large numbers of screws (large screw shear strength). The shear strength at the sheet bearing failure $P_n$ can be estimated by

$$P_n = n\alpha t dF_u\kappa_u(T) \tag{3.12}$$

in which, if $t_2 / t_1$ =1.0, $\alpha = 3.2\sqrt{t/d} \leq 2.1$ ; if $t_2 / t_1 \geq 2.5$ and $t_1 < 1.0mm$ , $\alpha = 3.2\sqrt{t/d} \leq 2.1$; if $t_2/t_1 \geq 2.5$ and $t_1 \geq 1.0mm$, $\alpha = 2.1$; otherwise, if $1.0 < t_2/t_1 < 2.5$, then obtain α by linear interpolation; $t$ is the thinnest of the two steel sheets; $n$ is the total number of screws, and $d$ is the nominal screw diameter.

(3) Sheet net-section failure (Type 3, Fig 3.2(c))

This failure mode occurs for the screwed connection with the large hole-diameter and large numbers of the holes in the sheet. The shear strength at the sheet net section failure $P_{net}$ can be estimated by

$$P_{net} = F_u A_e\kappa_u(T) \tag{3.13}$$

where, $A_e$ is the net cross-sectional area of the steel sheet.

(4) Screw shear failure (Type 4, Fig 3.2(d))

The screw shear fracture occurs for the screwed connection with small numbers of the screws, such as the two screwed-connection. The shear strength at the screw shear failure $P_s$ can be estimated by

$$P_s = mnA_s\tau_s\kappa_s(T) \tag{3.14}$$

where $m$ is the number of shear surfaces, $n$ is the total number of screws (2 or 8), $A_s$ is the nominal sectional area of the screw, $\tau_s$ is the shear strength of the screw at the ambient temperature

(Fig 2.9(a)) and $\kappa_s(T)$ is the reduction factor for the shear strength of the HS screw at temperature, $T$ (Fig 2.11(a)).

Following the screwed connection test explained in Section 3.4, Type 2 and 4 failure modes were observed. Fig 3.13 shows the shear strength (solid lines) estimated using the above equations corresponding to each failure mode. The test results of the two and eight-screwed connection specimens are shown by the marks in Fig 3.13. As shown in Fig 3.13 (a) and Table 3.2 (the two-screwed connections), it was clarified that the test results and the shear strength, $Ps$, (Type 4) obtained from Eq. (3.14) approximately agreed. At the ambient temperature, the shear strength, $P_n$, of the sheet bearing failure (Type 2) was the minimum value; however, the strength gap between $P_n$ and $P_s$ was very small, and it was considered that the screw shear failure (Type 4) at the ambient temperature occurred in the lead.

From Fig 3.13(b) (the eight-screwed connections), it was clarified that the test result at the ambient temperature was close to the shear strength, $Pn$, of the sheet bearing failure (Type 2), and the minimum values in four collapse modes resulting in the same failure modes at the ambient temperature for both the test and calculation results. The shear strength curve, $Ps$, of the screw shear failure above 400℃ significantly decreased because the reduction factor of the HS screws decreased (Fig 2.11(a)). The shear strength of eight-screwed connections from 400 to 700℃ was given by the screw shear failure, $Ps$, (Type4); this tendency was approximately the same as the experimental results. However, the test result at 400℃ was smaller than the shear strength curve, $Ps$, because the small damage of steel sheets(bearing failure around the holes) occurred, therefore, the full shear strength of screws was not exhibited. For the 800℃ test results, the failure mode changed from the screw shear failure to sheet bearing failure, because the shear strength of the steel sheet at 800℃ became very small. In this case, the calculation results for Type 4, were the minimum values in the four failure modes.

In the screwed connection test, the test results of the eight-screwed connection specimen exhibited two failure modes depending on the test temperatures; however, the reason could be explained by evaluating the shear strength of the screwed connection at elevated temperature Equations (3.11-3.14). The other failure modes (Types 1 and 3) were not observed in this experiment, therefore, the discussion on those failure modes and evaluation of the tensile strength for the screwed connection at elevated temperatures are required in future work. Additionally, the strength of the eight-screw connection specimen was 43.8 kN, which is lower than the strength calculated using Eq. (3.12). This discrepancy is due to a reduction in strength caused by not accounting for the group effect of the screws.
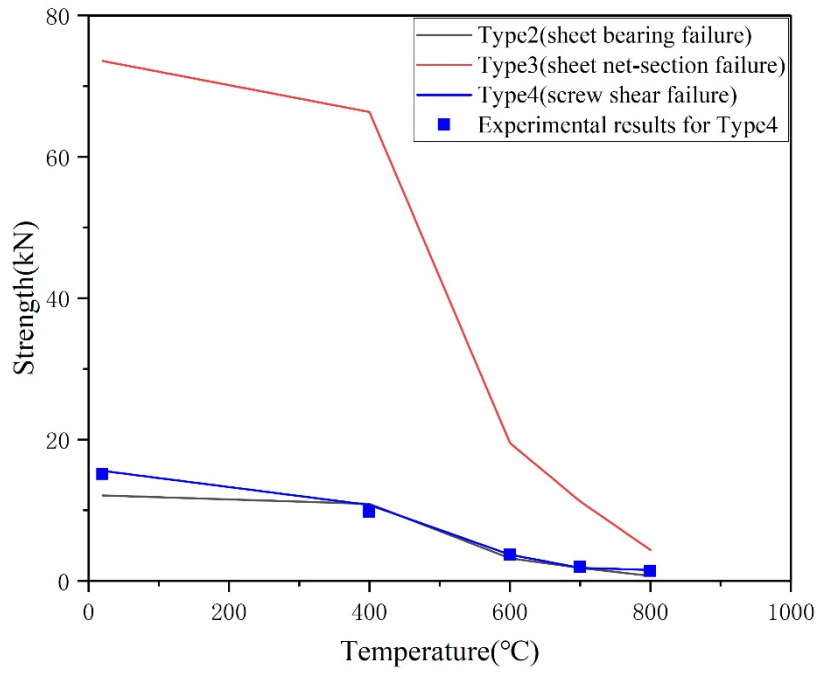
(a) Two screwed-connections
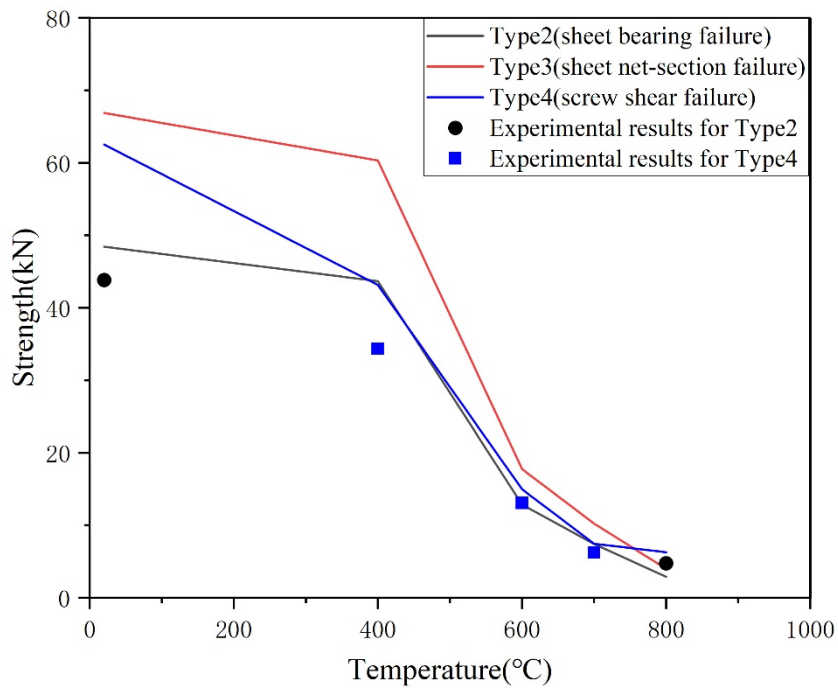


(b) Eight screwed-connections

Fig3.13 Comparison results between experimental and calculation results for screwed connections

## 3.6 Conclusions

Tensile tests for single overlapped screwed connections using HS screws at elevated temperatures were conducted to examine the load-bearing capacity of the screwed connection when screw shear failure occurred. The screwed connection using two screws exhibited screw shear failure regardless of the test temperature; however, using eight screws exhibited the transition of failure modes owing to the test temperature. That is, for the same specification screwed connections, sheet bearing failure occurred at the ambient temperature and 800$^{\circ}$C, whereas screw shear failure occurred between the test temperatures (400, 600 and 700$^{\circ}$C). Formulae for calculating the shear strength of the screw connection using the reduction factors for both the sheet tensile and screw shear strengths were proposed. The above transition of failure modes can be explained by evaluating the tensile strengths corresponding to each failure mode at elevated temperatures.

## References

[3.1] EN 1993-1-3 (2006), Eurocode 3 – Design of Steel Structures – Part 1-3: General Rules Supplementary Rules for Cold-Formed Members and Sheeting.

[3.2] American Iron and Steel Institute. North American Specification for the Design of CFS Structural Members, AISI S100-12[S]. Washington, DC, USA, 2012.

[3.3] Center for Cold-Formed Steel Structures, "AISI Specification Provisions for Screw Connections," CCFSS Technical Bulletin, vol.2.,no.1,Feb.1993,University of Missouri Rolla.

[3.4] Pekoz, T. "Design of Cold-Formed Steel Screw Connections," in Proceedings of the 10th International Specialty Conference on Cold-Formed Steel Structures, W.W.Yu and R.A. LaBoube, Eds., University of Missouri-Rolla, Oct. 1990

[3.5] Sato, T. and Ozaki, F. (2018), "Local buckling performance of steel thin square hollow section at high temperature", Journal of Structural and Construction Engineering (Transactions of AIJ), Vol. 83 No. 751, pp. 1381-1389, (in Japanese).

# Chapter 4 Shear tests of self-drilling screws after heating and cooling processes

## 4.1 Introduction

In Chapter 4, three types of self-drilling screws, manufactured using high-strength steel, martensitic high-strength stainless steel, and austenitic stainless-steel bars, were used in the tests, which was the same batch as used in Chapter 2. Shear loading tests were conducted on the self-drilling screws after the heating and cooling procedures. It was clarified that the reduction factor of HS screws decreased significantly when <500°C, compared with JIS Grade 4.8/8.8/12.8, super high-strength F14T, and high-strength F10T bolts. The post-fire shear strengths of HS and super high-strength F14T bolts reduced by more than 40% when the heated temperature reached 800 °C. The post-fire shear strengths and load-bearing capacities of the self-drilling screw were examined. Furthermore, the post-fire shear strengths were compared with the shear strengths at elevated temperatures. The reduction of post-fire shear strength was clarified, which provided the fundamental data necessary for the study of screwed-connections at post-fire conditions, as detailed in Chapter 5.

## 4.2 Overview of shear test for self-drilling screws after heating and cooling progress

### 4.2.1 Details for specimens

Three types of self-drilling screws, shown in Fig 4.1, were used as test specimens for the ambient shear tests performed after the heating and cooling procedures. These screws were manufactured using the same steels as those used in tensile/shear tests at elevated temperatures in Chapter 2. High-strength steel screws, manufactured using the initial steel JIS SWCH A18, are referred to as HS hereafter. Austenitic stainless-steel screws, manufactured using the initial stainless-steel JIS-SUS304J3, are referred to as ASUS. Martensitic stainless-steel screws, manufactured using the original stainless-steel lot JIS SUS410, are hereafter referred to as MSUS. The chemical components of the original steel-lot bars are listed in Table 4.1. The ASUS and MSUS screws contained higher contents of nickel and chromium alloys, responsible for improving the rest resistance, than that of HS screws. However, these alloys exhibit higher tensile strength at elevated temperatures than the general mild or high-strength carbon steels. Typically, HS screws are used for connecting cold-formed structures. MSUS screws are commonly used as stainless-steel structural components for the cold-formed structures. ASUS screws are preferred for non-structural components, such as the installations of interior and exterior decorative materials and aluminum sheets in metal roofing systems, which require water and corrosion resistances [4.1,4.2,4.3]. Those screws are usually used for structural, non-structural, and functional connections in cold-formed steel structures. Therefore, it is important to discuss those

post-fire performances. For each of the three types of screws, the nominal diameter was 5mm, and the length under the head position was 70 mm according to the previous study [4.1].



HS          ASUS          MSUS
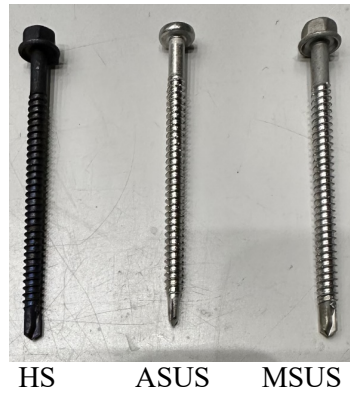
Fig 4.1 Test specimens

Table 4.1 Chemical compositions of screws

| Chemical(mass%)<br>Metal | C | Si | Mn | P | S | Al | Cu | Ni | Cr |
|---|---|---|---|---|---|---|---|---|---|
| SWCH18 A(HS) | 0.19 | 0.03 | 0.8 | 0.01 | 0.007 | 0.03 | 0.02 | 0.03 | 0.03 |
| SUS304J3(ASUS) | 0.025 | 0.25 | 1.6 | 0.034 | 0.001 | | 2.55 | 9.05 | 18.28 |
| SUS410(MSUS) | 0.1 | 0.4 | 0.37 | 0.023 | 0.001 | | | 0.23 | 12.03 |

### 4.2.2 The heating and cooling processes

To conduct the heating and cooling procedures on specimens, an electrical furnace (inner effective heating length: 800 mm, height: 500 mm, width: 450 mm) (Fig 4.2), the same as that used in previous research by Zhao et al. [4.4], was used. The three types of specimens underwent heating from ambient temperature to various test-temperature levels of 200–900 °C with intervals of 100 °C, as detailed in Table 4.2. The heating rate of the electrical furnace was set to 10 °C/min, which was consistent with that of previous research in Chapter 2 and 3. A sheathed thermocouple (sheathed diameter of thermocouple: 1.6 mm) was attached to the HS specimen (Fig 4.2) at a distance of one-third of that from the screw head where the shear modes occur in the experiment. The measured temperature of the specimens confirmedly reached the test target temperature. The specimens remained under the target temperature for 30 min to ensure uniform temperature distribution. Subsequently, the furnace was turned off, and the specimens were cooled in the furnace.

Table 4.2 Number of shear tests of screw specimens

|  | Temperature | | | | | | | | | Total |
|---|---|---|---|---|---|---|---|---|---|---|
|  | 20°C | 200°C | 300°C | 400°C | 500°C | 600°C | 700°C | 800°C | 900°C |  |
| HS | 3 | 3 | 3 | 3 | 3 | 3 | 3 | 3 | 3 | 27 |
| ASUS | 3 | 3 | 3 | 3 | 3 | 3 | 3 | 3 | 3 | 27 |
| MSUS | 3 | 3 | 3 | 3 | 3 | 3 | 3 | 3 | 3 | 27 |
| Total | - | - | - | - | - | - | - | - | - | 81 |
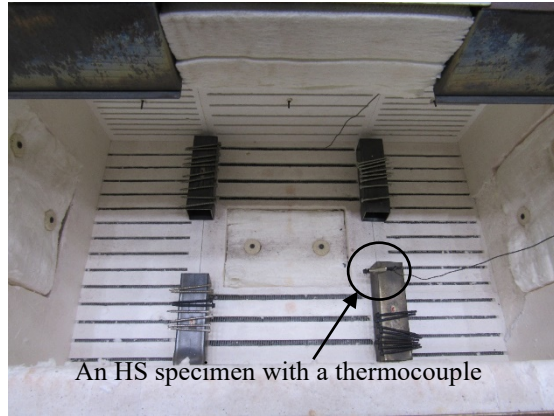
Fig 4.2. Screw specimens in the furnace
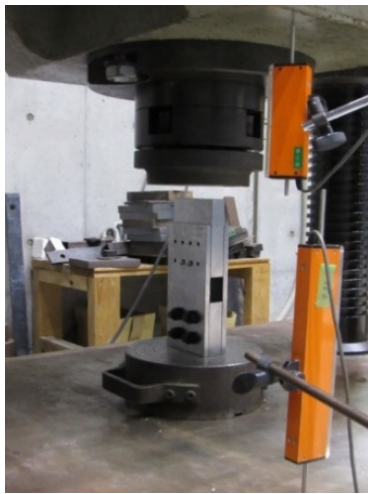


(a) Overview of shear test
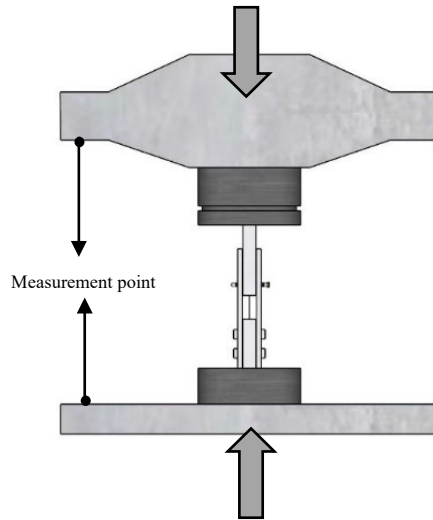
(b) Test system
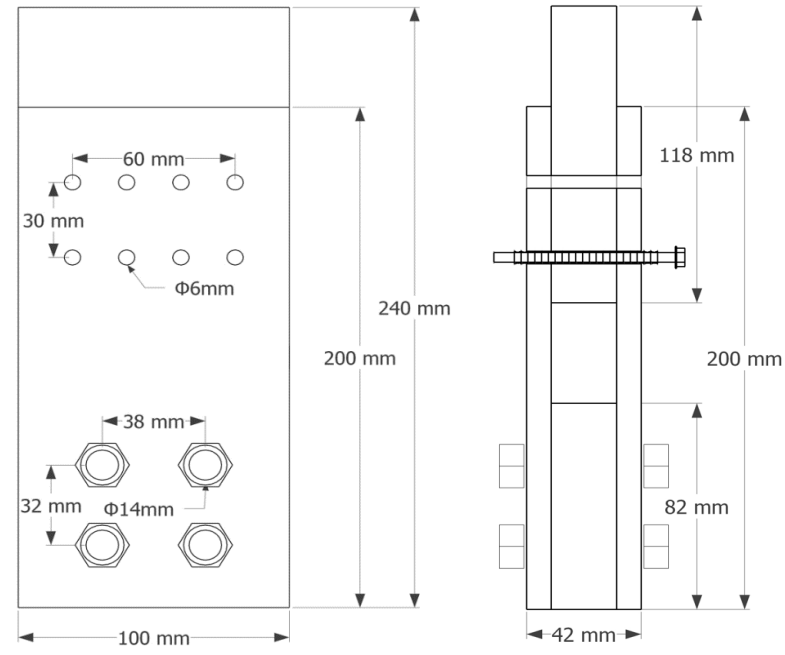


(c) Testing jig

Fig 4.3 Test systems and testing jig for shear tests

**4.2.3 The shear tests for heated specimens at ambient temperature**

After the heating and cooling procedures, shear tests were conducted on the screw specimens under ambient temperature conditions. As shown in Fig 4.3(a), a UH-200A universal testing machine with a maximum load capacity of 2000kN, as in a previous study by Ozaki et al. [4.1], was employed to perform shear tests on the screw specimens. To examine the shear strength of the screws, double-shear testing jigs composed of three steel plates were used. The same experimental jig was also used in a previous study for high-temperature screw shear tests (Fig 4.3) by Ozaki et al. [4.1]. To ensure the stability of the entire experimental jig, the three steel plates with a height and width of 240 and 100 mm, respectively, were connected in the testing jig using four high-strength bolts with a thread diameter of 12 mm. The steel plates were tightened by hands at the lower part (Fig 4.3(a) and (c)). The two screws were inserted into the top hole (diameter: 6 mm) of the experimental jig, which had a slightly larger diameter (5 mm) than the screw specimen for easy installation. As shown in Fig 4.3(b), the shear force, P, was applied to the top of the testing jig. For each test temperature, three-time tests were conducted, as listed in Table 4.2, and the mean value of shear strength was determined to consider the dispersion of the test results. Furthermore, two contact displacement transducers were located at the universal testing machine's upper and lower measurement points (Fig 4.3(b)). The measured relative displacement included the deformation of the screw specimens and testing jig. However, the stiffness of the testing jig was much greater than that of the screw; therefore, the measured relative displacement was equal to the deformation of the screw.

**4.3 Experimental results of post-fire shear strength for self-drilling screws**

Fig 4.4 shows the relationships between the test time and temperature during the heating and cooling procedures. The curves demonstrate that the specimens were heated at 10 °C/min to the target temperature and maintained at the target temperature for 30 min before being cooled in the furnace. As shown in Fig 4.4, the test specimens reached the target temperature. The cooling rate was 0.5–2 °C/min.

Fig 4.5 shows the shear test results of the HS, ASUS, and MSUS specimens after heating and cooling. The vertical axis represents the nominal shear stress $\tau$, which is determined by Eq. (4.1),

$$\tau = P/(m \cdot n \cdot A_s) \tag{4.1}$$

where $m$ and $n$ are the numbers of the shear planes of the steel jig plates and screws, respectively ($m$=2 and $n$=2); $A_s$ is the nominal sectional area of the screw ($19.6\ mm^2$); $P$ is the shear load for screw tests.

The horizontal axis represents the dimensionless relative deformation $\delta/d$, measured by displacement meters. $d$ represents nominal diameter of the screw; in this study, $d$=5 mm. The mean values of the shear strength, standard deviation (SD), coefficient of variation (CV), and reduction factors of shear strength at each heated temperature are listed in Table 4.3. The values of SD and CV for ASUS were small. Whereas, the values of CV for HS and MSUS screws were

slight growth over 600℃ because the effect of heat treatment during the manufacturing processes of the high-strength screw was reduced by heating and cooling processes of post-fire tests.

As shown in Fig 4.5, a stiffness-change point was observed in the test result curve from the beginning of loading to the point of shear strength. During the loading process until this point, the test results included the bending deformation of the screw that occurred in the hole of the testing jig. The shear deformation became dominant as the bent screw touched the side wall of the hole and was approximately under the sheared condition. The same behavior was observed in a previous study by Ozaki et al. [4.1]. Therefore, the stiffness increased after exceeding this point. For HS and MSUS specimens, the shear strengths decreased with increasing heated temperature, as shown in Fig 4.5 (a) and (b). However, the shear strengths of the ASUS specimens were unchanged, as shown in Fig 4.5 (c). All screw specimens exposed to high temperatures evidently exhibited a similar deformation capacity to the untreated specimens. The shear failure occurred at both the shear plane locations for each specimen as shown in Fig 4.6. Bending plastic deformation was observed in the screw specimens even after shear failure. In addition, noticeable color changes were observed as a result of the heating process.
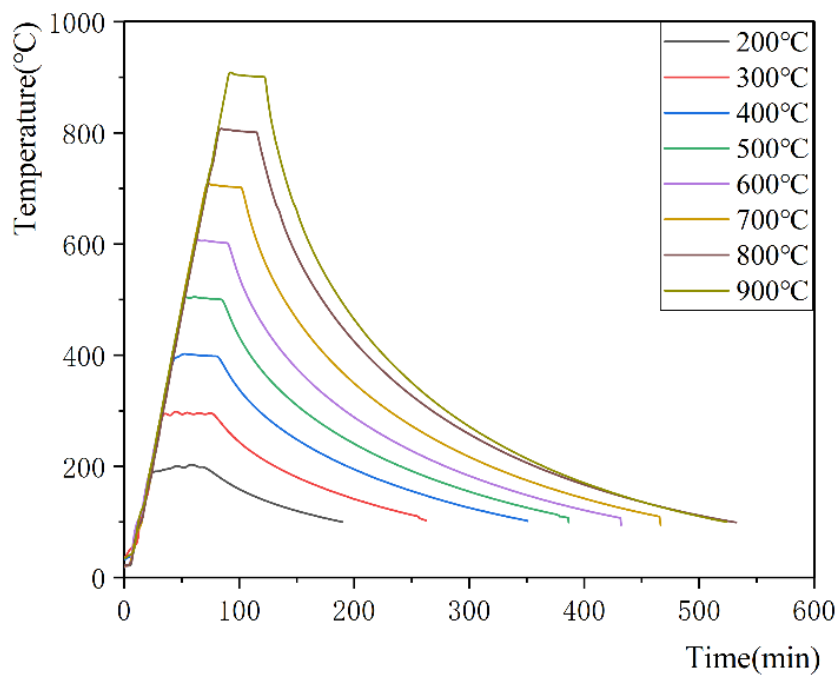


Fig4.4 Relationships between time and temperature following heating and cooling processes for screw specimens

60

Table 4.3 Mean values, SD, CV and reduction factors ($\kappa(T)$) of shear strength after heating and cooling procedure

| Screw types / Temperature | HS | | | | MSUS | | | | ASUS | | | |
|---|---|---|---|---|---|---|---|---|---|---|---|---|
| | Mean N/mm² | $\kappa_s^{cool}(T)$ | SD N/mm² | CV % | Mean N/mm² | $\kappa(T)$ | SD N/mm² | CV % | Mean N/mm² | $\kappa(T)$ | SD N/mm² | CV % |
| 20°C (Untreated) | 375.9 | 1.0 | 12.32 | 3.3 | 413.6 | 1.0 | 1.72 | 0.4 | 355.3 | 1 | 0.19 | 0.1 |
| 200°C | 366.7 | 0.98 | 37.98 | 10.4 | 381.4 | 0.92 | 20.95 | 5.5 | 360.9 | 1.02 | 0.16 | 0.04 |
| 300°C | 317.5 | 0.84 | 9.36 | 3.0 | 390.9 | 0.95 | 9.35 | 2.4 | 381.5 | 1.07 | 0.26 | 0.1 |
| 400°C | 307.4 | 0.82 | 12.44 | 4.1 | 396.6 | 0.96 | 18.06 | 4.6 | 364.2 | 1.03 | 1.25 | 0.3 |
| 500°C | 234.5 | 0.62 | 0.83 | 0.4 | 418.2 | 1.01 | 22.94 | 5.5 | 355.6 | 1 | 0.93 | 0.3 |
| 600°C | 227.9 | 0.61 | 10.54 | 4.6 | 316.6 | 0.77 | 23.56 | 7.4 | 335.3 | 0.94 | 2.26 | 0.7 |
| 700°C | 241.9 | 0.64 | 8.33 | 3.4 | 274.8 | 0.67 | 5.24 | 1.9 | 340 | 0.96 | 0.76 | 0.2 |
| 800°C | 211.4 | 0.56 | 2.75 | 1.3 | 281.9 | 0.68 | 33.97 | 12.1 | 345.6 | 0.97 | 1.04 | 0.3 |
| 900°C | 203.6 | 0.54 | 12.60 | 6.2 | 252.4 | 0.61 | 7.61 | 3.0 | 359.8 | 1.01 | 0.8 | 0.2 |
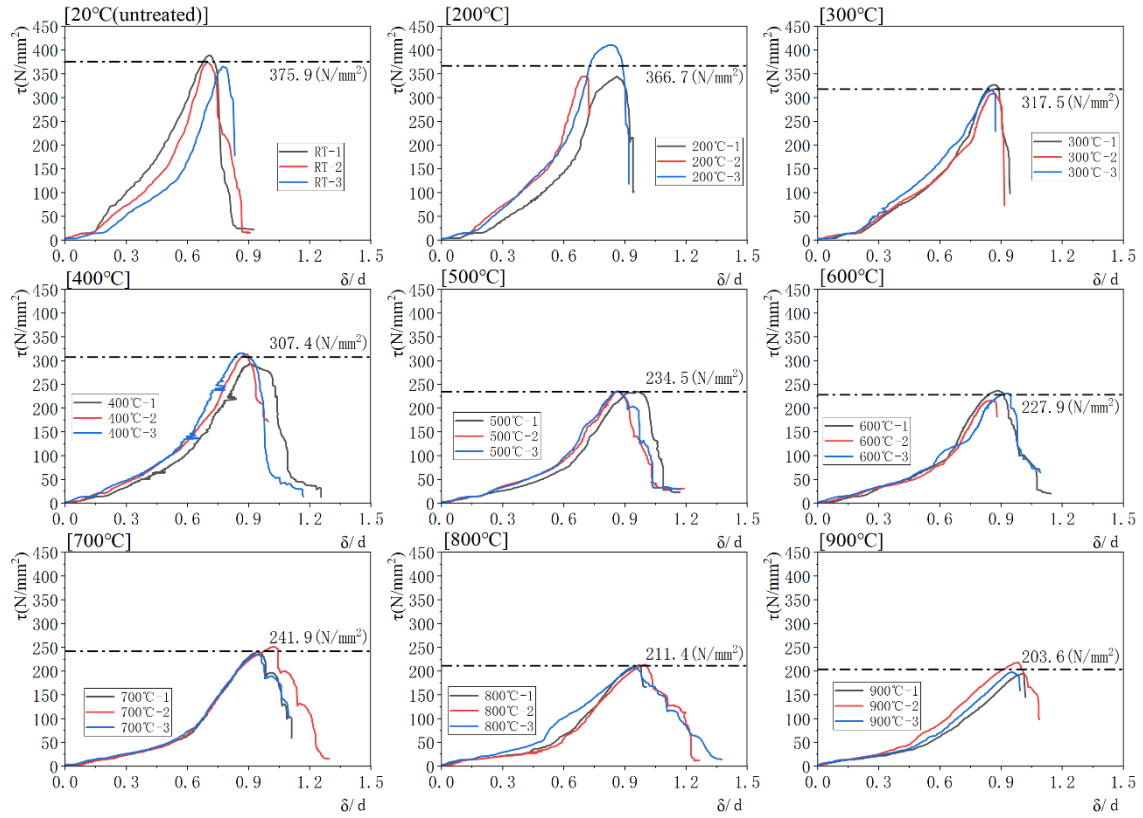
(a) HS specimens
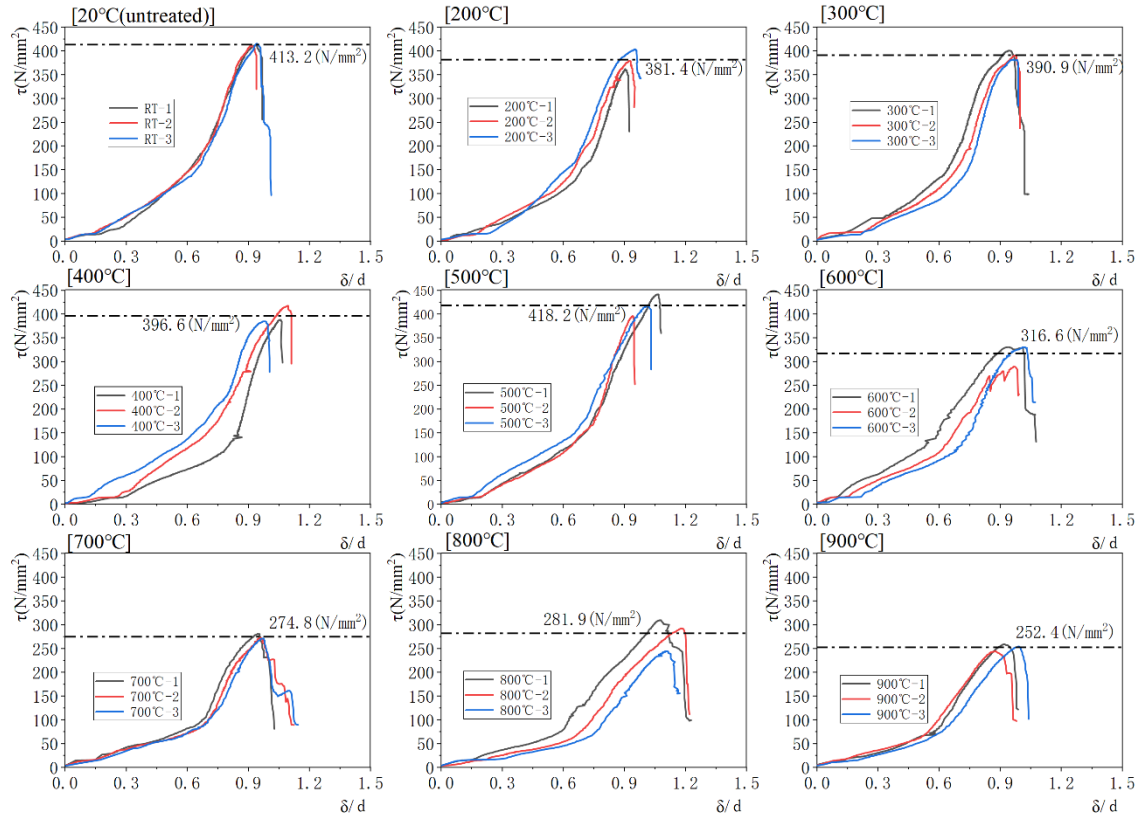


(b) MSUS specimens

Fig4.5 Experimental results of screw shear tests after heating and cooling processes

(c)ASUS specimens

Fig 4.5 Experimental results of screw shear tests after heating and cooling processes

① ② ③    ① ② ③    ① ② ③    ① ② ③    ① ② ③
20℃(untreated)    200℃    300℃    400℃    500℃

① ② ③    ① ② ③    ① ② ③    ① ② ③
600℃    700℃    800℃    900℃

(a) HS specimens

① ② ③    ① ② ③    ① ② ③    ① ② ③    ① ② ③
20℃(untreated)    200℃    300℃    400℃    500℃

① ② ③    ① ② ③    ① ② ③    ① ② ③
600℃    700℃    800℃    900℃

(b) MSUS specimens

① ② ③    ① ② ③    ① ② ③    ① ② ③    ① ② ③
20℃(untreated)    200℃    300℃    400℃    500℃

① ② ③    ① ② ③    ① ② ③    ① ② ③
600℃    700℃    800℃    900℃
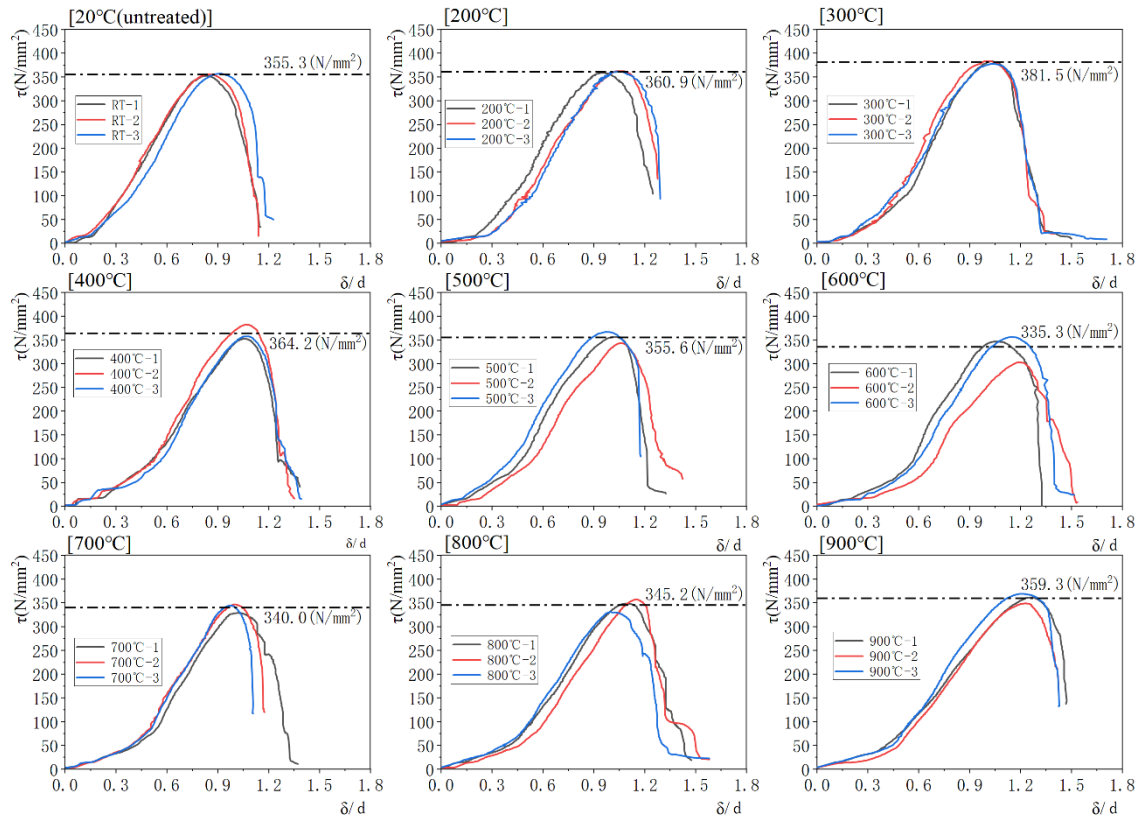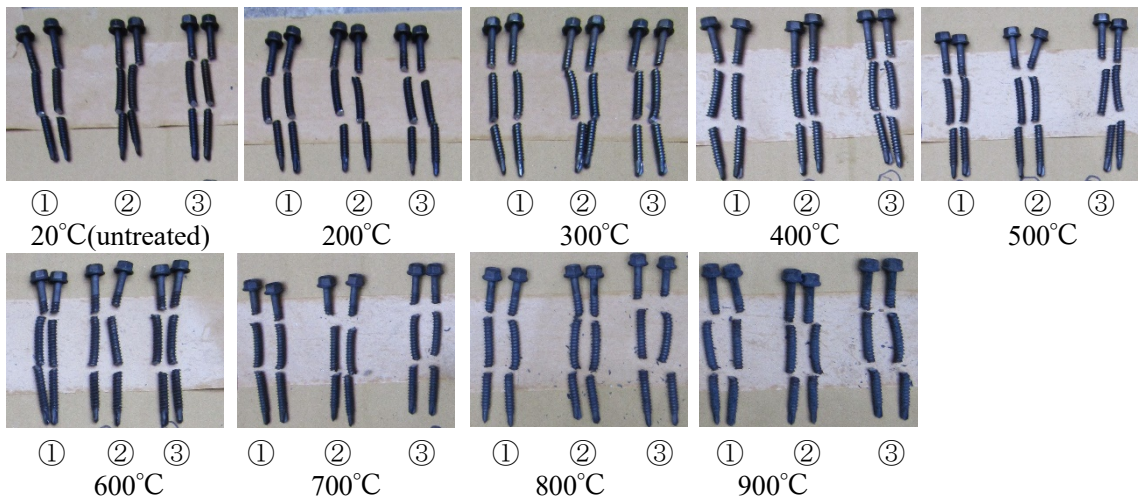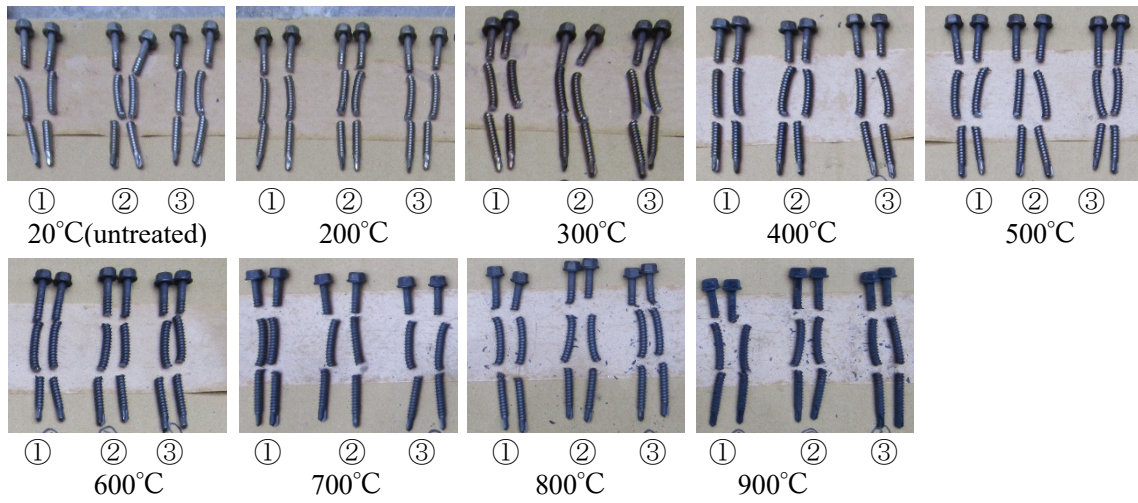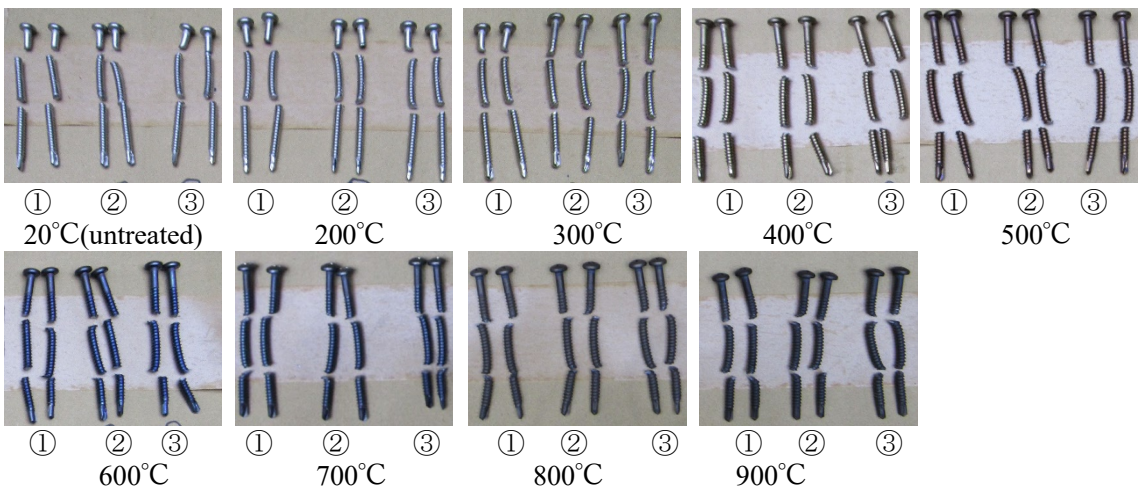
(c) ASUS specimens

Fig 4.6 Screw specimens after shear tests

Fig 4.7(a) shows the relationships between the shear strength and heated temperature for HS, MSUS, and ASUS specimens after the heating and cooling procedures. As shown in Fig 4.7(a), the shear strength of HS specimens noteworthily decreased continuously as the exposure temperature increased. Conversely, the shear strength of MSUS specimens reduced slightly and significantly when the heated temperatures were <500 °C and >500 °C, respectively. In contrast, ASUS specimens showed remarkable stability in post-fire shear strength, even after exposure to high-temperature regions such as 900 °C. Furthermore, HS specimens exhibited consistently lower post-fire shear strength than MSUS and ASUS specimens, specifically in the temperature range of 300–900 °C. This suggests that the strength of HS and MSUS specimens decreases significantly after exposure to fire, despite their high strength at ambient temperature. Fig 4.7(b) shows the reduction factor of shear strength for the three types of screw specimens examined in this study. The reduction factors are defined as the ratio of the shear strength of specimens at each heated temperature to that of the untreated specimens. For the MSUS and HS specimens, the reduction factor of shear strength decreased approximately by 40% after being heated to 900°C and cooled. Moreover, the reduction factor of shear strength for HS specimens significantly reduced by 40% while the heated temperature was 500°C, which is considered to be caused by the heat treatment process of HS during production from the carbon steel bar to the HS screws.
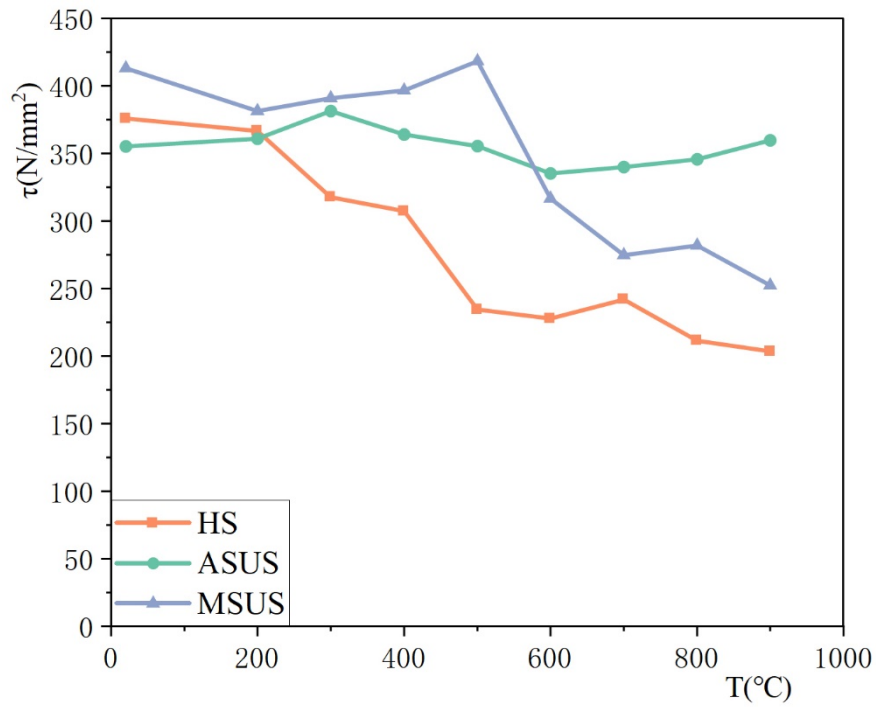
(a) Shear strength
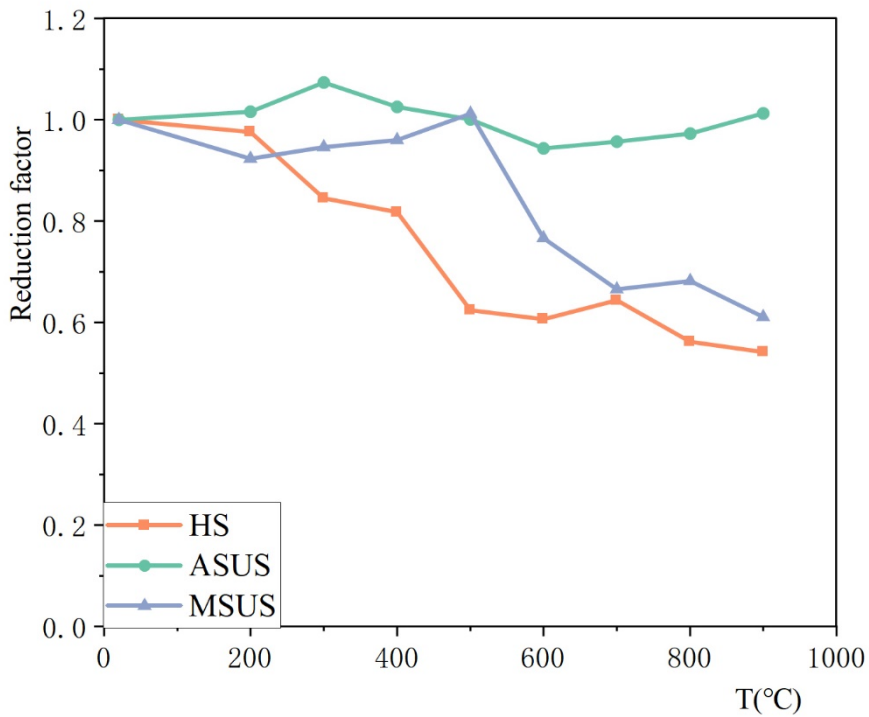


(b) Reduction factors of shear strength

Fig 4.7 Relationship between post-fire shear stress and temperature for screw specimens

## 4.4 Comparison of shear test results with past test results

The experimental results obtained in this study were compared with those of the previous study in Chapter 2, which conducted the same screw specimens that were manufactured in the same batch at elevated temperatures, as shown in Fig 4.8. For the HS specimens (Fig 4.8(a)), the shear strength decreased consistently from 20 to 400 °C. For MSUS screws, the shear strengths remained unchanged and decreased significantly below 400 °C and above 400 °C in elevated temperature tests, respectively. Similarly, the post-fire shear strength was almost unchanged below 400 °C, decreasing as the heated temperature increased, as shown in Fig 4.8(b). Furthermore, for the ASUS specimen, the shear strengths decreased with increasing elevated temperatures; however, the post-fire shear strength remained constant throughout the experiment in this study (Fig 4.8(c)).

The results of the post-fire shear strengths of the screw specimens in this study were compared with those of various steel bolts reported in previous studies; these were JIS 4.8/8.8/12.9 bolts by Kodama et al. [4.5] (the standard tensile strength $F_b$ at ambient temperature = 400N/mm$^2$, 800N/mm$^2$, 1200 N/mm$^2$, respectively), JIS high-strength bolts F10T [4.6] ($F_b$=1000 N/mm$^2$), stainless-steel bolts 10T-SUS [4.6] ($F_b$= 1000 N/mm$^2$), and super high strength bolts F14T by Han et al. [4.7] ($F_b$= 1400 N/mm$^2$). The comparison results are shown in Fig 4.9. The reduction factors of post-fire shear strength of HS, JIS 4.8/8.8/12.8, super high-strength F14T, and high-strength F10T bolts decreased with increasing heated temperatures (Fig4.9(a)). The post-fire shear strengths of HS and super high-strength F14T bolts reduced by more than 40% when the heated temperature reached 800 °C. However, the post-fire shear strength reduction factor of the HS specimens was found to be significantly reduced in comparison to other bolts when the heated temperature was below 600 °C, which may be attributed to the differing production processes and chemical compositions of HS screws. The reduction factor of the post-fire shear strength for ASUS, MSUS, and JIS 10T-SUS bolts followed a similar trend when the heated temperature was <500 °C. However, when the heated temperature was >500 °C, the post-fire shear strength of the MSUS specimens reduced by approximately 40% compared with ASUS and JIS 10T-SUS, as shown in Fig 4.9(b).

Based on the above discussion, since the strength of HS and MSUS screws for cold-formed steel structures is reduced after a fire, it is necessary to extensively examine the post-fire residual strength of HS and MSUS screws for cold-formed steel structures in order to ensure the safety of repair work when considering reusing or replacing cold-formed steel structural members.
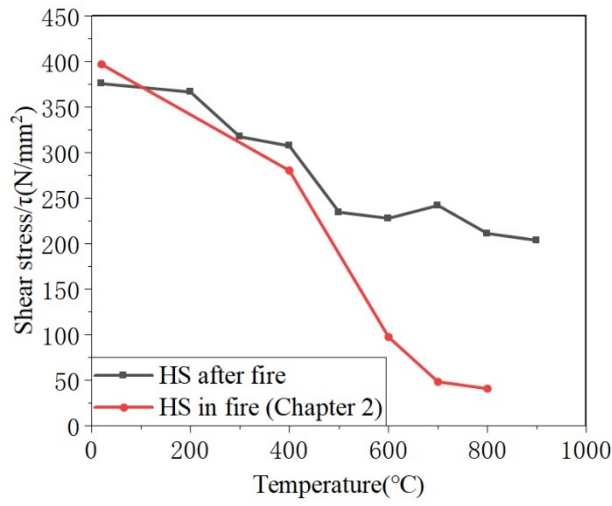
(a) HS
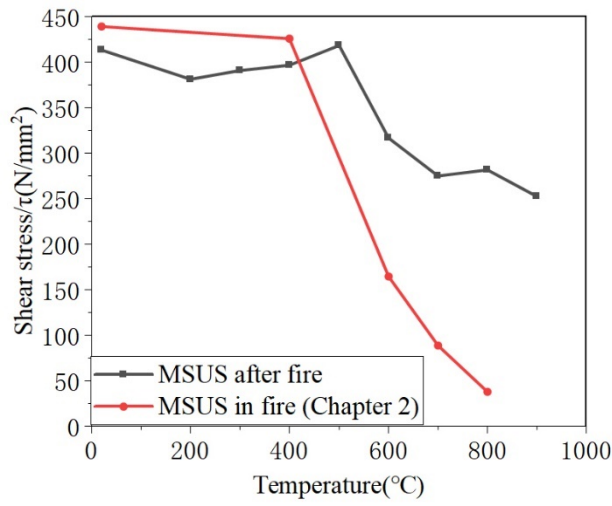


(b) MSUS
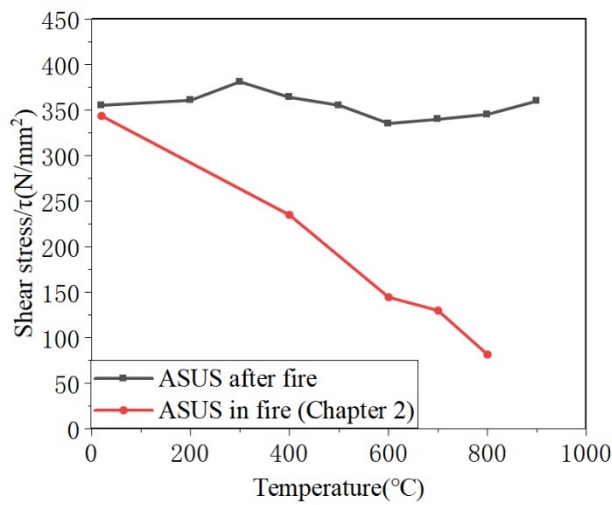


(c) ASUS

Fig4.8 Comparison results of screw specimens after/in fire
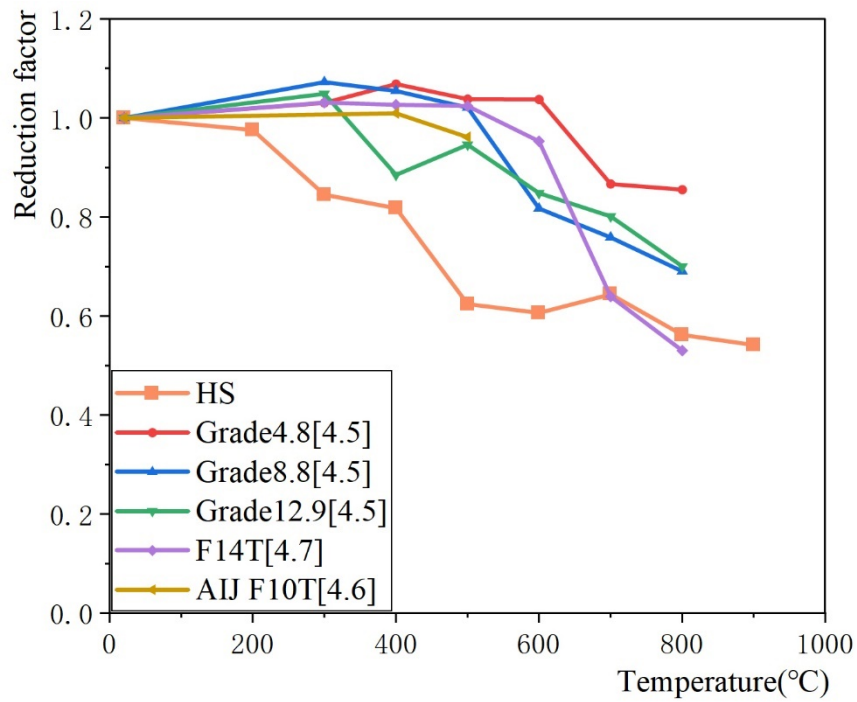
(a) The results of HS and the past researches
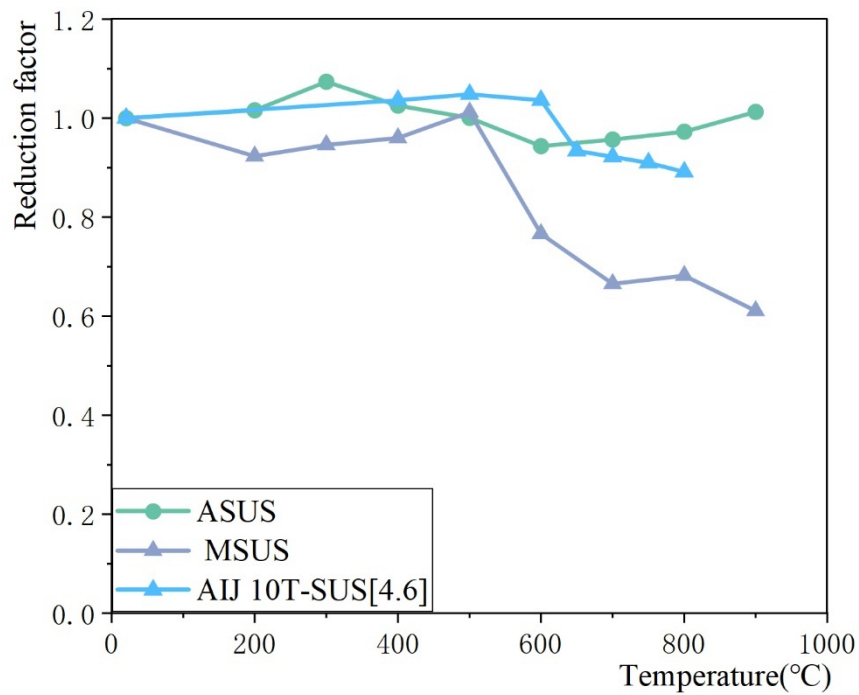


(b) The results of MSUS, ASUS and the past researches

Fig4.9 Comparison results of shear strength after fire

## 4.5 Conclusions

Shear tests were performed at ambient temperature on three types of self-drilling screws (nominal diameter: 5 mm, steel grades: HS (high-strength steel), MSUS (martensitic stainless-steel), and ASUS (austenitic stainless-steel) after heating and cooling procedures. The post-fire shear strength of the HS and MSUS screws decreases significantly when exposed to >500 ℃. In contrast, the post-fire shear strength of ASUS screws remains almost unchanged when exposed to high temperatures.

The experimental results in post-fire conditions were compared with those of the previous study at elevated temperatures in Chapter 2. For the HS specimens, the shear strength decreased consistently from 20 to 400 ℃. For the ASUS specimen, the shear strengths decreased with increasing elevated temperatures; however, the post-fire shear strength remained constant throughout the experiment in this study. Furthermore, for MSUS screws, the shear strengths remained unchanged and decreased significantly below 400 ℃ and above 400 ℃ in elevated temperature tests, respectively.

The results of the post-fire shear strengths of the screw specimens in this study were compared with those of various steel bolts. The post-fire shear strength of HS, JIS 4.8/8.8/12.8, super high-strength F14T, and high-strength F10T bolts decreased with increasing heated temperatures. However, when the heated temperature was below 600 ℃, it was shown that the post-fire shear strength reduction factor of the HS specimens was significantly lower than that of other bolts. This result may be related to the different production procedures and chemical compositions of HS screws.

**References**

[4.1] Ozaki, F., Liu, Y., Ye, K., 2022. Tensile and shear strength for a self-drilling screw and transition of failure modes and shear-strengths for self-drilling screwed connections at elevated-temperatures. J. Struct. Fire Eng. 13, 321–346

[4.2] KUROSAWA Miku, KISHIKI Shoichi, 2022. "Ultimate Strength of Screw Joint for Exterior Wall of Metal Panel", Summaries of technical papers of annual meeting, Architectural Institute of Japan, No.22442, pp. 883-884. (in Japanese).

[4.3] Jun Zhao, Zhuang Wang, Feng Qian, Yang Peng, Jun Dong, 2022. Finite element analysis of the shear capacity of stainless-steel screw connections, Structures, Vol.41, ISSN 2352-0124, pp.957-968.

[4.4] Zhao, X., Ozaki, F., Hirashima, T., Kimura, K., Murakami, Y., Suzuki, J., Yotsumoto, N., 2023. Bending-strength evaluation of wide-flange steel beams subjected to local buckling at elevated temperatures. JSFE 14, pp.202–227.

[4.5] KODAMA T., Ozaki, F., 2023. "shear strength of a bolt at elevated temperature and after heating and cooling processes", Summaries of technical papers of annual meeting, Architectural Institute of Japan. No.3084, pp. 177-178. ( in Japanese)

[4.6] Architectural Institute of Japan (AIJ) (2017), AIJ Guide Book for Fire-Resistive Performance of Structural Materials, Maruzen Publishing Co., Tokyo (in Japanese).

[4.7] Seokhyeon HAN, Fuminobu OZAKI, Kenji TADA, Junichi SUZUKI, 2022. "Damage evaluation for super high-strength bolted(F14T) connections after heating and cooling processes". Summaries of technical papers of annual meeting, Architectural Institute of Japan. No.3018, pp.35-36. (in Japanese)

# Chapter 5 Tensile tests for screwed connections after heating and cooling processes

## 5.1 Introduction

In Chapter 5, the post-fire shear strengths and load-bearing capacities of screwed connections have been examined by using two screwed-connection specimens, four screwed-connection specimens and eight screwed-connection specimens. Tensile loading tests were conducted on single overlapped screwed connections after the heating and cooling procedures to examine the transition of the failure modes between the ambient and exposed temperatures. Evaluation equations were proposed for each failure mode, which could predict the post-fire strength of screwed-connections.

## 5.2 Overview of tensile test for screw connections after heating and cooling processes

### 5.2.1 Details for specimens

Fig 5.1 shows the details of screwed-connection specimens, in which the edge and end distance were designed by the EN 1993-1-3(EC3) [5.1]. These connection specimens consist of two steel sheets and screws, as shown in Fig 5.3. The steel sheets were made of hot-rolled mild-carbon steel (SPHC for JIS G 3131 (Table 5.1), length: 300 mm, width: 80 mm, thickness: 1.6 mm). The screws were made of the same chemical components as the HS specimens (nominal diameter: 5 mm; length under the head position of the screw: 13 mm), as shown in Fig 5.2. HS screws are generally used for the screwed connection of cold-formed steel structures. Pilot holes with a diameter of 2 mm in were drilled into the screwed connecting portion. As shown in Fig 5.1, these specimens exhibited grips (length: 150 mm) at the upper and lower ends. The grips ensured that the entire specimens were in the center of the test machine. In total, three types of connection specimens were used in this study. The number of HS screws (Fig 5.3) in the connection was different between these specimens, which were two, four, and eight. The two-screwed connection specimens were used to examine the post-fire shear failure mode of the screws in the sheet connections. The connection specimen was designed to ensure sufficient strength of the steel sheet compared with the shear strength of two screws following the heating and cooling procedures. The four- and eight-screwed connection specimens were used to examine the probability of a change in failure modes by the heating and cooling procedures. The screwed connection specimens are listed in Table 5.1. For the screwed connection specimens, the end distance, $e_1$, from the center of the screw hole to the end line of the steel sheet was 15 mm, which was three times larger than the nominal screw diameter (d=5 mm) and designed to adhere to the EC3 [5.1] requirements for end distance ($e_1 \geq 1.5d$). According to EC3 [5.1], the end distance ($e_1$) (Fig 3.1) refers to the edge that is oriented in the same direction as the axial force. According to the specifications, the distance

between the centers of screws must not be <3d, and the distance from the center of a screw to the edge of the steel sheet must be at least 1.5d ($p_1, p_2 \geqslant 3d$, $e_2 \geqslant 1.5d$), as shown in Fig 3.1. To investigate the post-fire mechanical properties of the steel sheets, tensile tests were conducted on steel sheet specimens with length, width, and thickness of 550, 80, and 1.6 mm, respectively, after the heating and cooling procedures. (Fig 5.1)
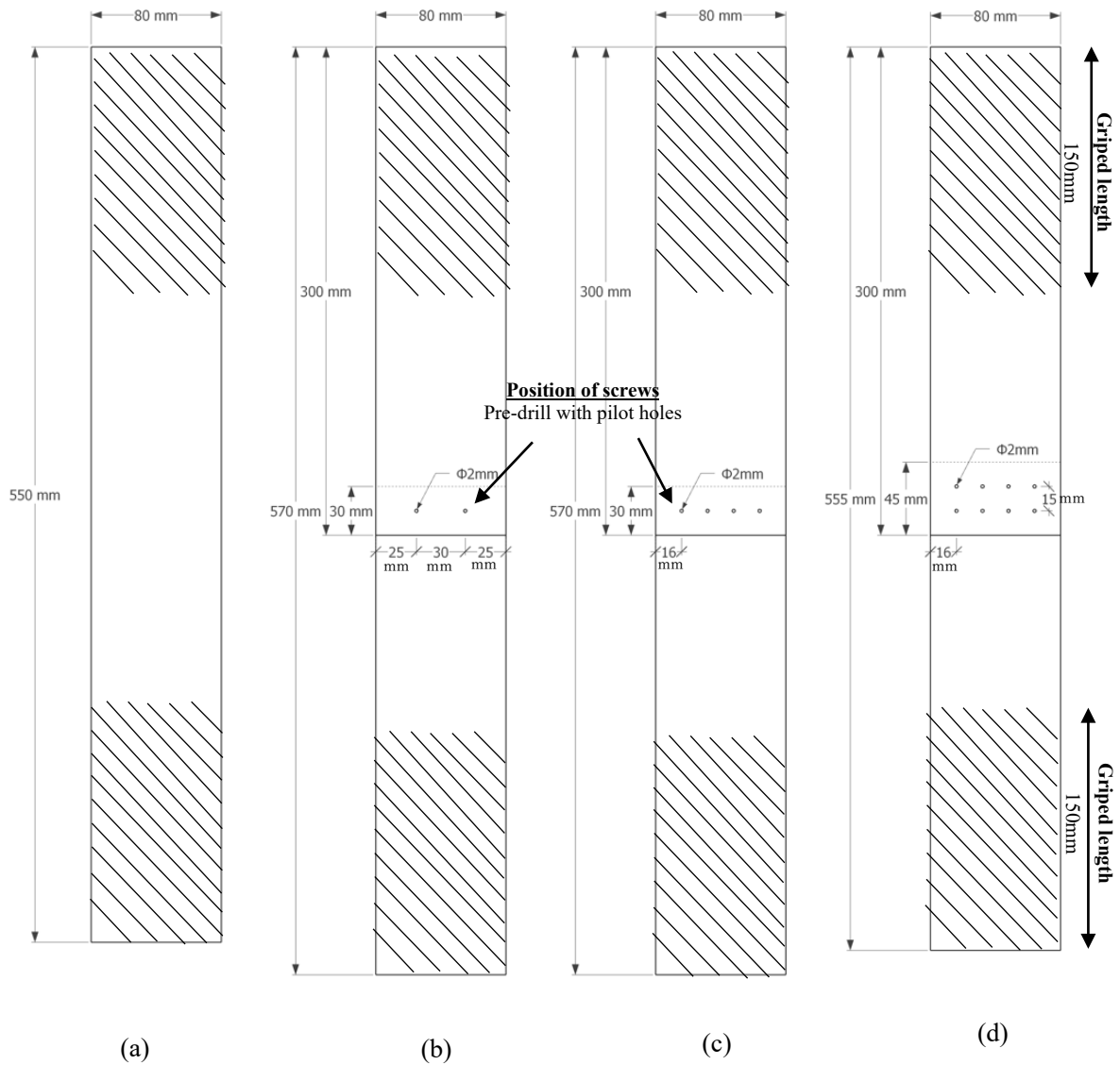


Fig5.1 Details of steel sheet specimens and screwed connection specimens

Table 5.1 Details of screwed connection specimens

| | Screw type | Steel sheet | Connection |
|---|---|---|---|
| **Screwed connection** | HS specimen<br>Diameter: 5mm<br><br>Length under screw head position: 15mm<br>Number of screws: 2, 4 and 8 | SPHC (JIS G 3131)<br>Thickness: 1.6mm<br>Width: 80mm<br><br>Number of sheets: 2 | Single one-lapped connection<br>Pitch length between screws: 30 and 16 mm<br>Edge distance: 25 and 16mm |



Fig5.2. Screw used for screwed connections
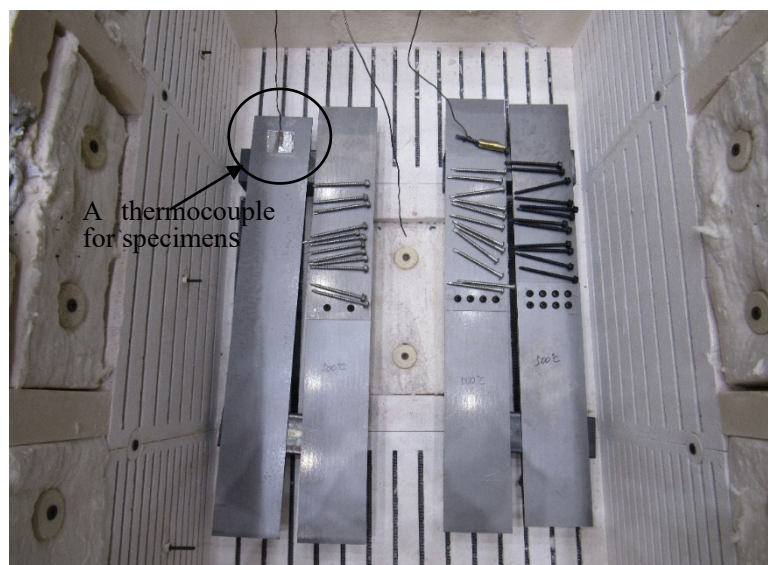


Fig5.3 Steel sheets and screwed-connection specimens in a furnace

74

## 5.2.2 The Heating and Cooling Processes

The heating and cooling procedures were the same as those used for the shear tests on screws described in Chapters 2, 3 and 4. Six target test temperatures of 20 (untreated specimens), 400, 500, 600, 700, and 800°C were employed for tensile tests on steel sheets (Fig 5.1(a)); furthermore, seven target temperatures of 20 (untreated specimens for the experiment), 400, 500, 600, 700, 750, and 800°C were employed for tensile tests on screwed-connection (Fig 5.1(b)–(d)). The steel sheet and screwed-connection specimens were subjected to the same heating and cooling procedures in the same electric furnace. A sheathed thermocouple (sheathed diameter of thermocouple: 1.6 mm) was attached to the steel sheet (Fig 5.3) 50 mm from the end of the specimens, and the measured temperature confirmedly reached the target temperature. These test specimens were held at the target temperature for 30 min to ensure uniform temperature distribution. Subsequently, the furnace was switched off, and the specimens were cooled in the furnace.

## 5.2.3 The tensile tests for heated specimens at ambient temperature

As shown in Fig 5.4, the same testing machine was used to perform the tensile tests on the screwed-connection specimens at ambient temperature. The steel sheet and screwed-connection specimens were set on the test machine. The grips of 150 mm on their upper and lower ends secured the position of screws in the center of the test machine. Furthermore, two contact high-sensitive displacement transducers were placed at the upper and lower measurement points of the universal testing machine to measure the deformation of specimens, as shown in Fig 5.4. The tensile force, $P$, was applied to the screwed connection specimen.

Fig 5.4 Test set-up of screwed connection specimens

## 5.3 Experimental results of steel sheets and screwed connections after heating and cooling processes

Fig 5.5 shows the relationships between time and temperature during the heating and cooling procedures. As shown in Fig 5.5, the test specimens reached the target temperature. The cooling rate was 0.5–2 ℃/min.

Fig 5.6 shows the relationships between the load and deformation of steel-sheet and screwed-connection specimens. The mechanical properties of steel sheets, including chemical metal and the nominal tensile strength, are listed in Table 5.2. The post-fire tensile test results on the maximum tensile load obtained from the tests on the screwed-connection specimens are summarized in Table 5.3. Moreover, the experimental results of the two-screw connection specimens after the fire, which exhibited screw shear failure modes, were compared to the shear test results for HS screws presented in Chapter 4, as shown in Fig 5.7. As shown in Fig 5.7, both results have a similar tendency with the heated temperature increasing. However, when the heating temperature was 500℃, the post-fire shear strength of the HS screws was lower than that of the two-screwed connection specimens, which were affected by the increasing post-fire tensile strength of the steel sheets under 500℃. Furthermore, Fig 5.8 shows the photographs of the screwed-connection specimens after the tensile tests.
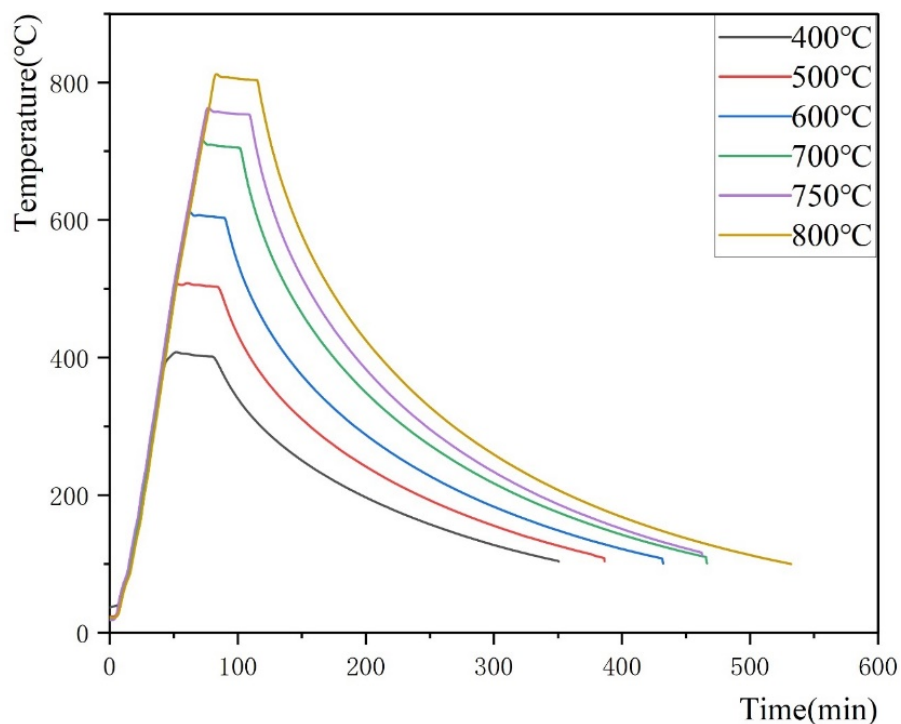


Fig 5.5 Relationships between time and temperature during the heating and cooling procedures

77
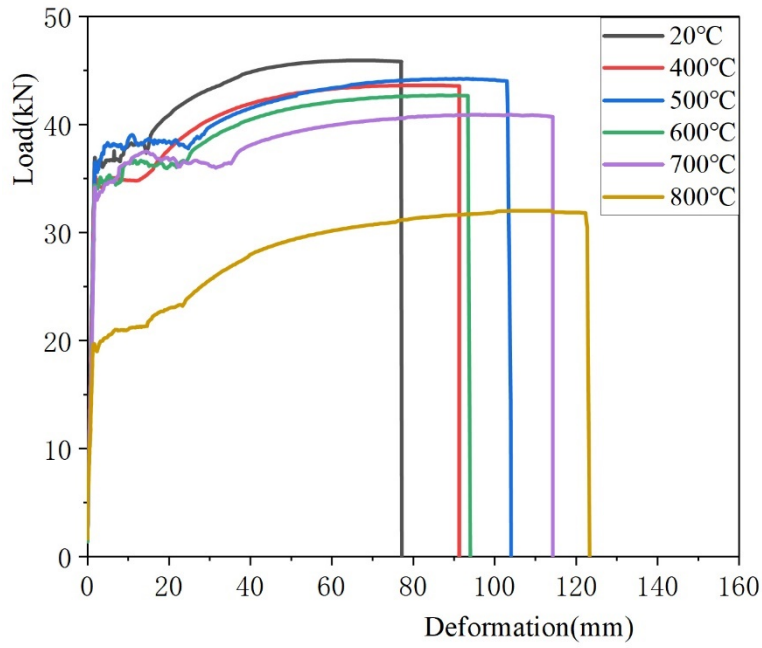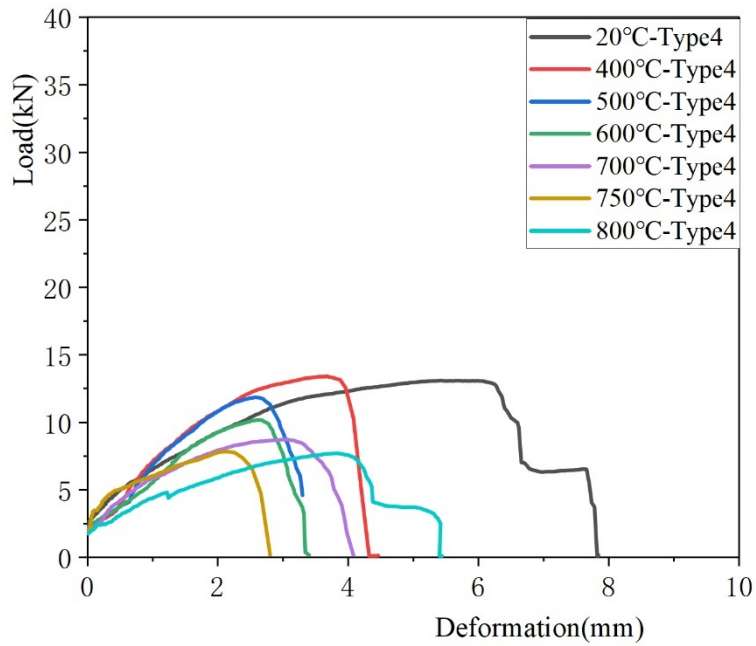
(a)Steel sheets



(b)Two-screwed connections

(Type2: Sheet bearing failure; Type3: Sheet net-section failure; Type4: Screw shear failure)

Fig 5.6 Relationships between load and deformation for steel sheets and screwed connections
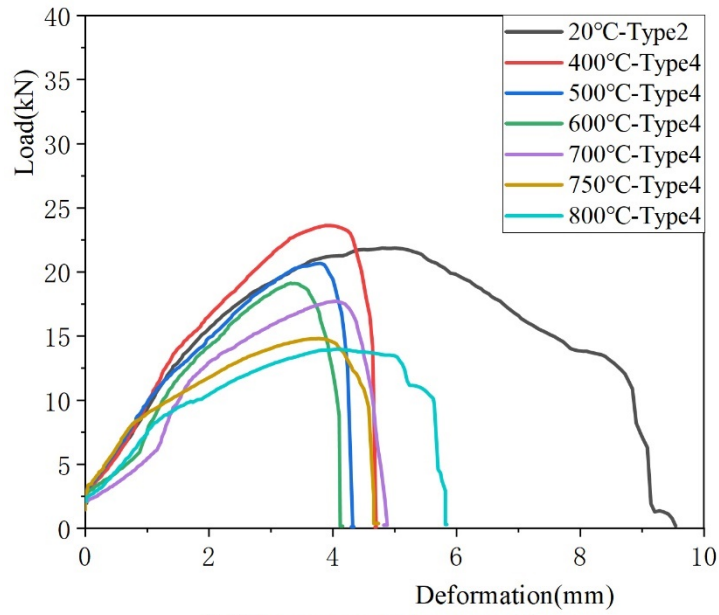
(c)Four-screwed connections
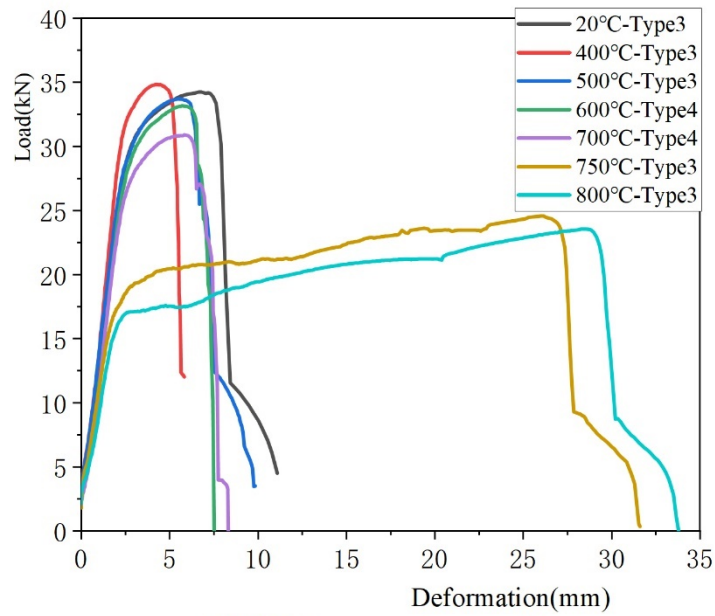


(d)Eight-screwed connections

(Type2: Sheet bearing failure; Type3: Sheet net-section failure; Type4: Screw shear failure)

Fig5.6 Relationships between load and deformation for steel sheets and screwed connections (Connected)
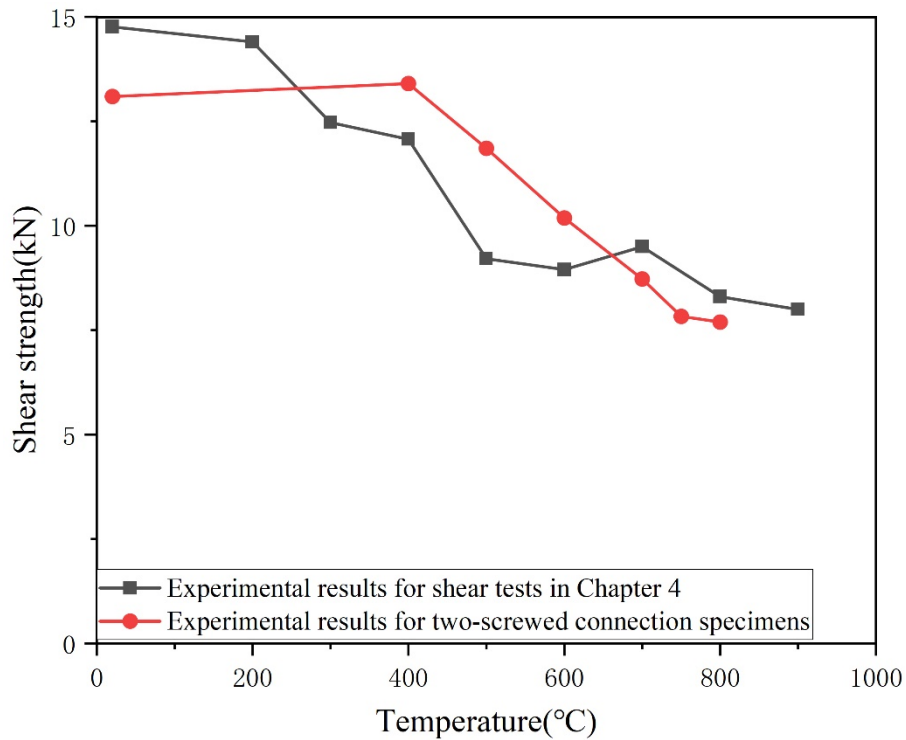
Fig 5.7 Comparison results between the shear tests of HS screws and the two-screwed connection specimens after fire

Table 5.2 Chemical compositions and mechanical properties of SPHC (JIS G 3131:2018)

| | Chemical Metal(mass%) | | | | Tensile strength (N/mm²) |
|---|---|---|---|---|---|
| SPHC | *C* | *Mn* | *P* | *S* | |
| | 0.12 | 0.60 | 0.045 | 0.035 | 270~440 |

Table 5.3 Results of tensile tests for steel sheets after heating and cooling procedures

| Temperature (°C) | Yield stress (MPa) | Reduction factor of yield stress | Tensile strength (MPa) | Reduction factor of tensile strength |
|---|---|---|---|---|
| 20°C (Untreated) | 288.5 | 1.0 | 358.9 | 1.0 |
| 400°C | 274.0 | 0.95 | 340.9 | 0.95 |
| 500°C | 285.3 | 0.99 | 345.6 | 0.96 |
| 600°C | 268.8 | 0.93 | 333.6 | 0.93 |
| 700°C | 267.3 | 0.93 | 319.5 | 0.89 |
| 800°C | 154.0 | 0.53 | 250.1 | 0.70 |

20°C(untreated)

Screw shear failure (Type4)



400°C

Screw shear failure (Type4)



500°C

Screw shear failure (Type4)



600°C

Screw shear failure (Type4)



700°C

Screw shear failure (Type4)



the holes of steel sheet are damaged
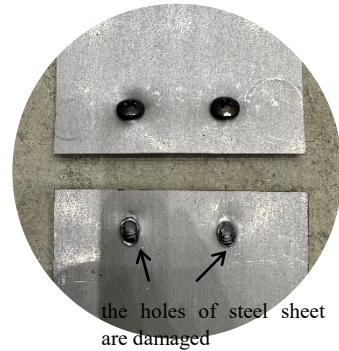
20°C(untreated)



750°C

Screw shear failure (Type4)



800°C

Screw shear failure (Type4)

(a) Two-screwed connection specimens after tests

Fig 5.8 Screwed connection specimens after tests

20℃(untreated)
Sheet bearing failure (Type2)

400℃
Screw shear failure (Type4)

500℃
Screw shear failure (Type4)

600℃
Screw shear failure (Type4)

700℃
Screw shear failure (Type4)

the holes of steel sheet are damaged

400℃

the holes of steel sheet are damaged

800℃

(b) Four-screwed connection specimens after tests

Fig 5.8 Screwed connection specimens after tests

750℃
Screw shear failure (Type4)

800℃
Screw shear failure (Type4)
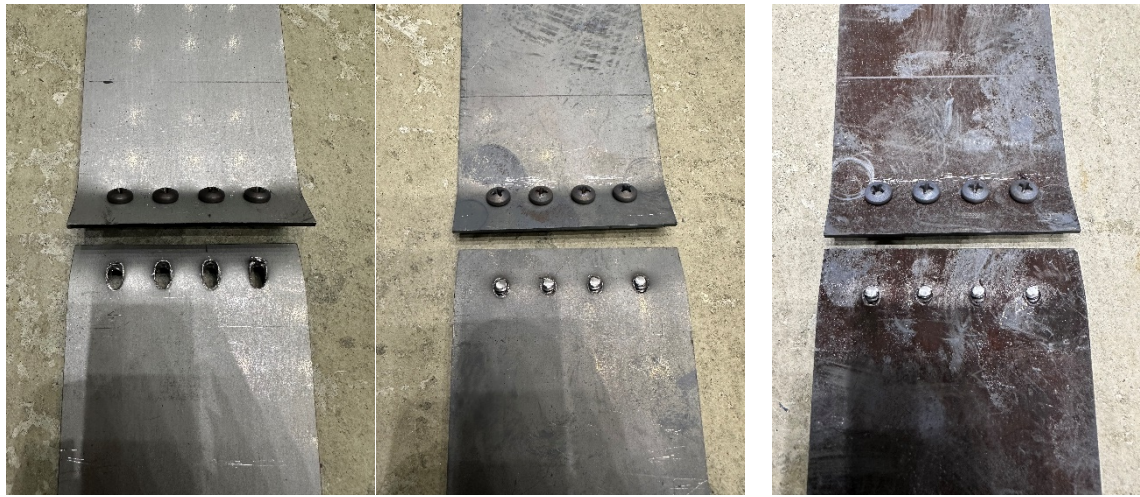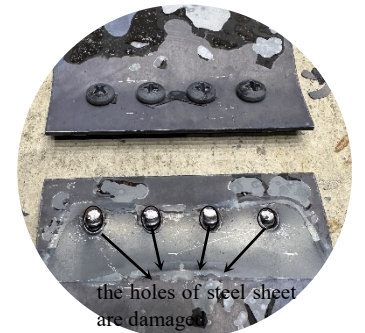
20℃(untreated)

Sheet net-section failure (Type3)

400℃

Sheet net-section failure (Type3)

500℃

Sheet net-section failure (Type3)

600℃

Screw shear failure (Type4)

700℃

Screw shear failure (Type4)

600℃

700℃

750℃

Sheet net-section failure (Type3)

800℃

Sheet net-section failure (Type3)

(c) Eight-screwed connection specimens after tests

Fig 5.8 Screwed connection specimens after tests

### 5.3.1 The steel sheet specimens

For steel-sheet specimens, the post-fire yield stress and tensile strength evidently decreased with the increase in the heated temperature. When exposed to 800 ℃ heated temperature, the tensile strength and yield stress of the steel-sheet specimens were reduced by 30% and 40%, respectively, compared with the untreated steel-sheet specimens (Fig 5.6 (a) and Table 5.3). The previously obtained results of post-fire yield strength and tensile strength (JIS SS400 by AIJ [5.2], Q690 by Li et al. [5.3], and Q235 by Zhang et al. [5.4]) were compared with those obtained in this study, as shown in Fig 5.9. The values of the post-fire yield strength and ultimate strength reduction factors of SPHC, JIS SS400, and Q235 steels were similar to those obtained for <700 ℃, whereas those of SPHC decreased by approximately 40% for 800 ℃. In addition, the post-fired yield strength and tensile reduction factors of SPHC and Q690 steel decreased with increasing heated temperature for >500 ℃.
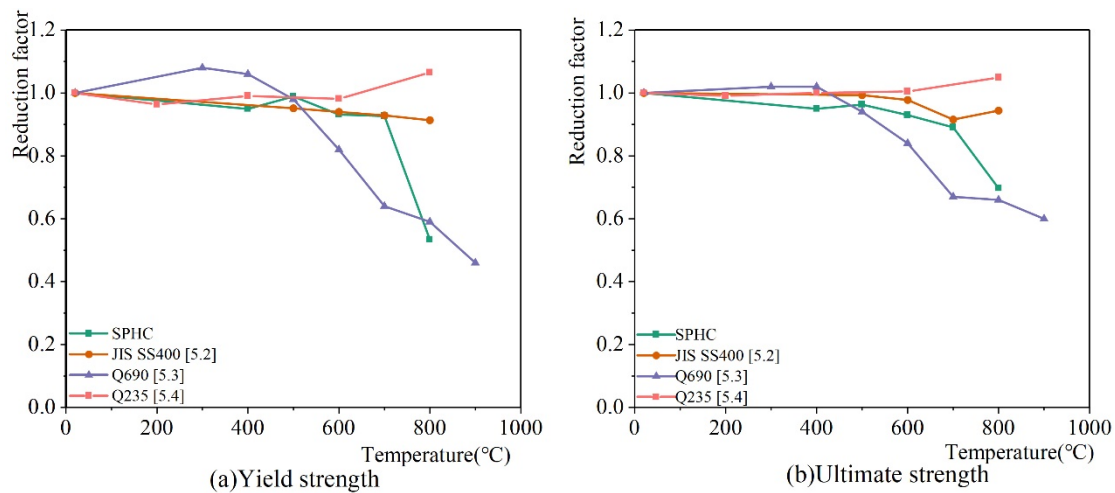


Fig 5.9 Comparison of post-fire mechanical properties for SPHC, JIS SS400, Q690 and Q235

### 5.3.2 Two-screwed connections

In this study, three types of failure modes for the screwed connection specimens were observed. For the two-screwed connection specimens (Fig 5.8(a)), screw shear failure modes (referred to as Type 4, Fig 3.2(d)) were observed in all heated temperature tests. Fig 3.2 shows four types of failure modes which were proposed as the same as that at elevated temperatures in Chapter 3.

For the two-screwed specimens (Fig5.6 (b) and Table 5.4), the post-fire strength of specimens decreased with increasing heated temperature. The untreated specimen deformed more than the others experiencing heating temperatures. This was owing to the bearing failure around the holes in the sheets (Fig 5.8(a)). The strength and deformation capacities of the two-screwed connections were lower than those of the steel sheets.

Table 5.4 Test results of screwed connections after heating and cooling procedures

| Temperature(℃) | Two-screwed connection | | Four-screwed connection | | Eight-screwed connection | |
| | Maximum load values(kN) | Failure mode | Maximum load values(kN) | Failure mode | Maximum load values(kN) | Failure mode |
| --- | --- | --- | --- | --- | --- | --- |
| 20℃ (Untreated) | 13.09 | Type4 | 21.86 | Type2 | 34.24 | Type3 |
| 400 | 13.40 | Type4 | 23.62 | Type4 | 34.83 | Type3 |
| 500 | 11.85 | Type4 | 20.68 | Type4 | 33.70 | Type3 |
| 600 | 10.19 | Type4 | 19.12 | Type4 | 33.12 | Type4 |
| 700 | 8.73 | Type4 | 17.71 | Type4 | 30.89 | Type4 |
| 750 | 7.83 | Type4 | 14.81 | Type4 | 24.57 | Type3 |
| 800 | 7.69 | Type4 | 13.98 | Type4 | 23.56 | Type3 |

### 5.3.3 Four-screwed connections

For the four-screwed connection specimens (Fig 5.8(b)), in the case of the untreated specimen, the sheet bearing failure around the screw holes (referred to as Type 2, Fig 3.2(b)) was observed; however, the screws were not fractured. Whereas, in other cases of 400–800 ℃ heating and cooling procedures, screw shear failure (Type 4) modes were observed.

Fig 5.6(c) and Table 5.4 show the test results of the four-screwed specimens. The tensile strength decreased with the increase in the heated temperature. The untreated specimen exhibited a larger deformation capacity than the other four-screwed connection specimens. This is owing to the plastic deformation and bearing failure around the screw holes (the sheet bearing failure (Type 2) (Fig 5.8(b)) observed in the untreated specimen. However, the deformation capacity remained almost unchanged for the specimens that experienced the heated temperature and underwent the screw shear failure (Type 4). In addition, the ultimate strength of the four-screwed specimens increased compared with the two-screwed specimens.

### 5.3.4 Eight-screwed connections

For the eight-screwed connection specimens (Fig 5.8(c)), sheet net-section failure (referred to as Type 3, Fig 3.2(c)) was observed for the untreated specimens and those treated at 400, 500, 750, and 800 ℃. However, the screw shear failure (Type 4) modes occurred when the heated temperatures were 600 and 700 ℃. These were proposed as the failure modes of the screwed-connection at elevated temperatures in Fig 3.2. The sheet longitudinal shear failure (referred to as Type 1, Fig 3.2 (a)) was not observed in this study.

For the eight-screwed specimens (Fig 5.6(d) and Table 5.4), the deformation capacities remained almost unchanged when the heated temperatures were lower than 700 ℃. However, when exposed to the heated temperatures of 750 and 800 ℃, the specimens showed large deformation, and the failure modes changed from the screw shear failure mode (Type 4) to the sheet net-section failure mode (Type 3).

## 5.4 Proposal equations based on failure modes for self-drilling screw connections after heating and cooling processes

Each post-fire failure mode of the screwed connection referred to in the study corresponds to those mentioned in Chapter 3, that is, four failure modes of screwed connections at elevated temperatures. These modes were considered to investigate the change in failure modes and corresponding equations for the screwed connection after the heating and cooling procedures. These equations were based on the failure modes equations at the elevated temperature in Chapter3. In this study, the equations corresponding to the elevated temperatures were extended to the post-fire situations by employing the post-fire reduction factors of the screws and steel sheets shown in Fig 5.10.
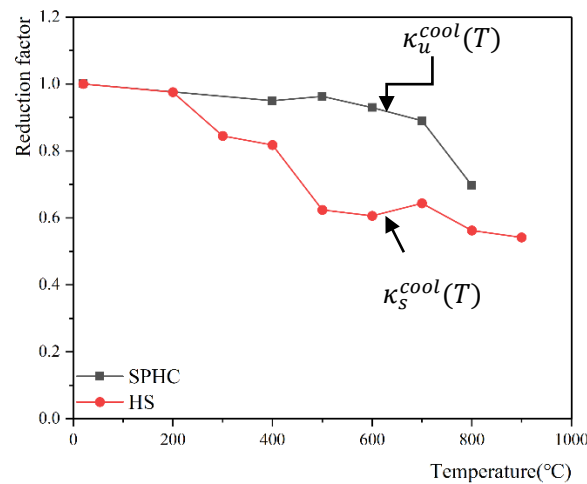


Fig 5.10 Reduction factors of HS screws and SPHC steel sheets

The following four equations were proposed for the post-fire failure modes:

(1) Sheet longitudinal shear failure after the heating and cooling procedures (Type 1, Fig 3.2(a))

In this case, the sheet fractures were due to the limited edge distances in the screwed connection. However, sheet longitudinal shear failure (Type1) was not observed in this study. The shear strength for the sheet longitudinal shear failure $P_u$ can be estimated by

$$P_u = F_u t e \kappa_u^{cool}(T) \tag{5.1}$$

where $F_u$ is the tensile strength (in this study, $F_u$ = 358.9 MPa) of the steel sheets at the ambient temperature, $e$ is the edge distance (screwed-connection specimen: 15 mm) in the connection, $t$ is the sheet thickness (1.6 mm), and $\kappa_u^{cool}(T)$ is the reduction factor of the post-fire tensile strength of the steel sheet after experiencing temperature $T$ (Fig 5.10 and Table 5.3).

(2) Sheet bearing failure after the heating and cooling procedures (Type 2, Fig 3.2(b))

This failure is caused by the sheet fractures due to the large diameter of the hole drilled in the thin sheet. This failure mode easily occurs for the connections with large numbers of screws (large screw shear strength). The shear strength for the sheet bearing failure $P_n$ can be estimated by

$$P_n = \alpha n t d F_u \kappa_u^{cool}(T) \tag{5.2}$$

86

in which, if $t_2 / t_1 = 1.0$, $\alpha = 3.2\sqrt{t/d} \leq 2.1$; if $t_2 / t_1 \geq 2.5$ and $t_1 < 1.0mm$, $\alpha = 3.2\sqrt{t/d} \leq 2.1$; if $t_2/t_1 \geq 2.5$ and $t_1 \geq 1.0mm$, $\alpha = 2.1$; otherwise, if $1.0 < t_2/t_1 < 2.5$, then obtain $\alpha$ by linear interpolation ( $t_1$ and $t_2$ are the thicknesses of connected steel sheets respectively); $t$ is the thinnest of the two steel sheets; $n$ is the total number of screws, and $d$ is the nominal screw diameter.

(3) Sheet net-section failure after the heating and cooling procedures (Type 3, Fig 3.2(c))

This failure mode occurs for screwed connections with large hole diameters and a large number of holes in the sheet. The post-fire shear strength for the sheet net section failure $P_{net}$ can be estimated by

$$P_{net} = F_u A_e \kappa_u^{cool}(T) \tag{5.3}$$

where $A_e$ is the net cross-sectional area of the steel sheet.

(4) Screw shear failure after the heating and cooling procedure (Type 4, Fig 3.2(d))

The screw shear fracture occurs for the screwed connection with small numbers of the screws, such as the two-screwed connections. The post-fire shear strength at the screw shear failure $P_s$ can be estimated by

$$P_s = mn A_s \tau_s \kappa_s^{cool}(T) \tag{5.4}$$

where $m$ is the number of shear surfaces, $n$ is the total number of screws (2, 4 or 8), $A_s$ is the nominal sectional area of the screw, $\tau_s$ is the post-fire shear strength of the HS screw at the ambient temperature (Fig4.7(a)), and $\kappa_s^{cool}(T)$ is the reduction factor of the post-fire shear strength of the HS screw after experiencing temperature $T$ (Fig 5.10 and Table 4.3).

## 5.5 Discussions between experimental results and proposal equations

According to the screwed connection tests (Section 5.3), Type 2–4 failure modes were observed. Fig 5.11 shows the tensile strength (solid lines) estimated from the above equations corresponding to each failure mode. The test results of the two-, four-, and eight-screwed connection specimens are shown by the marks ("●": Type2, "◆": Type3, "■": Type4) in .

For two-screwed connection specimens, the shear strengths, $P_s$, (Type4) obtained from Eq. (5.7) approximated the experimental results (Type 4), as shown in (a). However, the shear strength at the sheet bearing failure (Type 2, black line) was the lowest for the untreated two-screwed connection specimens; the theoretical calculation result were obtained using Eq. (5.2). The steel sheets around the holes of the untreated specimens exhibited sheet bearing failure, as shown in Fig 5.8(a). The calculated values of the sheet bearing failure (Type 2) and screw shear failure (Type 4) were approximately the same at any heated temperature. Therefore, the screw shear failure (Type 4) occurred while the steel sheets exhibited strength hardening with sheet bearing failure.

For untreated four-screwed connection specimens, the post-fire shear strength ($P_n$) at the sheet bearing failure (Type 2) calculated using Eq. (5.2) was considerably low (Fig 5.11(b)). Furthermore, the untreated four-screwed connection specimens underwent the sheet bearing failure mode (Type 2), as shown in Fig 5.8(b). However, owing to the significant reduction in the

post-fire reduction factor of screws with the increase in the heated temperature, the untreated four-screwed connection specimens underwent screw shear failure mode (Type 4) (Fig 5.8(b)). Correspondingly, the calculated shear strengths of screw shear failure (Type 4) were the lowest in the same situations. Although the calculated value of the shear strength at the sheet bearing failure (Type 2, black line) was the lowest for the heated temperature of 400 °C, bearing failure around the screw holes (Type 2) was observed (Fig 5.8(b)). In the experimental results, the screw shear failure (Type 4) occurred as mentioned above.

For eight-screwed connection specimens, sheet net-section failure (Type 3) occurred owing to the large number of screws. As shown in Fig 5.11(c), the calculation result of sheet net-section failure (Type 3) was the lowest, and the shear strength ($P_s$) of screws was much greater than that of steel sheets ($P_{net}$). Furthermore, the calculation results of sheet net-section failure (Type 3) for eight-screwed connections and four-screwed connections were lower than those for two-screwed connections because of the smaller net cross-sectional area of the steel sheet. However, for the heated temperatures of 500 and 600 °C, the calculated values of the post-fire shear strengths, $P_{net}$ and $P_s$, for the sheet net-section failure mode (Type 3) and screw shear failure (Type 4) matched closely owing to the significant reduction in the post-fire reduction factor of HS screws. Therefore, the screw shear failure modes (Type 4) occurred after experiencing 600 and 700 °C.

Although the experimental failure modes differed from the theoretical calculation results in some cases, the experimental results were almost consistent with the lowest value based on the equations proposed in this study. Therefore, the post-fire strength and failure modes of the screwed connections after heating and cooling can be evaluated by the proposed equations.

## 5.6 Conclusions

Tensile tests were performed on the single overlapped screwed connections using HS screws and steel sheets after heating and cooling procedures to evaluate the post-fire shear strength and load-bearing capacity of screwed connections.

The two-screwed connection specimens exhibited screw shear failure regardless of the heated temperature; the untreated four-screwed connection specimens underwent sheet bearing failure. Whereas, screw shear failure modes occurred in other cases of experiencing 400–800 °C heating and cooling procedures. Moreover, for the eight-screwed connection specimens, screw shear failure modes occurred when the heated temperatures were 600 and 700 °C, and sheet net-section failure was observed in other conditions. That is, failure modes changed even when screwed connections of the same specification were used.

Equations were proposed to calculate the post-fire shear strength of the screwed connection using the post-fire reduction factors for both sheet tensile and screw shear strengths. The aforementioned failure mode transitions can be explained by assessing the post-fire tensile strengths corresponding to each failure mode. Furthermore, these equations can be used to evaluate the post-fire loading capacities of screwed connections corresponding to each failure

mode.
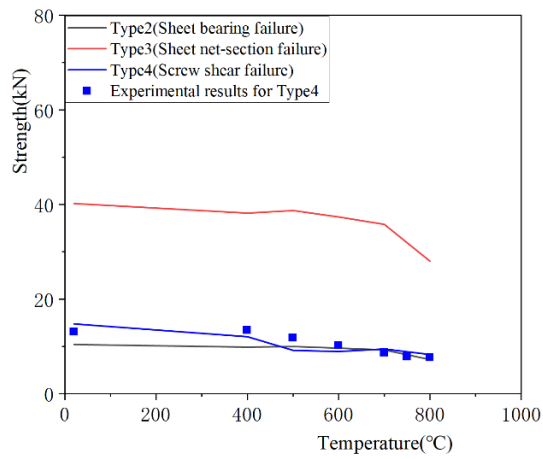


(a) Two-screwed connections
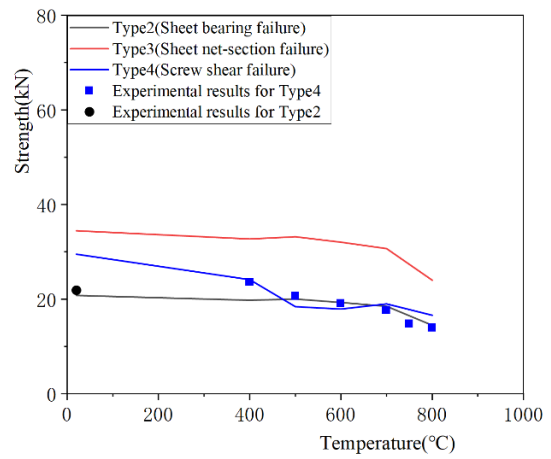


(b) Four-screwed connections
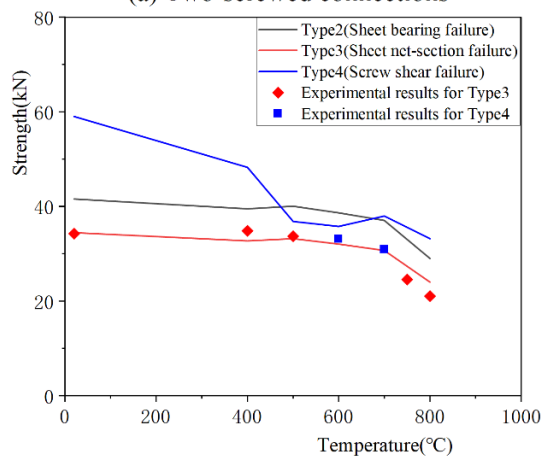


(c) Eight-screwed connections

Fig 5.11 Comparison results between experimental and calculation results for screwed connections

## References

[5.1] EN 1993-1-3 (2006), Eurocode 3 – Design of Steel Structures – Part 1-3: General Rules Supplementary Rules for Cold-Formed Members and Sheeting.

[5.2] Architectural Institute of Japan (AIJ) (2017), AIJ Guide Book for Fire-Resistive Performance of Structural Materials, Maruzen Publishing Co., Tokyo (in Japanese).

[5.3] Li, G.-Q., Lyu, H., Zhang, C., 2017. Post-fire mechanical properties of high strength Q690 structural steel. Journal of Constructional Steel Research 132, 108–116.

[5.4] Y.J. Zhang, Y. Zhu, S. Zhao, K.X. Hu, Experimental research on mechanical properties of steel cooled in different modes after high temperature treatment, Struct. Eng. 25 (5) (2009) 104–109. (in Chinese).

[5.5] Ozaki, F., Liu, Y., Ye, K., 2022. Tensile and shear strength for a self-drilling screw and transition of failure modes and shear-strengths for self-drilling screwed connections at elevated-temperatures. J. Struct. Fire Eng. 13, 321–346

[5.6] American Iron and Steel Institute. North American Specification for the Design of CFS Structural Members, AISI S100-12[S]. Washington, DC, USA, 2012.

# Chapter 6 Evaluation method based on failure modes and collapse temperatures for screw connections in/after fire

## 6.1 Introduction

This chapter presents an evaluation method based on failure modes and failure temperatures for screw connections in/after fire. This evaluation method involves varying parameters, including different sheet thicknesses of screwed-connections and loads which are based on designing by Guide for Designing Cold-formed Steel Structures 2nd Edition [6.1]. Subsequently, the theoretical evaluation formulas proposed in Chapters 3 and 5 for elevated temperatures and post-fire conditions, are employed to calculate and investigate the failure modes and failure temperatures. This ensures the structural integrity and safety of cold-formed steel structures at elevated temperatures and provides essential data for post-fire repair and reuse efforts, as well as investigating the residual strength after fire.

## 6.2 Details of evaluation method for screw connections

### 6.2.1 Structural calculation for screwed connection for cold-formed steel structures in Japan

The Guide for Designing Cold-formed Steel Structures 2nd Edition [6.1] outlines the structural calculation of the allowable shearing stress of the screwed connections based on four failure modes as shown in Fig 6.1. The allowable shearing stress is determined by the minimum value Eq. (6.1) of the screw pull-out failure formula Eq. (6.2), the sheet bearing failure formula for the screw head side steel sheet Eq. (6.3), the sheet bearing failure formula for the screw tip side steel sheet Eq. (6.4) and the screw shear failure formula Eq. (6.5). The allowable shear strength can be obtained by multiplying this allowable stress by the cross-sectional area of the screw determined by the nominal diameter of the screw. In calculating the allowable shear strength of a screwed connection, it is necessary to consider that the actual thickness of the steel may be less than the nominal thickness due to variations. Therefore, 90% of the nominal thickness is used as the design thickness. The long-term allowable shear strengths $Ras$(N) of each drilling screw are expressed as follows:

$$Ras = \min{(Ras1, Ras2, Ras3, Ras4)} \tag{6.1}$$

$$Ras1 = 2.2\eta^{0.5}(\tfrac{t_2}{d})^{1.5}F_2A_d, \ \eta = 3.1 - 5.6\left(\tfrac{t_1}{t_2}\right) + 3.5(\tfrac{t_1}{t_2})^2 \tag{6.2}$$

$$Ras2 = 0.43\left\{0.6 + 12\left(\tfrac{t_2}{d}\right)\right\}\left(\tfrac{t_1}{d}\right)F_1A_d \tag{6.3}$$

$$Ras3 = 0.43\left\{1.5 + 6.7\left(\tfrac{t_1}{d}\right)\right\}\left(\tfrac{t_2}{d}\right)F_2A_d \tag{6.4}$$

$$Ras4 = \left(\frac{F_d}{1.5\sqrt{3}}\right)A_{de} \qquad (6.5)$$

Where Ras1= Long-term allowable shear strength for the screw pull-out failure (N)

Ras2= Long-term allowable shear strength for the screw head side steel sheet failure (N)

Ras3= Long-term allowable shear strength for the screw tip side steel sheet failure (N)

Ras4= Long-term allowable shear strength for the screw shear failure (N)

$t_1$= Design thickness of screw head side steel plate (90% of nominal thickness) (mm)

$t_2$= Design thickness of screw tip side steel plate (90% of nominal thickness) (mm)

$F_1$= Standard strength of allowable stress for head side steel sheet (=235N/mm²)

$F_2$= Standard strength of allowable stress for tip side steel sheet (=235N/mm²)

$d$= Nominal diameter of drill screw (=4.8mm)

$F_d$= Standard strength of allowable stress for drill screw (=570 N/mm²)

$A_d$= Cross-sectional area of drill screw ($\pi d^2/4$) (mm²)

$A_{de}$= Effective cross-sectional area of drill screw ($0.55A_d$) (mm²)
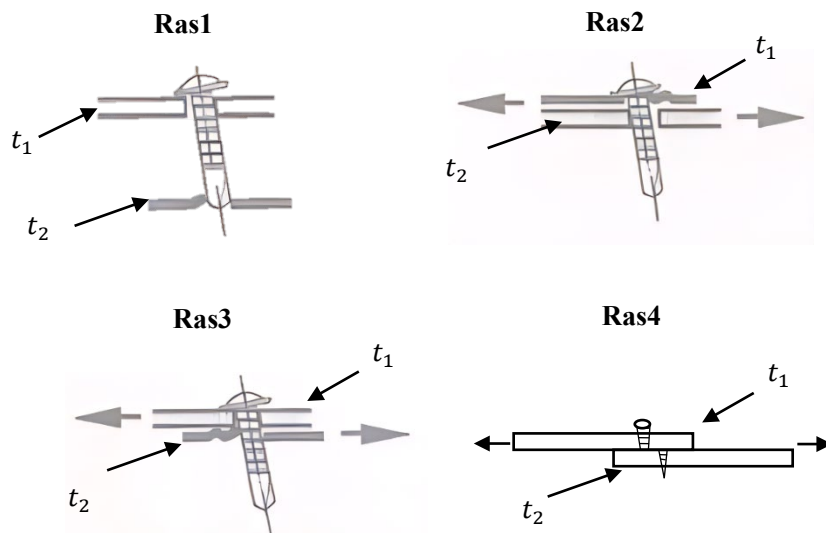


Fig 6.1 Failure modes of structural calculation for screwed connections

### 6.2.2 Details of parametrically designed screwed-connections

In order to investigate the performance of the design screwed-connection specimens during and after exposure to fire, the design screwed-connection specimens were connected with different sheet thicknesses according to the four design failure modes described in Section 6.2.1. Furthermore, in order to ascertain the influence of load on the screwed-connection specimens, different loads were applied to the same specimens. The details of four screwed-connection specimens and loads are shown in Table 6.1 and Fig 6.2. The edge distances of these design specimens meet Eurocode 3[6.2] specification requirements. The arrangements of screwed-connections are shown in Fig 6.2:

(a) When $t_1$=1.2 mm and $t_2$=1.6 mm, according to the structural design calculations based on section 6.2.1, a total of 5 screws are required to support a load of 6.5 kN. These screws are arranged in two rows, with 2 screws in one row and 3 screws in the other. For a load of 12 kN, a total of 9 screws are required, with 4 screws in one row and 5 screws in the other, as shown in Fig 6.2(a) and Table 6.1.

(b) When $t_1$=1.0 mm and $t_2$=2.3 mm, according to the structural design calculations based on section 6.2.1, a total of 3 screws are required to support a load of 5.5 kN in one row; For a load of 11kN, a total of 9 screws are required, with 3 screws in each row as shown in Fig 6.2(b) and Table 6.1.

(b) When $t_1$=3.2 mm and $t_2$=1.0 mm, according to the structural design calculations based on section 6.2.1, a total of 3 screws are required to support a load of 5.5 kN in one row; For a load of 11kN, a total of 9 screws are required, with 3 screws in each row as shown in Fig 6.2(c) and Table 6.1.

(b) When $t_1$=1.6 mm and $t_2$=3.2 mm, according to the structural design calculations based on section 6.2.1, a total of 4 screws are required to support a load of 8kN in one row; For a load of 16kN, a total of 8 screws are required, with 4 screws in each row as shown in Fig 6.2(d) and Table 6.1.

The width of steel sheets for all of the design specimens is 90mm. These specimens meet the requirements specified in EC3 [6.2] and AISI S100 [6.3] that the distance between the centers of screws shall not be less than $3d$ ($p_1,p_2 \geq 3d$) and the distance from the center of a screw to the edge of any part shall not be less than 1.5d ($e_1,$ $e_2 \geq 1.5d$), as shown in the Fig 3.1.

Table 6.1 The details of four screwed-connection specimens

| Design mode of allowable shearing stress (Ras1,Ras2,Ras3,Ras4) | $\bar{p}$ | Load(kN) ($P_{load}$) | steel thickness side of the screw head($t_1$) | steel thickness side of the screw tip($t_2$) | number of screws |
|---|---|---|---|---|---|
| Ras1 | 0.30 | 6.5kN | 1.2 | 1.6 | 5 |
| | 0.60 | 12kN | 1.2 | 1.6 | 9 |
| Ras2 | 0.31 | 5.5kN | 1.0 | 2.3 | 3 |
| | 0.62 | 11kN | 1.0 | 2.3 | 6 |
| Ras3 | 0.31 | 5.5kN | 3.2 | 1.0 | 3 |
| | 0.62 | 11kN | 3.2 | 1.0 | 6 |
| Ras4 | 0.30 | 8kN | 1.6 | 3.2 | 4 |
| | 0.60 | 16kN | 1.6 | 3.2 | 8 |

(a) $t_1$=1.2mm, $t_2$=1.6mm        (b) $t_1$=1.0mm, $t_2$=2.3mm

(c) $t_1$=3.2mm, $t_2$=1.0mm        (d) $t_1$=1.6mm, $t_2$=3.2mm
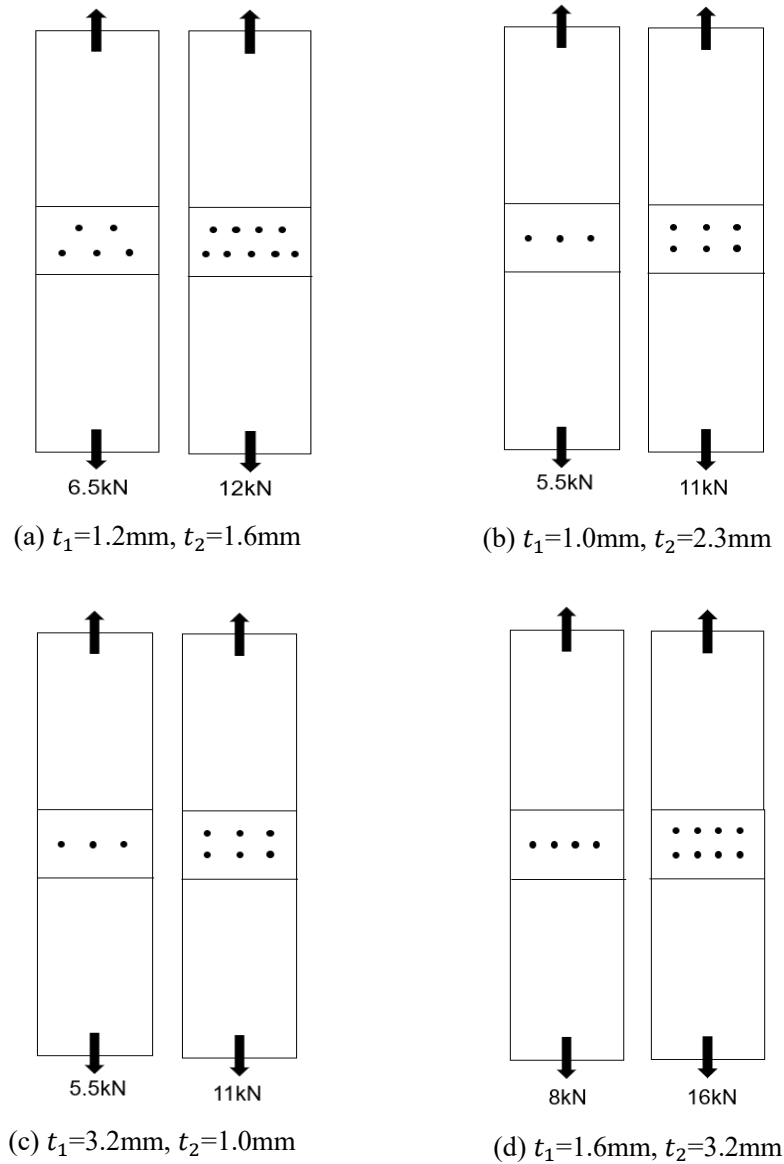
Fig 6.2 Details of design screwed connection specimens

## 6.3 Results and discussions of the parametric calculation of failure modes and failure temperatures in/after fire

To explore the performance of the above eight kinds of specimens at elevated temperatures and post-fire conditions, the theoretical evaluation formulas proposed in Chapters 3 and 5 for elevated temperatures and post-fire conditions, are employed to calculate and investigate the failure modes and collapse temperatures. Fig 6.3-6.6 and Table 6.2-6.5 show the results of failure modes and failure temperatures for screwed connections at elevated temperatures and post-fire conditions. The horizontals axis of Fig 6.3-6.6 are temperature and the verticals of Fig 6.3-6.6 are the values of strengths divided by load. Table 6.6 shows the results for the all of design screwed-connection specimens.

Following the conditions of $t_1$=1.2mm and $t_2$=1.6mm as shown in Fig 6.3 and Table 6.2, the failure mode is sheet bearing failure (Type 2) at a load of 6.5 kN under elevated temperature, with a collapse temperature of 584.2°C. At a load of 12 kN, the failure mode is the sheet net-section failure (Type 3), with a collapse temperature of 569.5°C. It can be observed that the collapse mode and collapse temperatures at elevated temperatures may vary depending on the applied load and the arrangement of screws. Then, after the heating and cooling processes, the screwed connections are not fractured and the residual strength was approximately twice that of the load at 800°C.

Under the conditions of $t_1$=1.0mm $t_2$=2.3mm as shown in Fig 6.4 and Table 6.3, whether at a load of 5.5kN or 11kN, the failure mode is sheet bearing failure (Type 2) at elevated temperature, with a collapse temperature of 540.9°C. The screwed connections are not fractured and the residual strength was approximately 1.5 times that of the load at 800°C after the heating and cooling processes.

Whether the load is 5.5kN or 11kN, sheet bearing failure (Type 2) at elevated temperature with a collapse temperature of 546.8°C is the failure mode under the case of $t_1$=3.2mm, $t_2$=1.0mm as shown in Fig 6.5 and Table 6.4. After the heating and cooling processes, the screwed connections remain intact, and the residual strength at 800°C was roughly 1.61 times that of the load.

Under the conditions of $t_1$=1.6mm $t_2$=3.2mm as shown in Fig 6.6 and Table 6.5, when the load applied 8kN, the failure mode is screw shear failure (Type 4) with a collapse temperature of 578.8°C. whereas, the failure mode is sheet net-section failure (Type 3) with a collapse temperature of 577.3°C when the load is applied 16kN. Moreover, even if the failure mode is not initially a screw shear failure mode at ambient temperature (20°C), it may shift to this mode at higher temperatures when the steel sheets are of greater thickness. A decreased net-section area of steel sheets has the effect of reducing the load-bearing capacity of the steel sheets. This results in a notable reduction in the tensile strength of the sheets and a corresponding decrease in their collapse temperature. Furthermore, the screwed connections are not fractured and the residual strength was approximately 1.9 times that of the load at 800°C after the heating and cooling processes.
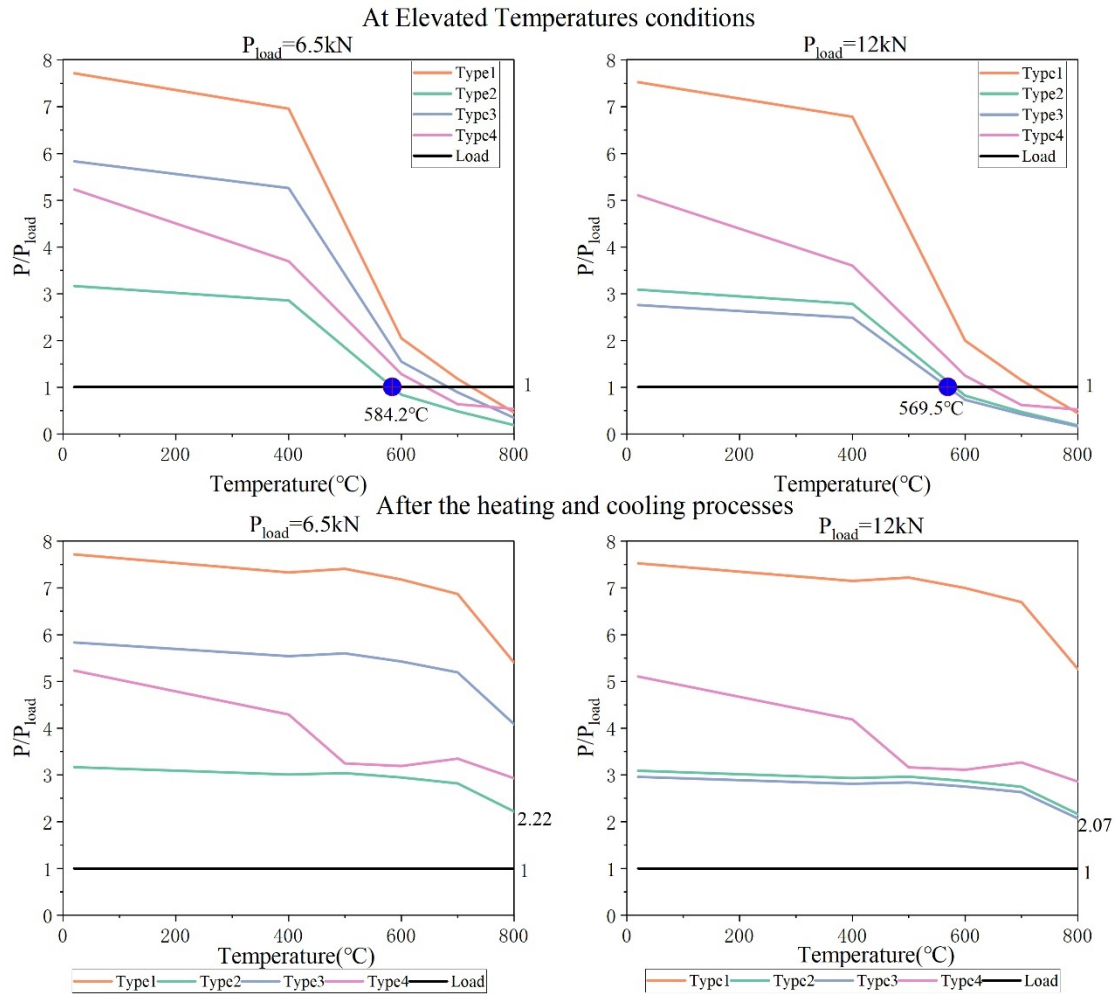
Fig6.3 The results for screwed connections when $t_1$=1.2mm and $t_2$=1.6mm

Table 6.2 The results for screwed connections when $t_1$=1.2mm and $t_2$=1.6mm

| $\bar{p}$ | Load(kN) (P_load) | t1 | t2 | Elevated temperatures | | | After fire | |
|---|---|---|---|---|---|---|---|---|
| | | | | failure mode | Collapse Temperature | Collapse Temperature | the failure mode for $P_{min}$ at 800°C | P/P_load |
| **0.30** | **6.5kN** | **1.2** | **1.6** | Type1 | 735.9 | N/A | Type2 | 2.22 |
| | | | | Type2 | 584.2 | N/A | | |
| | | | | Type3 | 695.5 | N/A | | |
| | | | | Type4 | 655.1 | N/A | | |
| **0.64** | **12kN** | **1.2** | **1.6** | Type1 | 721.7 | N/A | Type3 | 2.07 |
| | | | | Type2 | 581.7 | N/A | | |
| | | | | Type3 | 569.5 | N/A | | |
| | | | | Type4 | 639.8 | N/A | | |

Fig6.4 The results for screwed connections when $t_1$=1.0mm, $t_2$=2.3mm

Table 6.3 The results for screwed connections when $t_1$=1.0mm, $t_2$=2.3mm

| | | | | Elevated temperatures | | | After fire | |
|---|---|---|---|---|---|---|---|---|
| $\bar{p}$ | Load(kN) ($P_{load}$) | t1 | t2 | failure mode | Collapse Temperature | Collapse Temperature | the failure mode for $P_{min}$ at 800°C | $P/P_{load}$ |
| 0.31 | 5.5kN | 1.0 | 2.3 | Type1 | 641.1 | N/A | Type2 | 2.06 |
| | | | | Type2 | 540.9 | N/A | | |
| | | | | Type3 | 681.4 | N/A | | |
| | | | | Type4 | 589.4 | N/A | | |
| 0.62 | 11kN | 1.0 | 2.3 | Type1 | 641.1 | N/A | Type2 | 1.54 |
| | | | | Type2 | 540.9 | N/A | | |
| | | | | Type3 | 574.1 | N/A | | |
| | | | | Type4 | 589.4 | N/A | | |

97

Fig6.5 The results for screwed connections when $t_1$ =3.2mm,

Table 6.4 The results for screwed connections when $t_1$=3.2mm, $t_2$=1.0mm

| | | | | Elevated temperatures | | | After fire | |
|---|---|---|---|---|---|---|---|---|
| $\bar{p}$ | Load(kN) (P$_{load}$) | t1 | t2 | failure mode | Collapse Temperature | Collapse Temperature | the failure mode for P$_{min}$ at 800°C | P/P$_{load}$ |
| 0.31 | 5.5kN | 3.2 | 1.0 | Type1 | 790.7 | N/A | Type2 | 1.61 |
| | | | | Type2 | 546.8 | N/A | | |
| | | | | Type3 | 681.4 | N/A | | |
| | | | | Type4 | 589.4 | N/A | | |
| 0.62 | 11kN | 3.2 | 1.0 | Type1 | 790.7 | N/A | Type2 | 1.61 |
| | | | | Type2 | 546.8 | N/A | | |
| | | | | Type3 | 574.1 | N/A | | |
| | | | | Type4 | 589.4 | N/A | | |

Fig6.6 The results for screwed connections when $t_1$=1.6mm $t_2$=3.2mm

Table 6.5 The results for screwed connections when $t_1$=1.6mm $t_2$=3.2mm

| $\bar{p}$ | Load(kN) ($P_{load}$) | t1 | t2 | Elevated temperatures | | | After fire | |
|---|---|---|---|---|---|---|---|---|
| | | | | failure mode | Collapse Temperature | Collapse Temperature | the failure mode for $P_{min}$ at 800°C | $P/P_{load}$ |
| 0.30 | 8kN | 1.6 | 3.2 | Type1 | 703.8 | N/A | Type4 | 1.91 |
| | | | | Type2 | 583.2 | N/A | | |
| | | | | Type3 | 685.9 | N/A | | |
| | | | | Type4 | 578.8 | N/A | | |
| 0.60 | 16kN | 1.6 | 3.2 | Type1 | 703.8 | N/A | Type3 | 1.91 |
| | | | | Type2 | 583.2 | N/A | | |
| | | | | Type3 | 577.3 | N/A | | |
| | | | | Type4 | 578.8 | N/A | | |

99

Table 6.6 The results for all of screwed connection specimens

| $\bar{p}$ | Load(kN) (P$_{load}$) | steel thickness side of the screw head(t1) | steel thickness side of the screw tip(t2) | Design mode of allowable shearing stress (Ras1,Ras2,Ras3,Ras4) | number of screws (Design) | Elevated temperatures | | After fire | | |
|---|---|---|---|---|---|---|---|---|---|---|
| | | | | | | failure mode | Collapse Temperature | Collapse Temperature | the failure mode for P$_{min}$ at 800℃ | P/P$_{load}$ |
| 0.30 | 6.5kN | 1.2 | 1.6 | Ras1 | 5 | Type1 | 735.9 | N/A | Type2 | 2.22 |
| | | | | | | Type2 | 584.2 | N/A | | |
| | | | | | | Type3 | 695.5 | N/A | | |
| | | | | | | Type4 | 655.1 | N/A | | |
| 0.64 | 12kN | 1.2 | 1.6 | | 9 | Type1 | 721.7 | N/A | Type3 | 2.07 |
| | | | | | | Type2 | 581.7 | N/A | | |
| | | | | | | Type3 | 569.5 | N/A | | |
| | | | | | | Type4 | 639.8 | N/A | | |
| 0.31 | 5.5kN | 1 | 2.3 | Ras2 | 3 | Type1 | 641.1 | N/A | Type2 | 2.06 |
| | | | | | | Type2 | 540.9 | N/A | | |
| | | | | | | Type3 | 681.4 | N/A | | |
| | | | | | | Type4 | 589.4 | N/A | | |
| 0.62 | 11kN | 1 | 2.3 | | 6 | Type1 | 641.1 | N/A | Type2 | 1.54 |
| | | | | | | Type2 | 540.9 | N/A | | |
| | | | | | | Type3 | 574.1 | N/A | | |
| | | | | | | Type4 | 589.4 | N/A | | |

| $\bar{p}$ | Load(kN) (P$_{load}$) | steel thickness side of the screw head(t1) | steel thickness side of the screw tip(t2) | Design mode of allowable shearing stress (Ras1,Ras2,Ras3,Ras4) | number of screws (Design) | Elevated temperatures | | After fire | | |
|---|---|---|---|---|---|---|---|---|---|---|
| | | | | | | failure mode | Collapse Temperature | Collapse Temperature | the failure mode for P$_{min}$ at 800°C | P/P$_{load}$ |
| 0.31 | 5.5kN | 3.2 | 1 | Ras3 | 3 | Type1 | 790.7 | N/A | Type2 | 1.61 |
| | | | | | | Type2 | 546.8 | N/A | | |
| | | | | | | Type3 | 681.4 | N/A | | |
| | | | | | | Type4 | 589.4 | N/A | | |
| 0.62 | 11kN | 3.2 | 1 | | 6 | Type1 | 790.7 | N/A | Type2 | 1.61 |
| | | | | | | Type2 | 546.8 | N/A | | |
| | | | | | | Type3 | 574.1 | N/A | | |
| | | | | | | Type4 | 589.4 | N/A | | |
| 0.3 | 8kN | 1.6 | 3.2 | Ras4 | 4 | Type1 | 703.8 | N/A | Type4 | 1.91 |
| | | | | | | Type2 | 583.2 | N/A | | |
| | | | | | | Type3 | 685.9 | N/A | | |
| | | | | | | Type4 | 578.8 | N/A | | |
| 0.6 | 16kN | 1.6 | 3.2 | | 8 | Type1 | 703.8 | N/A | Type3 | 1.91 |
| | | | | | | Type2 | 583.2 | N/A | | |
| | | | | | | Type3 | 577.3 | N/A | | |
| | | | | | | Type4 | 578.8 | N/A | | |

## 6.4 Conclusions

This chapter presents an evaluation method based on failure modes and collapses temperatures for screw connections in and after the fire, with a particular focus on the influence of varying parameters such as sheet thickness and applied loads. Evaluation formulas proposed in Chapters 3 and 5 for elevated temperatures and post-fire conditions were employed to calculate and analyze the failure modes and collapse temperatures.

(1) Using the proposed formula to calculate the parameters, it has been determined that when the temperature exceeds 500 °C, the screw connection is highly susceptible to damage under high-temperature conditions. Moreover, even if the failure mode is not initially a screw shear failure mode at ambient temperature (20°C), it may shift to this mode at higher temperatures when the steel sheets are of greater thickness.

(2) The arrangement of screws and the distance between the centers of screws have a significant impact on the structural performance of a steel plate subjected to fire conditions. When the same steel sheet specification is maintained, an increase in the number of screws typically results in a reduction in the distance between the centers of screws, which leads to a decline in the load-bearing capacity of the steel plate, giving rise to a change in failure modes and a decrease in collapse temperatures.

(3) After the heating and cooling processes, the screwed connections exhibited considerable residual strength. This indicates that these connections can retain their structural integrity even after fire exposure, providing a theoretical basis for potential repair and reuse. For the various design specimens, the residual strength at 800°C was approximately 1.5 to 2 times the applied load, demonstrating the post-fire performances of these connections under extreme conditions.

Consequently, the evaluation formulas presented in Chapter 5 are able to effectively predict the performance of screw connections under conditions of elevated temperature and post-fire exposure. In particular, it is possible to ascertain the failure modes and collapse temperatures of screw connections using these formulas at elevated temperatures. Furthermore, this chapter provides a reliable method for evaluating cold-formed steel structure performance in fire and post-fire scenarios.

## References

[6.1] Guide for Designing Cold-formed Steel Structures 2nd Edition, Gihodo Shuppan Co.,Ltd., 2014 (in Japanese)

[6.2] EN 1993-1-3 (2006). Eurocode 3 – Design of Steel Structures – Part 1-3: General Rules Supplementary Rules for Cold-Formed Members and Sheeting.

[6.3] American Iron and Steel Institute. North American Specification for the Design of CFS Structural Members, AISI S100-12[S]. Washington, DC, USA, 2012.

# Chapter 7 Conclusions

## 7.1 Summaries and Conclusions

This paper examined the fire resistance and post-fire performance of self-drilling screws and those connections; then, evaluate equations based on different failure modes were proposed to clarified the transition of the failure modes with the changing temperatures and to extrapolate the collapse temperature for self-drilling screw connections. Subsequently, a parameter analysis was used to assess the fire resistance and post-fire performance of screw connections, as well as the effects of different steel plate thicknesses and screw counts on the failure mode and shear bearing capacity of screw connections under high temperature and post-fire conditions. The results of the analysis provide crucial information for ensuring the design's reliability.

### 7.1.1 Conclusions of Chapter 2

Three different types of screws made of high-strength steel (HS), martensitic high-strength stainless steel (MSUS), and austenitic stainless-steel (ASUS), which were widely used to connect the components of the cold-formed steel structure, underwent tensile and shear testing at elevated temperatures in steady-state scenarios.

According to the results of shear tests for screws at elevated temperatures, the HS screws exhibited a reduction factor on the shear strength at elevated temperatures above 600°C similar to those of the high-strength bolts (JIS F10 T). The MSUS screws possessed higher shear strength at elevated temperatures than the HS screws. The ASUS screws possessed the highest shear strength at elevated temperatures above 700°C, although they had the lowest shear strength at ambient temperature. Furthermore, according to the test results of both the tensile and shear tests using the above three types of drilling screws, the strength ratio of the shear to tensile strength at each elevated temperature was clarified.

### 7.1.2 Conclusions of Chapter 3

Tensile tests for single overlapped screwed connections using HS screws at elevated temperatures were conducted to examine the load-bearing capacity of the screwed connection. And formulae for calculating the shear strength of the screw connection using the reduction factors for both the sheet tensile and screw shear strengths were proposed based on four failure modes:(a) Sheet longitudinal shear failure (Type 1); (b) Sheet bearing failure (Type 2); (c) Sheet net-section failure (Type 3); (d) Screw shear failure (Type 4).

According to the results of tensile tests for screwed connections at elevated temperatures, the screwed connection specimens using eight HS screws demonstrated a transition in failure modes with changes in test temperature. That is, for the same specification screwed connections, sheet bearing failure occurred at the ambient temperature and 800°C, whereas screw shear failure occurred between the test temperatures (400, 600 and 700°C). The above transition of failure modes can be explained by evaluating the tensile strengths corresponding to each failure mode at

elevated temperatures. In conclusion, the proposed formula can be utilized to assess the behavior of screwed connections in a fire scenario, thereby facilitating the development of more precise and productive fire protection design strategies. Furthermore, it offers a scientific foundation for enhancing existing design methodologies and developing guidelines for improving the fire resistance performance of screwed connection structures.

### 7.1.3 Conclusions of Chapter 4

Shear tests were performed at ambient temperature on three types of self-drilling screws HS (high-strength steel), MSUS (martensitic stainless-steel), and ASUS (austenitic stainless-steel) after heating and cooling procedures. These three types of screws were the same as those in Chapter 2.

(1) Based on the results of shear tests conducted on three types of screws after the heating and cooling processes, the post-fire shear strength of HS and MSUS screws decreases significantly when exposed to temperatures exceeding 500 °C. Moreover, the reduction factor of shear strength for HS specimens significantly reduced by 40% while the heated temperature was 500°C, which is considered to be caused by the heat treatment process of HS during production from the carbon steel bar to the HS screws. In contrast, the shear strength of ASUS screws remains virtually unchanged, even at high temperatures.

(2) The experimental results for shear tests of screws obtained in this Chapter were compared with those at elevated temperatures in Chapter 2. For the HS specimens, the shear strength decreased consistently from 20 to 400 °C; Above 400 °C, the shear strength under high-temperature conditions decreased sharply compared to the post-fire shear strength. For the ASUS specimen, the shear strengths decreased with increasing elevated temperatures; however, the post-fire shear strength remained constant throughout the experiment in this study. Furthermore, for MSUS screws, the shear strengths remained unchanged and decreased significantly below 400 °C and above 400 °C in elevated temperature tests, respectively. Similarly, the post-fire shear strength was almost unchanged below 400 °C, decreasing as the heated temperature increased.

### 7.1.4 Conclusions of Chapter 5

Tensile tests for single overlapped screwed connections using HS screws after the heating and cooling processes were conducted to examine the load-bearing capacity of the screwed connection. And formulas for calculating the post-fire shear strength of the screw connection using the reduction factors for both the post-fire sheet tensile strengths and post-fire screw shear strengths were proposed based on four failure modes:(a) Sheet longitudinal shear failure (Type 1); (b) Sheet bearing failure (Type 2); (c) Sheet net-section failure (Type 3); (d) Screw shear failure (Type 4).

The transition of the failure modes between the ambient and the exposed temperatures were observed. According to the results of tensile tests for screwed connections after the heating and cooling processes, the two-screwed connection specimens exhibited screw shear failure regardless

of the heated temperature; the untreated four-screwed connection specimens underwent sheet bearing failure. Whereas, screw shear failure modes occurred in other cases of experiencing 400–800 °C heating and cooling procedures. Moreover, for the eight-screwed connection specimens, screw shear failure modes occurred when the heated temperatures were 600 and 700 °C, and sheet net-section failure was observed in other conditions. That is, failure modes changed even when screwed connections of the same specification were used. Furthermore, the aforementioned failure mode transitions can be explained by assessing the post-fire tensile strengths corresponding to each failure mode. Furthermore, these equations can be used to evaluate the post-fire loading capacities of screwed connections corresponding to each failure mode.

### 7.1.5 Conclusions of Chapter 6

An evaluation method based on failure modes and collapses temperatures for screw connections in and after the fire, with a particular focus on the influence of varying parameters such as sheet thickness and applied loads, was presented. It provides a reliable method for evaluating cold-formed steel structure performance in fire and post-fire scenarios. Evaluation formulas proposed in Chapters 3 and 5 for elevated temperatures and post-fire conditions were employed to calculate and analyze the failure modes and collapse temperatures in this Chapter.

(1) Using the proposed formula to calculate the parameters, it has been determined that when the temperature exceeds 500 °C, the screw connection is highly susceptible to damage under high-temperature conditions. Moreover, even if the failure mode is not initially a screw shear failure mode at ambient temperature (20°C), it may shift to this mode at higher temperatures when the steel sheets are of greater thickness.

(2) The arrangement of screws and the distance between the centers of screws have a significant impact on the structural performance of a steel plate subjected to fire conditions.

(3) After the heating and cooling processes, the screwed connections exhibited considerable residual strength. This indicates that these connections can retain their structural integrity even after fire exposure, providing a theoretical basis for potential repair and reuse. For the various design specimens, the residual strength at 800°C was approximately 1.5 to 2 times the applied load, demonstrating the post-fire performances of these connections under extreme conditions.

## 7.2 Future Works

The research presented in this study represents a significant advancement in the understanding of the fire resistance and post-fire performance of self-drilling screw connections in cold-formed steel structures. The current research is far from sufficient for developing comprehensive guidelines of a fire resistance design guide and a diagnostic method for post-fire repair or reuse for cold-formed steel structures. The present study did not consider the influence of thermal stress on the failure modes of joints. In the event of thermal expansion, specific failure modes may demonstrate a sudden decline in load following the attainment of peak load, which could

ultimately result in premature failure at elevated temperatures. It is therefore essential to investigate the behavior and deformation capacity of each failure mode under thermal changes. Further research will address the impact of thermal stress on the collapse temperature and failure modes of joints, to provide a more comprehensive risk assessment and improved design guidelines. On the basis of the aforementioned problems being resolved, further work is considered in two main areas.

1. For Fire-Resistant Design Methods:

(a) Finite element analysis can be conducted to simulate the experimental conditions and compare the results with the experimental data in this study. It can validate and optimize the proposed formulas for screwed-connections at elevated temperatures, ensuring their accuracy and reliability.

(b) Fire resistance for individual structural components of cold-formed steel structures should be investigated, such as the build-up beams using screws. It is recommended that detailed experimental studies and theoretical models be conducted to evaluate the behavior of these components under fire conditions. It will facilitate a more comprehensive comprehension of the fire resistance of cold-formed steel structures.

2. For Post-Fire Repair and Reuse Strategies:

(a) In this study, self-drilling screws and those connection specimens were allowed to cool naturally in the furnace after heating. It would be beneficial for future research to simulate real fire scenarios with greater accuracy by implementing water cooling after heating, in order to more closely resemble the actions of firefighting personnel.

(b) As the same as fire-resistant design methods, finite element analysis can be conducted to simulate the experimental conditions and compare the results with the experimental data in this study. Then it can optimize the proposed formulas for post-fire strengths of screwed-connections, ensuring their accuracy and reliability.

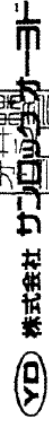**Appendix A:  Inspection Certificates for screw specimens**

HEX (HS)

製作番号 6061107-117100174

# 検 査 成 績 表
本社工場

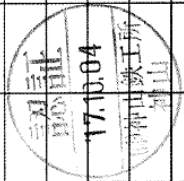株式会社神山鉃工所 様
株式会社マツウラ 様

(No. 8928　)

| 品　名 | 線　径 | 記　号 | | 仕　様 | | 束　数 | 質　量 | 出荷年月日 |
|---|---|---|---|---|---|---|---|---|
| SWCH18AP | 4.05 | | | 前鈍 | | 8 | 3.792 | 17/10/04 |

化学成分 % (×100, P・S・Al－×1000, B－×10000)

| | C | Si | Mn | P | S | Al | Cu | Ni | Cr |
|---|---|---|---|---|---|---|---|---|---|
| 鋼　番 | 19 | 3 | 80 | 10 | 7 | 30 | 2 | 3 | 3 |
| SF84359 | | | | | | | | | |
| 規　格 | 15 - 20 | ≦ 10 | 60 - 90 | ≦ 30 | ≦ 35 | 20 ≦ | ≦ 30 | ≦ 20 | ≦ 20 |

| 試験項目 | 実測値 | 引張荷重 N | 引張強さ | | 絞り % | 外観 | 質量 | 仕様 | 備考 |
|---|---|---|---|---|---|---|---|---|---|
| 線径 | + 0.000 − 0.020 | | Max 470 Min 410 | | 60.0 以上 | | | | |
| 01 | 4.038 | 5624 | 439 | | 82.3 | GOOD | 506 | C8474 | |
| 02 | 4.033 | | | | | GOOD | 485 | C8475 | |
| 03 | 4.034 | | | | | GOOD | 505 | C8476 | |
| 04 | 4.038 | | | | | GOOD | 468 | C8477 | |
| 05 | 4.037 | | | | | GOOD | 506 | C8478 | |
| 06 | 4.038 | | | | | GOOD | 400 | C8479 | |
| 07 | 4.037 | | | | | GOOD | 502 | C8480 | |
| 08 | 4.040 | | | | | GOOD | 420 | C8481 | |

検印 17.10.04 神山鉄工所 岡山

本証は朱印のあるもののみ有効とします。

〈C8474～C8481〉

109

# INSPECTION CERTIFICATE 検 査 証 明 書

No. 178285

Date 発行日 2017年 08月 22日

Shinsei Kogyo 新居工業株式会社
〒454-0921 名古屋市中川区中郷5
4-75 CHUGO NAKAGAWA-KU,
NAGOYA-CITY, 454-0921, JAPAN
TEL.〈052〉351-0504 FAX.〈052〉351-1098

Customer 需要家  株式会社 信光ステンレス  様

| Product No. 工番 | Commodity 品名 | Heat No. 製鋼番号 | Wire Diameter 線径(mm) | Number コイル数 | Total Mass 質量(kg) | Condition 納入状態 | Symbol of Grade 記号 |
|---|---|---|---|---|---|---|---|
| 7043375 | SUS410 | E83157 | 4.050 | 2 | 987.0 | BCS | WSB |

## Chemical Composition 化学成分 (%)

| Elements 成分 | C (×100) | Si (×100) | Mn (×100) | P (×1000) | S (×1000) | Cu (×100) | Ni (×100) | Cr (×100) | Mo (×100) |
|---|---|---|---|---|---|---|---|---|---|
| Specification 規格 | MAX. 15 | MAX. 100 | MAX. 100 | MAX. 40 | MAX. 30 | | MAX. 60 | 1150 -1350 | |
| Results 成績 | 10 | 40 | 37 | 23 | 1 | 23 | 1203 | |

## Inspection Results 検査結果

| Items 検査項目 | Wire Diameter 線径(mm) | Ovality 偏径差(mm) | Mass 質量(kg) | Tensile Strength 引張強さ(N/mm²) | Reduction of Area 絞り(%) | Remarks 備考 |
|---|---|---|---|---|---|---|
| Spec. 規格 | 4.050 +0,-0.02 | | | 460 - 640 | ≧65 | |
| Coil No. 3 | 4.050 | | 465.0 | 567 | 84  98405 | |
| 4 | 4.049 | | 522.0 | 562 | 85  98406 | |

上記製品はご指定の規格または仕様に従って製造され
その要求を満足していることを証明します。
We hereby certify that the material described herein
has been made in accordance with the rules of the contract.

品質管理係
Chief of Quality Assurance Section
品質保証・制御部 部長 S.Maeda

(認証 '17.9.27 (株)神山線工所 神山)

（ASUS）

# INSPECTION CERTIFICATE 検査報告書

**NIPPON SEISEN**

No. 22207
Date Of Issue 発行日 2013.02.13

| Contractor 契約先 | 株式会社 神山鉄工所 桜井工場 | 御中 |
| Description 品名 | 冷間圧造用ステンレス鋼線 | |
| Type Of Steel 鋼種名 | SUS 304J3 | |
| Net Mass 質量 | 325.0 kg | Number 員数 1 |

| Customer 需要家 | 田島スチール株式会社 本社 御中 |
| Size 寸法 | 4.05 |
| | JIS G 4315 WSB | Condition 仕上 SSP |
| 品番 CB | Order No. 受注番号 CC67537 |

## Chemical Composition 化学成分 (%)

| Elements 成分 | C | Si | Mn | P | S | Ni | Cr | Cu |
|---|---|---|---|---|---|---|---|---|
| Specification 規格 | 0.08 MAX | 1.00 MAX | 2.00 MAX | 0.045 MAX | 0.030 MAX | 8.00 10.50 | 17.00 19.00 | 1.00 3.00 |
| Heat No 号 溶解番号 X483D-2 | 0.025 | 0.25 | 1.60 | 0.034 | 0.001 | 9.05 | 18.28 | 2.55 |

## Inspection Results 検査結果

| Inspection Items 検査項目 | No. | Mass 質量 kg | Size 寸法 | Tensile Strength 引張強さ N/㎟ 引張強さ | 偏径差 | 伸び % | 絞り % MIN |
|---|---|---|---|---|---|---|---|
| Specification 規格 | | | 4.030 4.050 | 530 710 | 0.010 MAX | | 65 |
| Inspection No. 検査番号 3207-17348 | 1 | 325.0 | 4.046 以上 | 592 | 0.003 | 32 | 80 |

(神鉄 切断済）
(テスト材)

325.「330
g

認証証
'13.2.15
㈱神山鉄工所 神山

外観 ： 良

111

# Acknowledgments

Completing this dissertation has been a challenging yet rewarding journey and would not have been possible without the support and guidance of many people. I would like to take this opportunity to express my sincere gratitude to all those who have contributed to my academic and personal growth during this time.

First and foremost, I owe my deepest thanks to Professor Fuminobu Ozaki. When I first began my research, I often felt uncertain and overwhelmed by the complexity of my chosen field. Professor Ozaki provided not only the technical knowledge I needed but also a clear vision of how to approach research with purpose and structure. He helped me see the bigger picture, teaching me how to connect the dots between seemingly unrelated concepts and apply them to my work. His guidance extended well beyond the technical aspects of my work. He encouraged me to think critically, communicate my findings clearly, and present my research to others confidently and engagingly. I am immensely grateful to Professor Ozaki for his invaluable mentorship, which has played a pivotal role in my growth as a researcher. Without his unwavering guidance and support, this thesis would not have reached its current form.

I would like to extend my heartfelt thanks to Professor Yasuhiro Mori, whose gentle and patient guidance has been a constant source of encouragement throughout my time in the lab. His insightful suggestions and thorough explanations helped me overcome many challenges in my research, and his support has been crucial in the successful completion of this thesis. Special thanks go to Professor Takeo Hirashima, whose expertise and constructive feedback were instrumental in refining my research and guiding me through the complexities of my field. Furthermore, I am also deeply grateful to Professor Yo Hibino for his significant contributions and guidance throughout this process.

I'd like to take a moment to express my heartfelt gratitude to my amazing parents, Liwu Liu and Ruzhen Wang. They've been my rock since I moved to Japan in 2016, offering unwavering support, both emotionally and financially. Their belief in me has been a driving force, helping me push through the toughest times and pursue my academic dreams. They've been my biggest cheerleaders, always there to support every decision I've made.

During my period of leave from my studies, I was fortunate to meet my husband, Chao LIU, a talented architectural designer, and my soulmate. His unwavering love, patience, and support have consistently served as my primary source of strength. Upon my return to Japan to resume my studies the day after my wedding, I found his encouragement to be unwavering. I would not have reached my current position without his comprehension and endorsement of my aspirations.

I would like to express my gratitude to my colleagues and fellow students for their friendship and support as I have progressed through this remarkable academic experience. Their companionship, encouragement, and shared experiences have facilitated the navigation of challenging periods, and I am profoundly grateful for their presence in my life.

To all those who have contributed to this remarkable academic journey, I extend my sincerest gratitude. This thesis is the culmination of not only my efforts but also the collective support and guidance I have received along the way, and I am eager to share it with you all.

<div align="right">

Ying LIU

09/2024

</div>